

**THE ROLE OF HISTONE ACETYLATION IN THE CONTROL OF IMMUNE
CHECKPOINT EXPRESSION IN CD8⁺ T CELLS**

by

Ali Ghasemzadeh

A dissertation submitted to Johns Hopkins University in conformity with the
requirements for the degree Doctor of Philosophy

Baltimore, Maryland
July 2019

ABSTRACT:

T cell exhaustion is characterized by the expression of multiple immune checkpoint molecules on the surface of T cells and loss of effector functions. Epigenetic programs governing the coordinate expression of immune checkpoints and the implications of different patterns of checkpoint expression on T cell function are currently unknown. In this thesis we identify the environmental cytokine TGF- β 1 differentially controls the expression of PD-1 and other immune checkpoints. This differential regulation is driven in part by epigenetic programs involving histone acetylation that alter the promoters of immune checkpoint. Utilizing highly specific small molecule inhibitors of TGF- β 1 signaling and class I histone deacetylases allowed for differential programming of immune checkpoint expression on the T cell surface and led to different functional properties of CD8+ T cells. This programming could be altered both *in vitro* and *in vivo*. Lastly, we show that treatment with HDAC inhibitors leads to a more profound exhaustion phenotype in both chronic viral infection and tumor models; however, the combination of HDAC inhibitors and checkpoint blockade agents have a synergistic effect on T cell function and anti-tumor immunity.

Readers:

Dr. Charles G. Drake (PhD Advisor)

Dr. Jonathan D. Powell

Thesis Committee:

Dr. Charles G. Drake (PhD Advisor)

Dr. Jonathan Powell (Committee Chair)

Dr. Srinivasan Yegnasubramanian

Dr. Christopher Gamper

ACKNOWLEDGEMENTS:

I would like to thank my PhD advisor, Dr. Charles Drake, for his guidance and mentorship over the course of my studies. His unwavering support and belief in me made it possible to carry out this research. Chuck is a passionate scientist and an excellent role-model as a physician-scientist and I hope I can live up to his example.

This thesis is dedicated to my family, without whom I would have never set forth on this path. Their help and advice at every stage has made it possible for me to pursue my dreams.

This work was made possible by the contributions of many collaborators and friends. There are too many to name individually, but I appreciate their contributions of time, energy, thoughts and ideas, reagents, and skills to this project. I am grateful for the friendships that have developed as a result of this work and hope that these data can in some small way contribute to our understanding of the immune system.

TABLE OF CONTENTS:

Abstract.....ii

Acknowledgements.....iv

Table of Contents.....v

List of Figures.....vi

Introduction.....1

Chapter 1: TGF- β 1 differentially regulates PD-1 from other immune checkpoints.....14

Chapter 2: Histone Acetylation Regulates Immune Checkpoint Expression.....27

Chapter 3: Inhibition of the TGF- β 1 / Class I HDAC Axis Promotes the Differentiation of Functionally Distinct T Cell Subsets.....47

Chapter 4: Modulation of checkpoint expression profiles on T cells *in vivo*.....62

Chapter 5: Entinostat synergizes with checkpoint blockade to generate anti-tumor immunity.....89

Conclusions and Future Directions.....107

References.....117

Curriculum Vitae.....128

LIST OF FIGURES

Figure 1: PD-1 expression is upregulated by TGF- β 1 in a Smad3 dependent manner.....	23
Figure 2: CTLA-4 and TIM-3 expression is downregulated by TGF- β 1.....	25
Figure 3: Histone acetylation is increased at the promoters of immune checkpoints during T cell activation.....	40
Figure 4: Selected acetylation tracks from immune checkpoint and T cell activation genes.....	41
Figure 5: Drug screen reveals class I specific HDAC inhibitors enhance the expression of TIM-3.....	43
Figure 6: TGF- β 1 and Entinostat differentially affect the acetylation of immune checkpoint promoters.....	44
Figure 7: Combining SIS3 and entinostat additively enhances expression of TIM-3.....	45
Figure 8: Combination of entinostat and SIS3 results in the largest fold change difference in promoter acetylation in CTLA-4 and TIM-3.....	46
Figure 9: PD-1 and TIM-3 mark two clusters of discordantly regulated immune checkpoints.....	57
Figure 10: Promoter acetylation status is directly related to RNA expression of immune checkpoint genes.....	59
Figure 11: PD-1 and TIM-3 are discordantly regulated and associated with different functional states.....	60
Figure 12: TGF- β 1 and HDAC inhibition change the distribution of T cell population level checkpoint expression.....	61
Figure 13: TGF- β 1/Class I HDAC inhibition increases the number of checkpoints expressed on CD8+ T cells.....	78
Figure 14: TGF- β 1/Class I HDAC inhibition induces the expression of multiple checkpoints in acute infection.....	79
Figure 15: TGF- β 1/Class I HDAC inhibition induces the expression of multiple checkpoints in chronic infection.....	81

Figure 16: HDAC inhibition promotes T cell expansion during the priming phase of infection.....	83
Figure 17: Cytokine production is altered by TGF- β 1/Class I HDAC inhibition during acute and chronic infection.....	84
Figure 18: TCF1 expression is retained in a higher proportion of antigen-specific CD8+ T cells in mice treated with class I HDAC inhibition.....	86
Figure 19: Tbet and Eomes expression are similar between TGF-b1/class I HDAC inhibited CD8+ T cells.....	87
Figure 20: LCMV virus levels are higher in the serum of class I HDAC inhibited mice.....	88
Figure 21: Entinostat in combination with anti-CTLA-4 leads to survival advantage.....	99
Figure 22: Combination anti-CTLA-4 and HDACi treatment lead to T cell infiltration to tumor and effector function.....	101
Figure 23: Combination entinostat and anti-CTLA-4 treatment lead to cytokine production in CD8+ TIL.....	103
Figure 24: Anti-CTLA-4 reduces the percentage of regulatory T cells in the TME.....	105

CHAPTER 1

Introduction

Cancer can be recognized by the immune system

The process by which a normal tissue transforms into a malignant mass is driven by the accumulation of mutations in the genome¹. These mutations confer a proliferative or survival advantage to the cell that contains the mutation relative to other cells of that tissue. From a therapeutic standpoint, the development of medications that can target the specific mutations of a tumor has been challenging. In contrast, the immune system can take advantage of this feature of tumors and potentially recognize the multitude of new antigenic specificities that are provided by the tumor^{2,3}. However, patients often present with advanced cancer, indicating that this theoretical tumor recognition mechanism by which the immune system may target and destroy tumors either does not exist, or is held in check by the tumor.

Evidence to support the claim that cancers can be shaped by and interact with the immune system came from an elegant series of experiments done using the MCA-induced sarcoma cancer model. In this model MCA is injected subcutaneously in a mouse and due to the mutations induced by MCA, cancer develops. MCA was injected in both wildtype and RAG knockout mice which lack B and T cells⁴. After the tumors developed, they were excised and re-implanted in either wildtype or RAG knockout mice. Tumors grown in WT mice were able to continue growing in WT and RAG knockout mice. Tumors grown in RAG knockout mice were able to grow in RAG knockout mice; however, they were unable to grow well in WT mice. This suggested that the lack of B and T cells during the development and growth of the primary tumor led the tumor being recognized when re-implanted in wildtype mice, reducing its growth.

Insights such as this one led to a more general theory called the immune editing hypothesis⁵.

The cancer immunoediting hypothesis was first proposed by MacFarlane Burnet and Lewis Thomas in the 1950s⁶. They proposed that the main function of the immune system was not rejection of transplant allografts, rather, it had developed to hunt and eliminate tumors. Over time, this idea was developed into what is now referred to as the 3E's of cancer immunoediting: Elimination, Equilibrium, and Escape. Together these have now become a part of the new "Hallmarks of Cancer"¹. Why the immune system cannot restrain tumors during the elimination phase and how they progress to escape has been an active area of research. Early tumors are quickly recognized by the immune system and eliminated⁷. These cells undergo various changes during the malignant transformation process and the stresses involved in this cause them to be recognized by the immune system. In this process, innate cytokines such as the type I interferons, and innate stress ligands such as NKG2D play important roles^{5,7}. However, as the cancer progresses, the immune system reaches an equilibrium stage in which it no longer is eliminating the tumor but has reached a state of growth arrest⁸. The evidence for this being a distinct phase is weak because it has been the hardest to model in mice. Unfortunately, many tumors will progress through this stage and reach Escape. In this phase, the tumor has acquired characteristics that make it insensitive to immune pressure. Numerous mechanisms have been described including loss of MHC expression, mutations in the JAK/STAT signaling pathway, secretion of immunosuppressive cytokines, recruitment of suppressive cell populations such as Tregs

and Myeloid-derived suppressor cells (MDSC), and upregulation of checkpoint ligands⁹⁻¹⁵.

Immune checkpoints and T cell exhaustion

Among the mechanisms of immune resistance and tumor escape from immune surveillance, the best studied and most clinically applicable currently is the engagement of immune checkpoints¹⁶. Immune checkpoints are a family of biologically related but molecularly distinct cell surface receptors that are expressed on T cells. Their evolutionary purpose appears to be in dampening the immune response to restrain the development of autoimmunity and tissue damage during a normal immune response to a pathogen. CTLA-4 knockout mice develop autoimmunity and die within 3-4 weeks of birth^{17,18}. CTLA-4 knockout T cells demonstrate significant upregulation of activation markers, and these mice exhibit severe myocarditis, pancreatitis, and infiltration of the liver, spleen, and lung with T cells. Similarly, PD-1 knockout mice develop high levels of serum immunoglobulins and cardiomyopathy as well as a mild lupus like phenotype¹⁹⁻²¹. Interestingly, the phenotype seen in PD-1 knockout animals is milder and develops later in life compared to that seen in CTLA-4 knockout mice, suggesting that despite the similar types of function, they are non-overlapping and may have distinct functions and signaling mechanisms.

Immune checkpoints are normally upregulated during acute T cell activation. Upon activation naïve T cells express multiple immune checkpoints, though the kinetics by which they become expressed are different. These include: PD-1, CTLA-4, LAG-3, and

TIM-3²². The expression of these checkpoints is subsequently downregulated. However, T cells that are chronically stimulated through the T cell receptor, such as in the setting of cancer and chronic infections maintain high levels of expression of immune checkpoints. Chronic stimulation and inflammation drives T cells to a dysfunctional, TCR signaling-driven state called exhaustion. Exhausted T cells have several distinguishing characteristics. They express multiple immune checkpoints, have reduced proliferative potential, and undergo a hierarchical loss of cytokine production capacity. Usually, IL-2 production is lost first, followed by TNF α and IFN γ ²²⁻²⁶. Granzyme B production is usually retained and exhausted T cells that have lost the ability to proliferate or produce other cytokines but retain granzyme B production are not inert. Studies have shown that these hypofunctional T cells are important in maintaining the stalemate between host and pathogen. Depletion of these T cells leads to pathogen proliferation and loss of infection control²⁷.

CTLA-4: the first immune checkpoint

CTLA-associated antigen 4 was the first immune checkpoint discovered. It was the first shown with blockade of CTLA-4 by monoclonal antibody that disrupting the interaction between checkpoint and ligand can lead to anti-tumor immunity²⁸. CTLA-4 is thought to function by dampening the activation of T cells. T cell activation is complex, and this process usually requires two signals. Signal one is delivered by the interaction of a TCR with its cognate peptide presented in the context of class I MHC. Signal two is a co-stimulatory signal, the most well-studied is the interaction between CD28 on T cells and CD80 or CD86 on antigen-presenting cells. The combination of two signals drives full

T cell activation. T cell expression of CTLA-4 hijacks this process by competing with CD28 to bind to CD80 and CD86. Because the affinity of CTLA-4 for CD80/86 is 4 times greater than CD28, it is able to outcompete it for binding, leading to a negative signal delivered to the T cell²⁹. In patients, administration of anti-CTLA-4 leads to a considerable level of T cell activation and is associated with a higher rate of immune-related adverse events (irAE) compared to PD-1 blockade³⁰. CTLA-4 is constitutively expressed at high levels on regulatory T cells where it likely plays a role in their suppressive function^{15,31,32}.

PD-1: a major resistance mechanism in humans

The blockade of PD-1 has led to deep and durable clinical responses in patients in multiple cancer types^{10,33-38}. Thus, a great deal of excitement has been generated about PD-1 blockade; however, the mechanisms by which it functions and is regulated are not well understood. Interestingly, recent evidence suggests that both PD-1 and CTLA-4 signaling converge around the CD28 pathway^{39,40}. While CTLA-4 competes for the ligand of CD28, PD-1 signaling itself appears to function to activate phosphatases that suppress CD28 co-stimulatory signaling. This may explain, in part, why co-blockade of PD-1 and CTLA-4 has synergistic therapeutic effect. The ligand for PD-1, PD-L1, is not constitutively expressed on most tissues⁴¹. In some tumors it becomes upregulated as a result of tumorigenesis and the oncogene Myc and the bromodomain BRD4 have been shown to play a role in this⁴²⁻⁴⁴. In other settings, PD-L1 expression is upregulated in response to IFN γ signaling in the environment⁴⁵. In the context of tumors, this is called adaptive immune resistance⁴⁶. Thus, tumors can sense an attack by T cells and upregulate PD-L1 as a molecular shield. Antibodies that block the interaction between

PD-1 and PD-L1 reinvigorate T cells. These T cells begin to proliferate and gain cytokine production and cytotoxicity.

The expression of PD-1 itself is upregulated during T cell activation as a consequence of TCR signaling. NFATc1 is a major regulator of PD-1 and drives its expression⁴⁷. The transcription factor Tbet, which is associated with effector function and Th1 differentiation, has been shown to be a negative regulator of PD-1 expression⁴⁸. Similarly, Blimp1 has been shown to repress NFATc1-dependent PD-1 expression⁴⁹. In contrast, FoxO1 has been shown to sustain the expression of PD-1 during chronic viral infection⁵⁰. Interestingly, the environment has also been shown to influence PD-1 expression. Smad3 signaling downstream of TGF- β 1, can upregulate the expression of PD-1 through direct Smad3 binding of the PD-1 promoter⁵¹. It has also been shown that TGF- β 1 can indirectly enhance PD-1 expression through Smad3 mediated degradation of the chromatin remodeler Satb1⁵². Satb1 targets the class I HDAC NuRD complex to the PD-1 locus, leading its deacetylation and repression. These mechanisms indicate the PD-1 expression can be modulated by a variety of transcription factors in a context dependent manner. However, our understanding of the genetic and epigenetic factors that govern the expression of other checkpoints besides PD-1, is relatively sparse and is an area of active inquiry.

Epigenetic regulation of T cell exhaustion

Development is a complex process involving the expression and silencing of large networks of genes and integration of signals from the environment. These large,

coordinated changes are driven by transcription factors and must be stabilized and inherited in subsequent cellular progeny. Thus, epigenetic alterations, the modification of DNA or associated factors that have information content and can be passed from generation to generation without alteration of the DNA sequence itself, are required⁵³. Epigenetic modifications modulate the accessibility of the underlying chromatin to transcription factors and thus facilitate the expression or silencing of genes. A theoretical model to have in mind about how this process may work is as follows: Cues such as TCR or TGF- β 1 signaling modify the activity of particular transcription factors and allow for their binding throughout the genome. These transcription factors usually have the ability to modify the chromatin around them, either directly, or through the recruitment of chromatin modifying enzymes. These changes then further solidify the gene expression change or may influence the expression of networks of other genes. This in turn can now induce the silencing or expression of families of other transcription factors that can now in turn begin this cycle again, modifying networks of genes. In this way, the T cell becomes committed to a particular lineage or phenotype.

The most well-studied epigenetic modification is direct methylation of cytosine residues of CpG dinucleotides in the DNA. DNA methylation leads to the silencing of gene expression. DNA methylation is deposited and maintained by the DNA methyltransferase family of enzymes DNMT1, 3A, and 3B^{54,55}. Of these family members, DNMT3A and 3B are capable of depositing *de novo* methylation marks, and thus are able to dynamically regulate gene expression⁵⁶. These enzymes play a key role in maintaining lineage stability and restricting T cell plasticity. DNMT3a silences IFN γ

expression during Th2 differentiation⁵⁷. It has recently been shown that DNMT3a is important for the methylation of TCF7 leading to silencing of its expression to restrict the frequency of memory-precursor T cells^{58,59}. Genome-wide studies of T cell methylation status during different stages of effector and memory differentiation have revealed that methylation status generally correlates well with gene silencing⁶⁰. In T cells, IFN γ and granzyme B gene promoters become demethylated during the acquisition of effector function while genes such as TCF7 which are expressed at high levels in naïve and memory T cells become silenced. Thus, the acquisition of distinct methylation profiles in T cells likely corresponds to the execution of unique genetic programs during different stages of differentiation and development.

DNA methylation has also been implicated in the control of PD-1 expression. In acute infection, the PD-1 promoter is transiently demethylated and subsequently remethylated. The duration of this is directly related to the length of TCR stimulation. However, in chronic infection PD-1 is demethylated and remains demethylated, even when viral loads decrease⁶¹⁻⁶³. Thus, PD-1 expression remains high.

A second category of epigenetic modification involves post-translational modifications of the histone tail. DNA is wrapped around histone cores, forming the substrate of chromatin. Modifications to histones facilitate the transition between condensed and relaxed chromatin configurations, allowing for transcription factors to gain access to the underlying chromatin. Different modifications can be made to histone tails and the combined sum of these interactions dictates the accessibility of the underlying DNA. The modification of histone tails can facilitate the recruitment of

proteins that can read the epigenetic code and allow for transcription or gene silencing to occur^{64,65}. The actions of different epigenetic marks have been profiled genome-wide, and functions have been described for each set. Specific histone marks associate with different regulatory elements of the genome. Histone acetylation is generally associated with transcriptional activation. H3K27 and H3K9 acetylation both mark active promoters, with H3K27 also marking enhancer elements in the genome. While histone tail acetylation is generally associated with transcriptional activation, histone methylation is more complex. H3K4-mono, di, and tri-methylation are all associated with transcriptional activation. H3K27-trimethylation is strongly associated with transcriptional repression and epigenetic silencing and is deposited by EZH2, the catalytic component of the PRC2 repressor complex^{64,65}. The zinc finger protein CTCF has been described as an insulator, protecting a promoter from the effects of a nearby enhancer⁶⁶.

The role of histone marks in the control of T cell biology has been studied in the context of single genes, as well as in genome-wide sequencing studies. Araki and colleagues studied the role of H3K9 acetylation on the induction and expression of the transcription factor Eomes and two of its targets, granzyme B and perforin⁶⁷. They found that H3K9 acetylation was increased in the promoter of Eomes in memory T cells leading to higher expression of both Eomes and its downstream targets. Treatment with a histone acetyltransferase inhibitor, curcumin, prevented H3K9 acetylation and abrogated the expression difference between naïve and memory T cells. Further emphasizing the importance of histone acetylation states in naïve and memory T cells,

DiSpirito and Shen demonstrated that histone H3 diacetylation was increased on a per cell basis in memory T cells compared to naïve T cells⁶⁸. Furthermore, memory CD8+ T cells that had been primed in the absence of CD4+ T cells had a lower level of H3 diacetylation. The demonstration of the dependence of a CD8+ T cell's epigenetic state on CD4+ T cell help highlights an important mechanism by which helper T cells likely influence the functional capability of CD8+ T cells, though the exact mechanism by which this occurs is unknown.

Chromatin landscapes and their relationship to T cell exhaustion have recently been an area of active inquiry, with several reports in both chronic viral infection and tumor models examining this question. Exhausted T cells demonstrate a different transcriptional profile compared to both memory and effector T cell populations²⁵. Besides overexpression of inhibitory receptors, these cells demonstrate alterations in T cell receptor and cytokine signaling pathways, expression of distinct sets of transcription factors, altered expression of chemotactic and adhesion genes, and changes in genes important in regulating metabolism. Despite the differences in expression pattern of genes between exhausted and memory T cells, there is little known about the epigenetic programs that control these differences in gene expression. Studies utilizing ATAC-seq technology have addressed this question^{69–71}. ATAC-seq or assay for transposase-accessible chromatin using sequencing, utilizes the transposase Tn5 to insert sequencing adapters in regions of open chromatin. These regions of open chromatin can subsequently be sequenced and mapped to a reference genome.

Exhausted T cells treated with anti-PD-1/L1 antibodies undergo proliferation and gain effector function. However, if treatment with the antibody is stopped the cells quickly lose effector function and become exhausted. Therefore, it does not appear that treatment with anti-PD-1/L1 antibodies reprograms exhausted T cells to become functional memory cells. ATAC-seq studies demonstrated that the chromatin landscape of exhausted T cells is distinct from memory and effector T cells⁷²⁻⁷⁴. Treatment with checkpoint blockade does not alter the chromatin landscape. Rather, it changes the patterns of transcription factor binding to available binding sites throughout the genome. This explains why after cessation of treatment T cells revert to the exhausted phenotype.

These data highlight the important role of epigenetic modifications and chromatin landscapes in the control of T cell exhaustion. However, we still understand little about the epigenetic factors that control the expression patterns of immune checkpoints on T cells and the contribution of these patterns to T cell exhaustion.

Overview of this Thesis:

The overall goal of this dissertation is to understand the role of histone acetylation in the differential control of immune checkpoint expression on CD8+ T cells and its contribution to the regulation of T cell exhaustion.

In this series of experiments, I have:

1. Shown that TGF- β 1 differentially regulates the expression of immune checkpoints including PD-1 and CTLA-4, LAG-3, and TIM-3

2. Demonstrated the role of histone acetylation in checkpoint expression control.
3. Evaluated the effect of TGF- β 1 and HDAC inhibition on T cell checkpoint expression, function, and differentiation.
4. Characterized the effects of TGF- β 1 and HDAC inhibition on T cell function *in vivo* in acute and chronic viral infection.
5. Explored the efficacy of combinations of immune checkpoint inhibitors and HDAC inhibitors as a cancer immunotherapy in a challenging prostate cancer model.

This thesis identifies a novel mechanism by which environmental factors epigenetically control T cell exhaustion and has implications for combination immunotherapy design in the clinic.

CHAPTER 1

TGF- β 1 differentially regulates PD-1 from other immune checkpoints

Introduction

Upon engagement of a T cell receptor by its cognate antigen presented in the context of an appropriate MHC molecule, T cells begin to proliferate and produce effector molecules. During this activation process PD-1 and other immune checkpoints are upregulated and expressed on the T cell surface⁷⁵. The evolutionary role of this expression is thought to be prevention of “exuberant” activation and damage to the host. Evidence supporting this idea can be found in the autoimmune phenotypes seen in mice with genetic deletion of CTLA-4 or PD-1, and the immune-related side effects seen in patients treated clinically with antibodies targeting these checkpoints^{17,18,20,21,30}.

In normal T cell activation, T cells express immune checkpoints during initial priming and expansion. As the pathogen is cleared and T cell memory develops the expression of checkpoints is downregulated. In the context of chronic activation in cancer and chronic infection, this expression remains elevated and contributes to T cell dysfunction^{76,77}. Blocking the interaction between immune checkpoints and their ligands improves T cell function leading to proliferation and expression of effector molecules. However, this effect is temporary. T cells removed from chronic antigen exposure do not become memory T cells with intact effector function. Studies into this phenomenon have revealed reprogramming at the epigenetic level contributes to T cells “remembering” their exhausted phenotype even in the absence of chronic antigen exposure.

Exhausted T cells found in tumors and chronic infection often express several other immune checkpoints in addition to PD-1. The co-expression of these proteins has

led to the idea that their expression is co-regulated⁷⁸⁻⁸⁰. Indeed, there is evidence suggesting that these checkpoints are co-regulated by NFAT family proteins as well as the zinc-finger transcription factor GATA3. TGF- β 1, an immunoregulatory cytokine highly expressed in the tumor microenvironment has been shown to upregulate PD-1 expression via Smad3 signaling and epigenetic remodeling^{51,52}. High levels of TGF- β 1 in the TME have been shown to correlate with poor outcome in multiple cancers⁸¹⁻⁸³. We became interested in testing the hypothesis that TGF- β 1 can regulate other immune checkpoints in a similar fashion.

Results

PD-1 expression is upregulated by TGF- β 1 in human CD8+ T cells

We first sought to verify that we could recreate the published observation that TGF- β 1 upregulates PD-1 expression. Human PBMC isolated from healthy donors were thawed and allowed to rest overnight in complete media. Subsequently, CD8+ T cells were isolated by magnetic bead based separation and activated *in vitro* with anti-CD3/anti-CD28 microbeads in the presence or absence of 5 ng/mL human TGF- β 1 for 4 days. Each day cells were collected and mRNA and protein level expression of PD-1 was quantified. PD-1 mRNA expression was doubled in CD8+ cells stimulated in the presence of TGF- β 1 compared to control CD3/CD28 stimulated cells as early as 24 hours post stimulation. Expression remained consistently elevated compared to control and continued to increase out to 4 days (Fig. 1A). On day 4 cells were analyzed by flow cytometry for PD-1 expression (Fig 1B). Dead cells and doublets were excluded from

analysis. Measured over 5 different human donors, the expression of PD-1 was significantly upregulated by TGF- β 1. Mean fluorescence intensity of PD-1 in CD3/CD28 stimulated cells was 1392 compared to 2507 in TGF- β 1 stimulated cells, representing a 1.8 fold increase in expression.

To confirm that this effect was at least in part due to TGF- β 1 signaling through Smad3, we utilized the small molecule inhibitor SIS3. SIS3 is an indole derivative found to specifically inhibit the phosphorylation of Smad3, while leaving Smad2 function intact. 5 μ M SIS3 was added at the beginning of the experiment to the media and experiment was carried out similarly to those described above with TGF- β 1. On a transcriptional level, SIS3 suppressed PD-1 expression as early as 24 hours after activation (Fig. 1D). This phenotype was similarly seen on the protein level, with expression being suppressed out to 4 days post stimulation. While exogenous TGF- β 1 was not added to the media in these *in vitro* experiments, fetal bovine serum used in making T cell media contains TGF- β 1. The basal signaling of this low level TGF- β 1 was suppressed by SIS3, indicating the dependence of TGF- β 1 mediated PD-1 upregulation on Smad3 signaling.

Expression of CTLA-4 and TIM-3 is downregulated by TGF- β 1

Having confirmed that TGF- β 1 upregulates the expression of PD-1, we hypothesized that it would have similar effect on the expression of other immune checkpoints. To test this hypothesis we activated magnetic bead isolated CD8+ T cells from human PBMC with CD3/CD28 microbeads in the presence or absence of 5ng/mL TGF- β 1. Using the same experimental setup as above, RNA was isolated every 24 hours

and the expression level of CTLA-4 and TIM-3 was determined (Fig. 2A). CTLA-4 expression was reduced by approximately 30% as early as 24 hours post stimulation and reduced expression was maintained throughout the stimulation. TIM-3 mRNA expression was almost entirely suppressed during the first 48 hours when T cells were stimulated in the presence of TGF- β 1. At 72 hours expression began and continued to increase to 96 hours but did not reach the same levels as control stimulated T cells. At the protein level, both CTLA-4 and TIM-3 expression were markedly decreased in the presence of TGF- β 1, compared to stimulation only control (Fig. 2B). Together, these surprising results indicate that PD-1 is regulated differentially by TGF- β 1. While PD-1 expression is upregulated by TGF- β 1, the expression of two other checkpoint molecules that have been thought to be co-regulated with PD-1 was found to be downregulated.

To test the hypothesis that TGF- β 1 mediated downregulation of CTLA-4 and TIM-3 was due to signaling downstream of Smad3, we utilized SIS3 to selectively inhibit the phosphorylation of Smad3, blocking its signaling action. While PD-1 expression on both the RNA and protein level was decreased by activation in the presence of SIS3, the expression of both CTLA-4 and TIM-3 was enhanced (Fig. 2C, 2D). This indicates that TGF- β 1 present at low levels in the serum of the media in the absence of exogenously added TGF- β 1, was sufficient to signal through Smad3 to suppress expression of CTLA-4 and TIM-3 during T cell activation *in vitro*.

Discussion

In this chapter, we have confirmed that published observations demonstrating TGF- β 1 upregulates the expression of PD-1 can be reproduced. A large body of

correlative data in the literature suggests that PD-1 and other immune checkpoints are co-regulated and that the expression of more checkpoint molecule types on the surface of the same T cell indicates the level or depth of exhaustion and dysfunction. Our finding that TGF- β 1 downregulates the expression of CTLA-4 and TIM-3 is contrary to that notion. TGF- β 1 has known immunoregulatory effects that have been well studied. It is involved in the generation and development of peripheral Tregs, inhibition of TCR signaling, inhibition of T cell proliferation. Mice expressing a dominant-negative TGF- β RII had an age-associated wasting disease characterized by multi-organ inflammation and development of autoantibodies⁸⁴. Collectively, multiple lines of evidence establish the importance of TGF- β 1 in maintaining immune homeostasis and preventing autoimmunity. In this context, one could expect if TGF- β 1 upregulates the expression of PD-1, it would have similar effect on other immune checkpoints known to be important for the maintenance of self-tolerance and prevention of autoimmunity.

Smad3 has been shown to directly bind the PD-1 promoter, leading to transcription⁵¹. Furthermore, TGF- β 1 has been shown to lead to the degradation of SATB1 through an unidentified mechanism. SATB1 physically interacts with and recruits the NuRD complex, a component of the histone deacetylase machinery. Under physiological conditions, TCR stimulations leads to an increase in SATB1 expression, which in turn recruits the NuRD complex to the PD-1 promoter, thereby limiting its expression. In the presence of TGF- β 1, SATB1 is degraded, leading to enhanced expression of PD-1 and higher Smad3 occupancy of the PD-1 promoter⁵². This mechanism cannot explain why TGF- β 1 signaling downstream of Smad3 leads to the

reduction in expression of CTLA-4 and TIM-3. Smad3 has been shown to have a relatively low affinity for DNA, despite the presence of a DNA binding domain. Thus, its recruitment to binding sites throughout the genome is dependent on binding partners that help recruit it. These binding partners in turn dictate the activity of Smad3. It is possible that different binding partners are responsible for the recruitment of Smad3 to CTLA-4 and TIM-3 promoters, leading to transcriptional repression. It is also possible that Smad3 is not being directly recruited to the promoters of these genes and is responsible for the degradation of a positive regulatory factor important for their expression, leading to loss of expression. The co-regulation of CTLA-4 and TIM-3 suggests a similar and potentially chromatin level program responsible for their shared regulation. In summary these data indicate that TGF- β 1 mediated Smad3 signaling differentially regulates the expression of PD-1 from CTLA-4 and TIM-3.

Materials and Methods

Human T cells

The Johns Hopkins HATS clinic provided leukaphoresis product and human PBMC were isolated by Ficoll gradient. PBMC were stored in liquid nitrogen and thawed prior to use. Human T cells were isolated from bulk PBMC using CD8+ T cell isolation kit (Miltenyi Biotech).

In vitro Activation of T cells

Human CD8+ T cells were activated *in vitro* with anti-human CD3/CD28 microbeads at a ratio of 1:1 per manufacturer instructions (Invitrogen). Human TGF- β 1 was purchased

(PeproTech) as a lyophilized product and suspended in complete T cell media. T cells were activated in the presence or absence of 5 ng/mL of TGF- β 1. For the experiments examining the inhibition of Smad3 signaling the inhibitor SIS3 was used at a concentration of 5 μ M (Sigma). SIS3 was dissolved in DMSO at a 10 mM stock concentration and dissolved in T cell culture media to working concentration. T cell media was made as follows: RPMI 1640 (90%), Fetal Bovine Serum (10%), Penicillin-Streptomycin (100 U/mL), L-glutamine (4 mM), HEPES (1M), Minimum essential amino acids, 50 μ M beta-mercaptoethanol.

qRT-PCR

Cells were collected from culture dishes, washed once in PBS, and lysed in RLT buffer (Qiagen). RNA was extracted using the Qiagen RNeasy kit per the manufacturer's instruction. Total RNA was converted to cDNA using the superscript II reverse transcription enzyme. Primer probe sets were purchased from Integrated DNA Technologies and quantitative PCR was carried out using LightCycler 480 master mix on a LightCycler 480 instrument (Roche).

Flow Cytometry

Samples were stained in FACS buffer (PBS containing 1% BSA) at room temperature for 30 minutes. The following antibodies were used and purchased from BD Biosciences: PD-1(EH12.1), CD4(OKT4), CD8(RPA-T8), CD3(UCHT1). Human anti-TIM-3 was purchased from R&D (344823). Anti-CTLA-4 was purchased from Biolegend (L3D10). CTLA-4 staining was carried out on the cell surface for 30 mins followed by sample fixation and

permeabilization with the EBioscience FoxP3 transcription factor kit and subsequently stained intracellularly. Samples were acquired on a BD LSR II.

Statistics

For comparison between treatment groups, unpaired t-test was used. Statistical analysis was carried out using GraphPad Prism v 7.0.

Figure 1

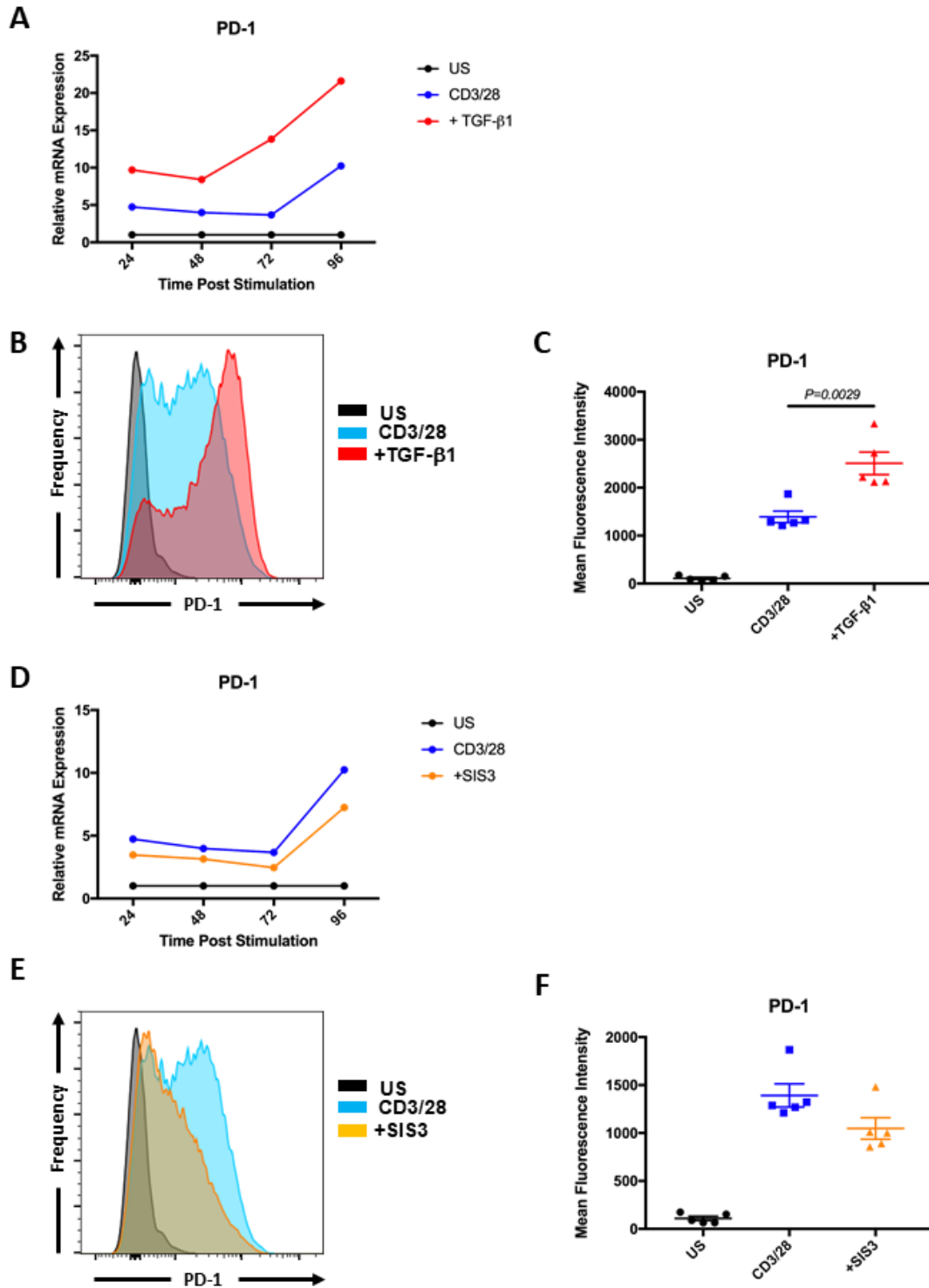
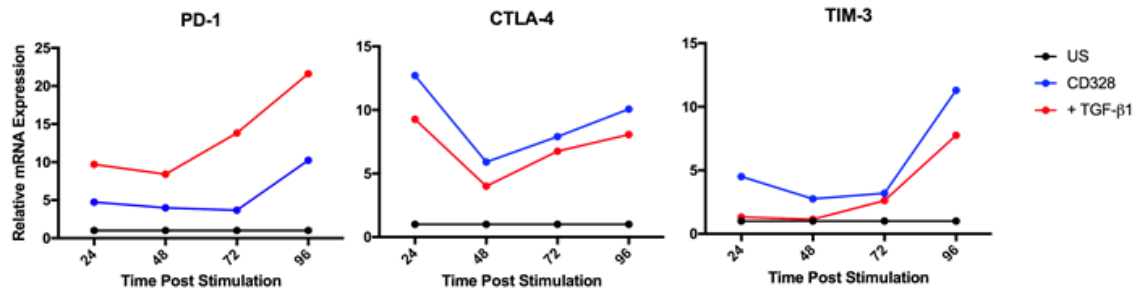


Figure 1: PD-1 expression is upregulated by TGF- β 1 in a Smad3 dependent manner.

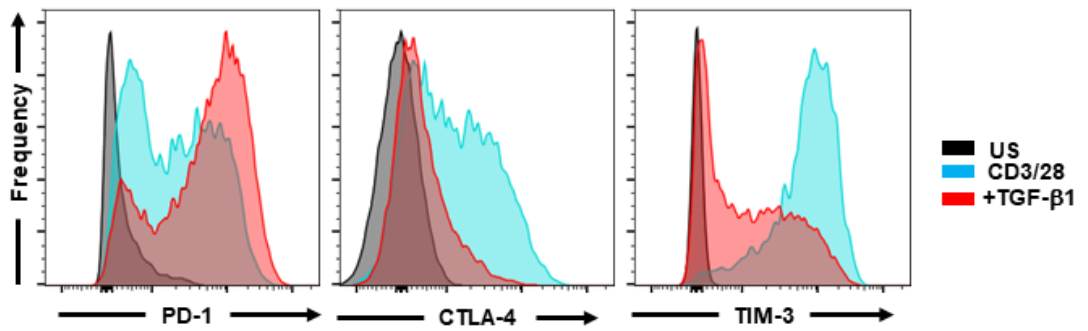
Human CD8⁺ T cells were activated with anti-CD3/CD28 microbeads in the presence of 5 ng/mL TGF- β 1 and analyzed for expression of PD-1 mRNA by qPCR (A) or PD-1 protein expression on the cell surface by flow cytometry (B & C). T cells were activated with anti-CD3/CD28 microbeads in the presence of 5 μ M SIS3 analyzed for expression of PD-1 mRNA by qPCR (D) or PD-1 protein expression on the cell surface by flow cytometry (E & F).

Figure 2

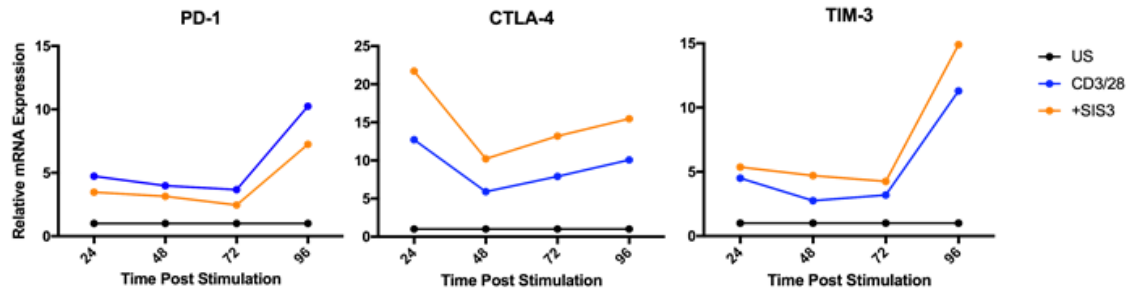
A



B



C



D

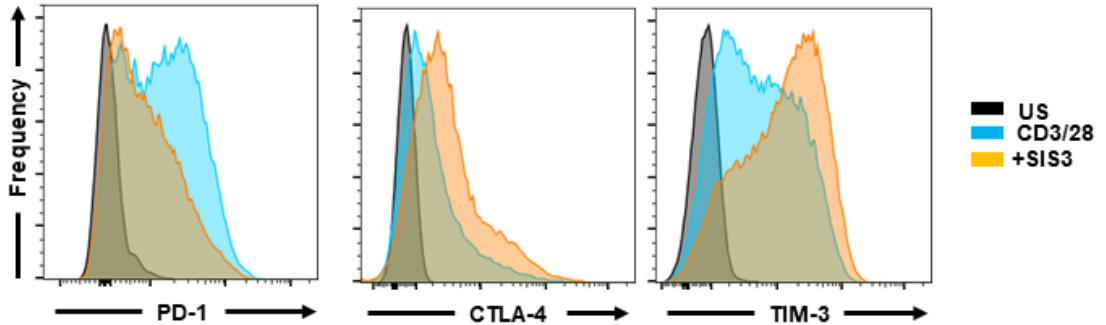


Figure 2: CTLA-4 and TIM-3 expression is downregulated by TGF- β 1

A) Human CD8⁺ T cells were activated with anti-CD3/CD28 microbeads and expression of PD-1, CTLA-4, and TIM-3 mRNA was measured by qRT-PCR. B) CD8⁺ T cells activated as in (A) were stained for expression of CTLA-4 and TIM-3 and analyzed by flow cytometry. C) Human CD8⁺ T cells were activated as in (A) in the presence or absence of 5 μ M SIS3 and PD-1, CTLA-4, and TIM-3 mRNA was measured by qRT-PCR. D) CD8⁺ T cells activated as in (C) were stained for expression of CTLA-4 and TIM-3 and analyzed by flow cytometry.

CHAPTER 2

Histone Acetylation Regulates Immune Checkpoint Expression

Introduction

The lifespan of a T cell is marked by large, coordinated changes in gene expression. In this regard, T cells are an excellent model system for the study of genetic and epigenetic changes associated with cellular differentiation and the plasticity of cell identity and its maintenance. Naïve T cells are quiescent and express genes important for the maintenance of long-lived cells. Within hours after activation, the expression of genes involved in cell cycle control and proliferation, and those involved in glycolytic metabolism are rapidly induced⁸⁵. Importantly, the expression of a large number of genes is downregulated during activation, indicating that programs of transcriptional repression are implemented simultaneously with those promoting transcriptional activation. These gene expression pattern changes are accompanied by epigenetic modifications to the underlying chromatin. Epigenetic modifications such as methylation of DNA and post-translational modifications to the histone tails in the form of methylation and acetylation allow for change in the accessibility of the chromatin to transcriptional machinery, ultimately allowing for either gene expression or silencing.

Studies of epigenetic changes in T cells during differentiation of naïve to effector to memory T cells have been carried out; however, relatively little is known about the epigenetic changes that accompany transition to the T cell exhausted state^{53,86–90}.

Several recent studies have attempted to elucidate some of the mechanisms at involved in both the chronic viral infection LCMV model and tumor models^{72–74,91–93}. Utilizing the Assay for Transposase-Accessible Chromatin using sequencing (ATAC-seq), these studies found that a relatively small number of chromatin accessible regions are specific only to

exhausted T cells and a majority are shared with effector T cells. Furthermore, blocking the PD-1/PD-L1 axis with antibodies did not lead to a change in the chromatin accessibility profiles of the exhausted T cells. Although blocking the PD-1/PD-L1 axis was accompanied by T cell proliferation and the production of cytokines and effector molecules, these T cells reverted to the exhausted phenotype once antibody administration was stopped. The lack of epigenetic change induced by PD-1 blockade likely represents the lack of change in the chromatin level exhaustion program. Thus, when antibody administration was stopped, T cells “remembered” that they were exhausted. Importantly, in these studies chromatin accessibility was assayed; however, chromatin marks were not interrogated. Therefore, it is unclear which set of epigenetic marks are involved in this programming or if they can be targeted pharmacologically.

In this chapter, we utilize chromatin immunoprecipitation followed by sequencing (ChIP-seq) to understand the role of histone acetylation in regulating the expression of checkpoint molecules. We next examine how the addition of TGF- β 1 differentially acetylates the genome compared to stimulation alone and hypothesize that this may underlie the differences in how TGF- β 1 regulates the expression of checkpoint molecules. Due to the involvement of histone acetylation, we conduct a limited drug screen examining pharmacological inhibitors of components of the histone acetylation machinery and find that class I HDAC inhibitors can selectively target the expression of genes suppressed by TGF- β 1. We show that combining TGF- β 1 signaling inhibitor and class I HDAC inhibitor additively promote the expression of checkpoints

that were downregulated by TGF- β 1, thereby suggesting that these two pathways cooperate in the regulation of immune checkpoints.

Results

To examine the role of histone acetylation in the control of CD8+ T cell checkpoint molecule expression, we activated human CD8+ T cells with anti-CD3/anti-CD28 microbeads for 96 hours. CHIP-seq for histone H3 pan-acetylation was carried out. This detects histone acetylation at H3K9 and H3K27 both of which are strongly associated with active transcriptional start sites and enhancers. We compared the level of histone H3 acetylation in annotated gene promoters and body between unstimulated and stimulated CD8+ T cells in a statistical manner using the CSAW algorithm, a software package for differential binding analysis of ChIP-seq data by dividing the genome into windows, then comparing the read enrichment within these windows between samples.

32,868 differentially regulated regions were identified with increased histone H3 acetylation in stimulated cells compared to unstimulated. Another 28,459 differentially regulated regions were identified which lost acetylation during T cell activation. Figure 1 demonstrates a number of the most upregulated genes during T cell activation. Genes with known checkpoint function have been shown in red and other genes in blue.

Among the genes that were enriched for histone acetylation are those involved in T cell activation such as IRF4, MIR21, IL2RA (high-affinity subunit of the IL2 receptor), and CISH. Interestingly a majority of immune checkpoints have significantly increased histone acetylation during activation. TNFRSF18 (encoding GITR), TNFRSF4 (encoding

OX40), CTLA4, TNFRSF9 (encoding 4-1BB), PDCD1 (encoding PD-1), LAG3, and HAVCR2 (encoding TIM-3) were all significantly enhanced during activation. This increase in histone acetylation fits with the known increase in their expression during activation. A table of the top 50 up and downregulated acetylated regions is included in this chapter (Table 1).

Histone acetylation changes during activation were mostly confined to the promoter and transcriptional start site, though in some genes changes were seen in intronic regions and exons downstream of the promoter (Fig. 4). Sharp peaks of acetylation can be seen at the transcriptional start site, which is characteristic of histone acetylation marks, particularly H3K27Ac which marks active and poised promoters.

Large changes in acetylation during activation led us to hypothesize that acetylation may control expression of immune checkpoints and this expression could be controlled pharmacologically. To test this hypothesis, we conducted a limited drug screen examining the effects of inhibitors targeting various components of the histone acetylation machinery (Fig. 5). Human CD8⁺ T cells were isolated from PBMC by magnetic separation and activated with anti-CD3/anti-CD28 microbeads for 96 hours. Expression of PD-1 and TIM-3 was assessed by flow cytometry. We chose these two inhibitory molecules due to the difference in their regulation that was witnessed when exposed to TGF- β 1. We reasoned that the possibility might exist that histone acetylation modifiers may have a differential effect on the expression of these immune checkpoints. As had been seen previously, TGF- β 1 increased the expression of PD-1 while reducing the expression of TIM-3, and inhibition of Smad3 signaling downstream of TGF- β 1 with

the small molecule inhibitor SIS3 led to a reduction in PD-1 expression and increase in TIM-3 expression. The selective p300 histone acetyltransferase inhibitor C646 (HATi) was used to inhibit the deposition of acetylation marks. This did not have a significant effect on the checkpoint expression. Vorinostat, a pan histone deacetylase inhibitor (HDACi), givinostat, a broad spectrum HDACi, and ACY1215, a selective HDAC6 inhibitor did not affect the expression of PD-1 or TIM-3 compared to control. Entinostat, a selective inhibitor of the class I HDAC family, encompassing members HDAC 1, 2, 3, and 8, increased the expression of TIM-3 but not PD-1. Further confirming this effect, mocetinostat, another selective class I HDAC inhibitor also increased the expression of TIM-3 but not PD-1.

Class I HDAC inhibition increased the expression of TIM-3 in our limited drug screen without affecting expression of PD-1. This led us to hypothesize that CD8⁺ T cells stimulated in the presence of TGF- β 1 or Class I HDAC inhibitor will have different chromatin landscapes in the regions surrounding the regulatory regions of immune checkpoint genes. To test this hypothesis, we performed ChIP-seq on human CD8⁺ T cells that were stimulated in the presence of either 5 ng/mL TGF- β 1 or 100 nM Entinostat for 4 days (Fig 6). Indeed, While the TGF- β 1 condition promoted the acetylation of PD-1 associated regulatory regions, it reduced the acetylation of regulatory regions associated with LAG-3, TIM-3, and CTLA-4. Entinostat promoted the acetylation of regulatory regions associated with LAG-3, TIM-3, and CTLA-4, but not PD-1. This result indicates that differential epigenetic regulation of these regions takes place through the actions of both Smad3 and class I HDACs.

The involvement of both Smad3 and class I HDAC in differential epigenetic remodeling of immune checkpoint gene regulatory regions led us to hypothesize that they might be part of the same pathway, regulating checkpoint chromatin landscapes. To test this hypothesis pharmacologically, human CD8+ T cells were activated *in vitro* for 96 hours using anti-CD3/anti-CD28 microbeads in the presence of TGF- β 1, SIS3, entinostat, or the combination of SIS3 and entinostat. Indeed, the combination of SIS3 and entinostat additively enhanced the protein level expression of TIM-3 indicating that Smad3 and class I HDAC likely function cooperatively to regulate the expression of TIM-3 (Fig. 7). We carried out ChIP-seq on CD8+ T cells activated in the presence of the combination of entinostat and SIS3 to test the hypothesis that this will lead to the largest fold change difference in acetylation pattern at PD-1 compared to the regulatory regions of CTLA-4, LAG-3, and TIM-3. In the case of CTLA-4 and TIM-3 this proved to be true, leading to the largest fold change difference (Fig. 8). LAG-3 however did not follow the same pattern as we had seen previously. This may be because LAG-3 did not display as strong of a change in its acetylation level as CTLA-4 and TIM-3 in response to either TGF- β 1 or HDAC inhibition suggesting that it might be regulated by a distinct mechanism.

Discussion

Most immune checkpoints are also considered activation markers. Their expression is reliably increased during T cell activation with different kinetics. PD-1 expression can be detected as early as 1-day post activation, with LAG-3 and TIM-3

expression becoming detectable at day 2 onwards. During *in vitro* activation, the expression of these markers peaks at day 5-8 and gradually declines after. These observations would suggest that the genetic and epigenetic regulation of checkpoint expression is governed by a shared, TCR signaling dependent program. Indeed, TCR signaling is an important regulator of checkpoint expression leading to the downstream induction of NFATc1 which has been linked to PD-1 expression control. Besides NFATc1, control of PD-1 expression has been linked to the transcription factors Tbet, Eomes, and FoxO1. Tbet, which is a master regulator of Th1 type T cell differentiation has been linked as a repressor of PD-1 expression. In contrast, FoxO1 has been shown to maintain PD-1 expression during chronic viral infection. The role of individual transcription factors in the control of expression of other immune checkpoints is less well studied. Tbet and NFIL3 have been reported to promote the expression of TIM-3^{94,95}. This is supported by studies that report IL-12, an inducer of Tbet expression, to strongly promote TIM-3 expression. An NFAT binding site has been reported in the promoter of CTLA-4, and its loss results in loss of CTLA-4 expression⁹⁶. Thus, the notion that a similar genetic program involving shared transcription factors co-regulates checkpoint expression on T cells is not without basis.

Transcription factors aid in the recruitment of other molecular components required for gene expression modification. However, most transcription factors, with exception of pioneer factors, cannot access the underlying DNA without the chromatin becoming accessible first. For this to occur, epigenetic alterations take place, facilitating the opening or closing of chromatin. Thus, cooperation between epigenetic marks and

transcription factors facilitates gene expression or repression. In this chapter, we examined the patterns of histone acetylation genome-wide in CD8⁺ T cells activated under different conditions. Just as the expression of multiple checkpoints is induced by T cell activation, we saw similar induction of histone acetylation in the proximal promoters of these genes and at transcriptional start sites. In this regard, checkpoints were regulated similarly in CD8⁺ T cells.

We demonstrated in the previous chapter that TGF- β 1 upregulates the expression of PD-1 but downregulates the expression of CTLA-4 and TIM-3, and that this was dependent on Smad3 signaling. In T cells, Smad3 has been shown to be involved in epigenetic regulation of PD-1 through action on the chromatin remodeler Satb1^{52,97}. Satb1 recruits the NuRD HDAC complex to the PD-1 promoter, leading to loss of PD-1 expression. TGF- β 1 exposure leads to the degradation of Satb1, loss of NuRD recruitment and increased PD-1 expression. Interestingly, experiments examining the expression of CTLA-4, LAG-3, and TIM-3 in Satb1 knockout OT-1 T cells showed loss of LAG-3 expression and unchanged CTLA-4 and TIM-3 expression. This indirectly supports our finding that TGF- β 1 differentially affects T cell checkpoint expression in a manner dependent on the action of HDAC enzymes.

Surprisingly, we found that class I HDAC inhibition alone was sufficient to increase TIM-3 expression during acute activation, without affecting the expression of PD-1. Pan HDAC inhibitors such as vorinostat and givinostat did not affect the expression, nor did inhibition of HDAC6. This result is slightly confusing in that the pan-HDAC inhibitors also inhibit the activity of class I HDACs. However, this did not lead to a

change in TIM-3 expression. One potential explanation is that the inhibition of other HDAC enzymes such as the class IIa (HDAC 4, 5, 7, and 9), class IIb (HDAC 6, and 10) and class IV (HDAC 11) members by the pan HDAC inhibitor leads to enhanced expression of negative regulatory factors that can counteract the effect of class I HDAC inhibition. This could be explored by comparing the gene expression profiles of pan-HDAC inhibitor and class I HDAC inhibitor treated T cells and may be informative for understanding the negative regulators of checkpoint expression in T cells.

Given the enhanced expression of immune checkpoints such as CTLA-4 and TIM-3 by class I specific HDAC inhibitors, we sought to compare the chromatin landscape in this condition with that induced by TGF- β 1, which had downregulated their expression. We found acetylation of the PD-1 promoter went up with TGF- β 1 but not the promoters of TIM-3 and CTLA-4. Furthermore, we found that class I HDAC inhibition increased the acetylation of the CTLA-4 and TIM-3 promoters but not PD-1. From this we concluded that TGF- β 1 and class I HDAC inhibition differentially program the promoters of immune checkpoint genes. Because the effect of HDAC inhibition led to an increase in the expression of genes that were downregulated by TGF- β 1, we hypothesized that combining entinostat with SIS3 would lead to an even larger upregulation of immune checkpoints. We hypothesized that these effects would be additive, suggesting that both Smad3 and class I HDACs are functioning within the same pathway. However, synergistic effects would suggest that these are two different, yet cooperative pathways involved in checkpoint expression control. To test this hypothesis, we combined SIS3 and entinostat and found that the effects were additive in increasing the expression of

TIM-3. At the chromatin level, this correlated with the largest changes that we had seen in promoter acetylation. Both TIM-3 and CTLA-4 exhibited larger fold change differences in acetylation in comparison to the TGF- β 1 condition when SIS3 was combined with entinostat, demonstrating that Smad3 signaling and class I HDACs are cooperating in the regulation of at least a subset of immune checkpoint genes. Whether this cooperation is a direct physical interaction between Smad3 and class I HDAC or a pathway level interaction whereby one regulates the activity of the other is unknown and a question that can be pursued in future studies.

In summary, in this chapter we have demonstrated that histone acetylation is increased in the promoters of immune checkpoint genes during T cell activation. This is generally a uniform phenomenon across all immune checkpoints and correlates with their increased expression. However, TGF- β 1 differentially regulates this process. It increases the expression and acetylation of PD-1 and decreases the expression of TIM-3 and CTLA-4. This is dependent on the actions of Smad3 in cooperation with the class I HDAC family of deacetylase enzymes. Inhibition of either Smad3 or class I HDAC activity can increase the expression of TIM-3 and CTLA-4, and the combination of these two inhibitors additively increases the expression of CTLA-4 and TIM-3.

Materials and Methods

Human T cells

The Johns Hopkins HATS clinic provided leukaphoresis product and human PBMC were isolated by Ficoll gradient. PBMC were stored in liquid nitrogen and thawed prior to use.

Human T cells were isolated from bulk PBMC using CD8+ T cell isolation kit (Miltenyi Biotech).

In vitro Activation of T cells

Human CD8+ T cells were activated *in vitro* with anti-human CD3/CD28 microbeads at a ratio of 1:1 per manufacturer instructions (Invitrogen). Human TGF- β 1 was purchased (Peprotech) as a lyophilized product and suspended in complete T cell media. T cells were activated in the presence or absence of 5 ng/mL of TGF- β 1. For the experiments examining the inhibition of Smad3 signaling the inhibitor SIS3 was used at a concentration of 5 μ M (Sigma). SIS3 was dissolved in DMSO at a 10 mM stock concentration and dissolved in T cell culture media to working concentration. T cell media was made as follows: RPMI 1640 (90%), Fetal Bovine Serum (10%), Penicillin-Streptomycin (100 U/mL), L-glutamine (4 mM), HEPES (1M), Minimum essential amino acids, 50 μ M beta-mercaptoethanol.

Flow Cytometry

Samples were stained in FACS buffer (PBS containing 1% BSA) at room temperature for 30 minutes. The following antibodies were used and purchased from BD Biosciences: PD-1(EH12.1), CD4(OKT4), CD8(RPA-T8), CD3(UCHT1). Human anti-TIM-3 was purchased from R&D (344823). Anti-CTLA-4 was purchased from Biolegend (L3D10). CTLA-4 staining was carried out on the cell surface for 30 mins followed by sample fixation and permeabilization with the EBioscience FoxP3 transcription factor kit and subsequently stained intracellularly. Samples were acquired on a BD LSR II.

ChIP-Seq

Samples for CHIP-seq were fixed using 1-2% formaldehyde and cell pellets were snap frozen and stored at -80°C prior to CHIP. Samples were then processed using the Diagenode iDeal CHIP Seq kit for Histones according to the manufacturer protocol. CHIP-seq was performed by Diagenode in Belgium. Samples were sheared for 12 cycles of 30 seconds on and 30 seconds off by sonication using a Bioruptor Pico. CHIP was performed with 2 µg of anti-panacetyl-Histone H3 antibody (EMD Milipore). Sequencing was performed on an Illumina HiSeq 3000. Reads were mapped to the human genome version hg38. CSAW was used to carryout differential binding analysis. Graphs were generated in R.

Figure 3

**H3KAc ChIP-Seq
Unstimulated vs STIM**

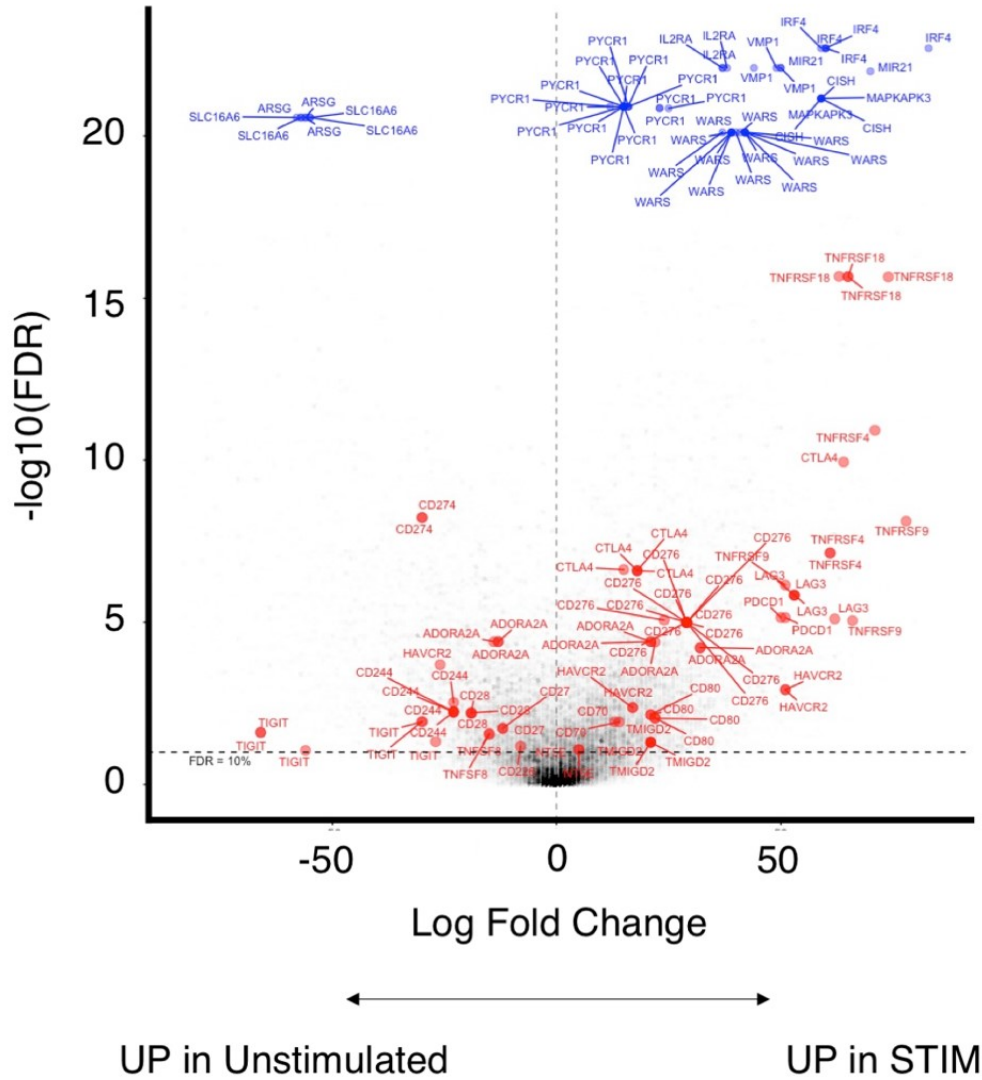


Figure 3: Histone acetylation is increased at the promoters of immune checkpoints during T cell activation

T cells activated *in vitro* demonstrate increased acetylation of immune checkpoint genes (in red) as well as other genes associated with T cell activation (blue).

Figure 4

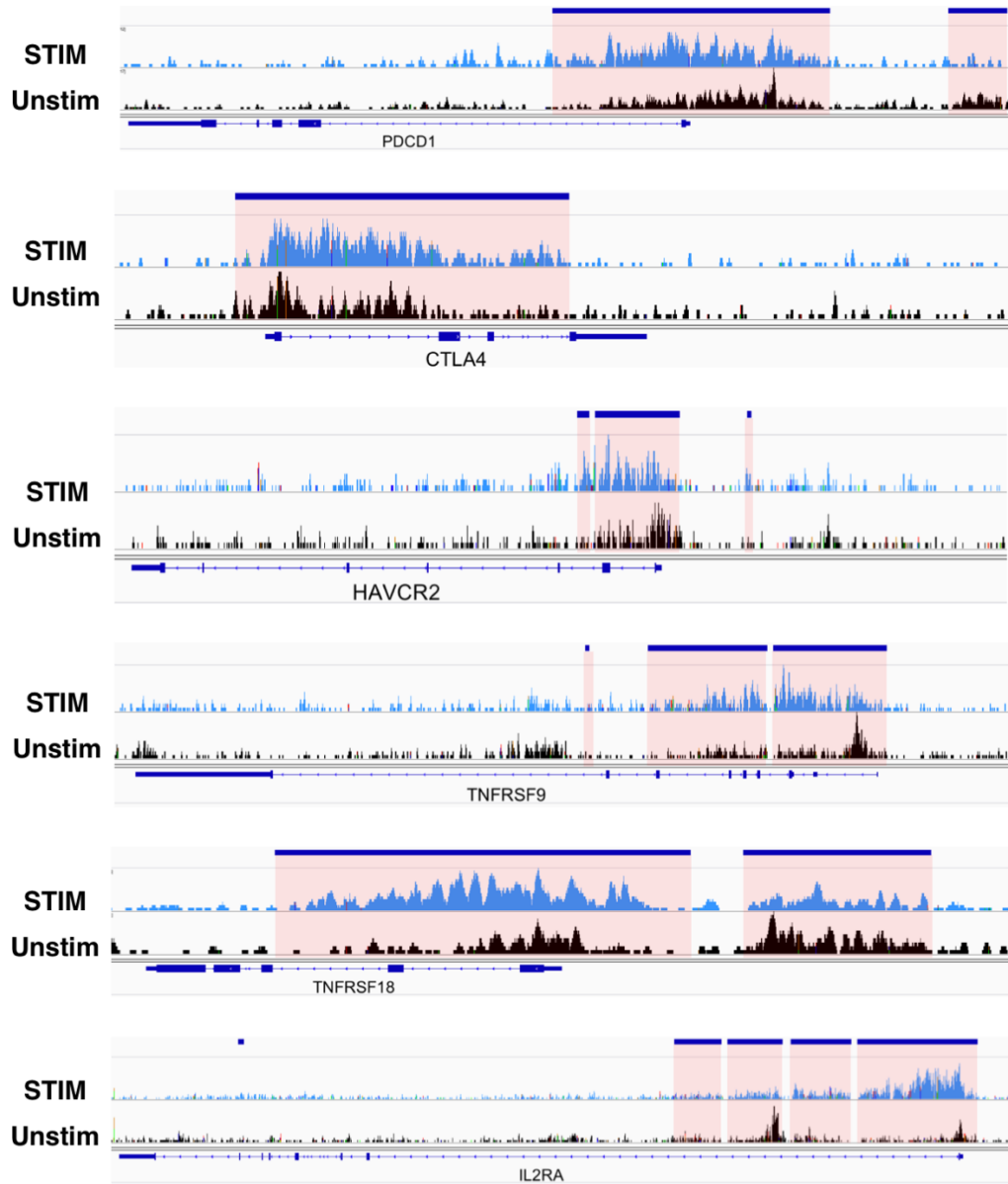


Figure 4: Selected acetylation tracks from immune checkpoint and T cell activation genes

Genes are shown with the unstimulated condition in black on the bottom and stimulated on the top. Peaks show areas of acetylation enrichment detected by sequencing. Blue lines and pink boxes mark areas detected as being differentially enriched for histone H3 acetylation by CSAW software statistical analysis.

Table 1

Increased Acetylation in Stimulated CD8 T cells					Decreased Acetylation in Stimulated CD8 T cells						
Rank	Gene	logFC.up	logFC.down	PValue	FDR	Rank	Gene	logFC.up	logFC.down	PValue	FDR
1	VMP1	42	2	5.00E-46	1.29E-41	1	PIK3CD	0	43	4.28E-45	6.57E-41
2	MIR21	48	2	5.60E-46	1.29E-41	2	KLF2	0	32	3.03E-42	3.50E-38
3	IRF4	64	0	7.18E-39	2.24E-35	3	ARSG	0	55	4.99E-41	3.18E-37
4	IL2RA	35	0	1.61E-37	4.35E-34	4	SLC16A6	0	57	5.18E-41	3.18E-37
5	CISH	65	8	5.78E-34	7.30E-31	5	LINC00861	0	33	1.23E-39	5.97E-36
6	MAPKAPK3	65	8	5.78E-34	7.30E-31	6	ARRDC3-AS1	5	59	3.64E-39	1.60E-35
7	PYCR1	16	0	6.55E-34	7.96E-31	7	ARRDC3	0	81	3.98E-39	1.60E-35
8	RNF19A	83	0	1.79E-32	1.83E-29	8	ATXN7	0	37	5.11E-39	1.96E-35
9	WARS	35	3	7.24E-32	5.95E-29	9	RASGRP2	0	38	1.86E-37	4.75E-34
10	WDR25	59	3	1.06E-31	7.31E-29	10	RIPOR2	0	51	2.19E-35	3.54E-32
11	LINC00963	57	4	3.02E-30	1.68E-27	11	FGD3	0	35	5.86E-35	9.31E-32
12	MKI67	24	2	3.55E-30	1.89E-27	12	LOC729683	0	82	1.12E-34	1.63E-31
13	ODF3B	27	0	3.69E-30	1.91E-27	13	LIMD2	0	81	1.10E-34	1.63E-31
14	RAD54L	30	0	3.77E-30	1.91E-27	14	IL16	0	79	2.02E-34	2.74E-31
15	BIRC5	20	0	4.83E-30	2.30E-27	15	MIR150	0	29	1.10E-32	1.14E-29
16	TYMP	77	0	1.05E-29	4.41E-27	16	PIK3IP1	0	52	1.95E-32	1.91E-29
17	PKMYT1	24	1	9.90E-29	3.74E-26	17	PIK3IP1-AS1	0	83	3.12E-32	2.96E-29
18	CSF1	35	0	1.28E-28	4.83E-26	18	PSMB8-AS1	0	44	5.65E-32	4.84E-29
19	ATF3	58	0	1.35E-28	5.05E-26	19	PSMB8	0	43	5.65E-32	4.84E-29
20	MCM2	27	7	6.83E-28	2.26E-25	20	PSMB9	0	45	5.65E-32	4.84E-29
21	TPRA1	60	7	1.29E-27	4.08E-25	21	EVL	0	56	3.07E-31	2.04E-28
22	MZB1	75	0	3.57E-27	1.04E-24	22	TC2N	0	51	1.22E-30	6.85E-28
23	PFKFB4	30	2	7.90E-27	2.27E-24	23	CCM2	0	26	3.55E-30	1.89E-27
24	DCAF16	50	3	1.09E-26	3.07E-24	24	LINC00528	0	39	1.79E-29	7.25E-27
25	NCAPG	35	9	1.20E-26	3.33E-24	25	BID	0	40	1.84E-29	7.25E-27
26	VEGFA	57	0	2.66E-26	7.29E-24	26	UMODL1	0	49	6.07E-29	2.30E-26
27	LONP1	13	17	6.90E-26	1.83E-23	27	IL7R	1	78	3.06E-28	1.04E-25
28	CDC25A	30	1	9.55E-26	2.47E-23	28	ISG20	0	39	6.38E-28	2.16E-25
29	MASTL	28	0	9.94E-26	2.55E-23	29	SETD1B	0	79	6.87E-28	2.26E-25
30	FOS	50	0	1.06E-25	2.70E-23	30	LINC01089	0	79	6.87E-28	2.26E-25
31	YME1L1	47	1	1.11E-25	2.80E-23	31	RHOF	0	78	6.87E-28	2.26E-25
32	CATSPERD	45	17	1.29E-25	3.12E-23	32	JADE2	1	27	1.69E-27	5.28E-25
33	MIR155HG	43	1	1.55E-25	3.74E-23	33	FCMR	0	77	2.49E-27	7.57E-25
34	ZBTB32	49	0	3.15E-25	7.53E-23	34	PPP2R5C	0	83	3.26E-27	9.71E-25
35	MIR6865	33	0	1.16E-24	2.74E-22	35	GIMAP7	0	40	2.56E-26	7.07E-24
36	MIR6864	41	0	1.42E-24	3.34E-22	36	RPRD2	0	39	2.62E-26	7.21E-24
37	CAMTA2	46	0	1.64E-24	3.85E-22	37	TRAF3IP3	0	36	3.82E-26	1.03E-23
38	SPAG7	38	8	2.51E-24	5.78E-22	38	MIR650	0	35	4.01E-26	1.08E-23
39	SNX9	31	3	4.72E-24	1.06E-21	39	TXNIP	0	62	2.93E-25	7.02E-23
40	SCD	48	0	7.31E-24	1.60E-21	40	CAMK2D	0	45	1.48E-24	3.47E-22
41	MIR210HG	24	2	1.26E-23	2.63E-21	41	SORL1	0	76	3.13E-24	7.07E-22
42	LIF	39	0	1.26E-23	2.63E-21	42	DBP	0	46	5.09E-24	1.15E-21
43	ZFPL1	34	0	1.40E-23	2.89E-21	43	CFLAR	0	30	5.92E-24	1.32E-21
44	MIR210	30	2	1.41E-23	2.90E-21	44	CORO1A	0	28	8.01E-24	1.75E-21
45	CDCA5	37	0	1.49E-23	2.98E-21	45	CD96	0	37	1.03E-23	2.19E-21
46	TNFRSF18	62	0	2.39E-23	4.60E-21	46	LDB1	0	44	1.49E-23	2.98E-21
47	PLK1	20	2	3.35E-23	6.39E-21	47	RNF44	0	42	1.62E-23	3.19E-21
48	ADM2	26	0	3.76E-23	7.13E-21	48	BCL9L	0	83	2.74E-23	5.23E-21
49	NFIL3	56	0	4.06E-23	7.66E-21	49	SH2B3	0	29	1.22E-22	2.25E-20
50	UBE2C	22	5	6.55E-23	1.22E-20	50	CDC37L1	0	29	1.33E-22	2.43E-20

Table 1: Top 50 genes associated with increased or decreased promoter acetylation

Figure 5

Effect of TGF- β 1 and HDACi on Checkpoint Expression

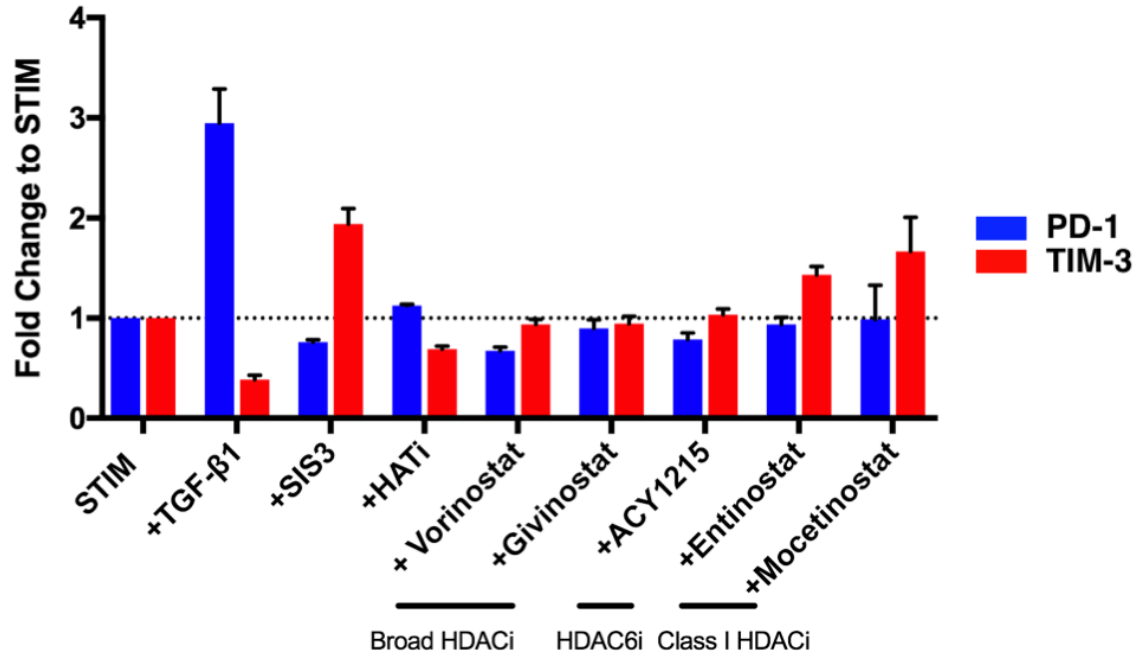


Figure 5: Drug screen reveals class I specific HDAC inhibitors enhance the expression of TIM-3

Human CD8+ T cells were activated with anti-CD3/anti-CD28 microbeads *in vitro* for 96 hours. Expression of TIM-3 was profiled by flow cytometry and mean fluorescence intensity was normalized to the control simulation only condition.

Figure 6

**H3KAc ChIP-Seq
TGF β vs Entinostat**

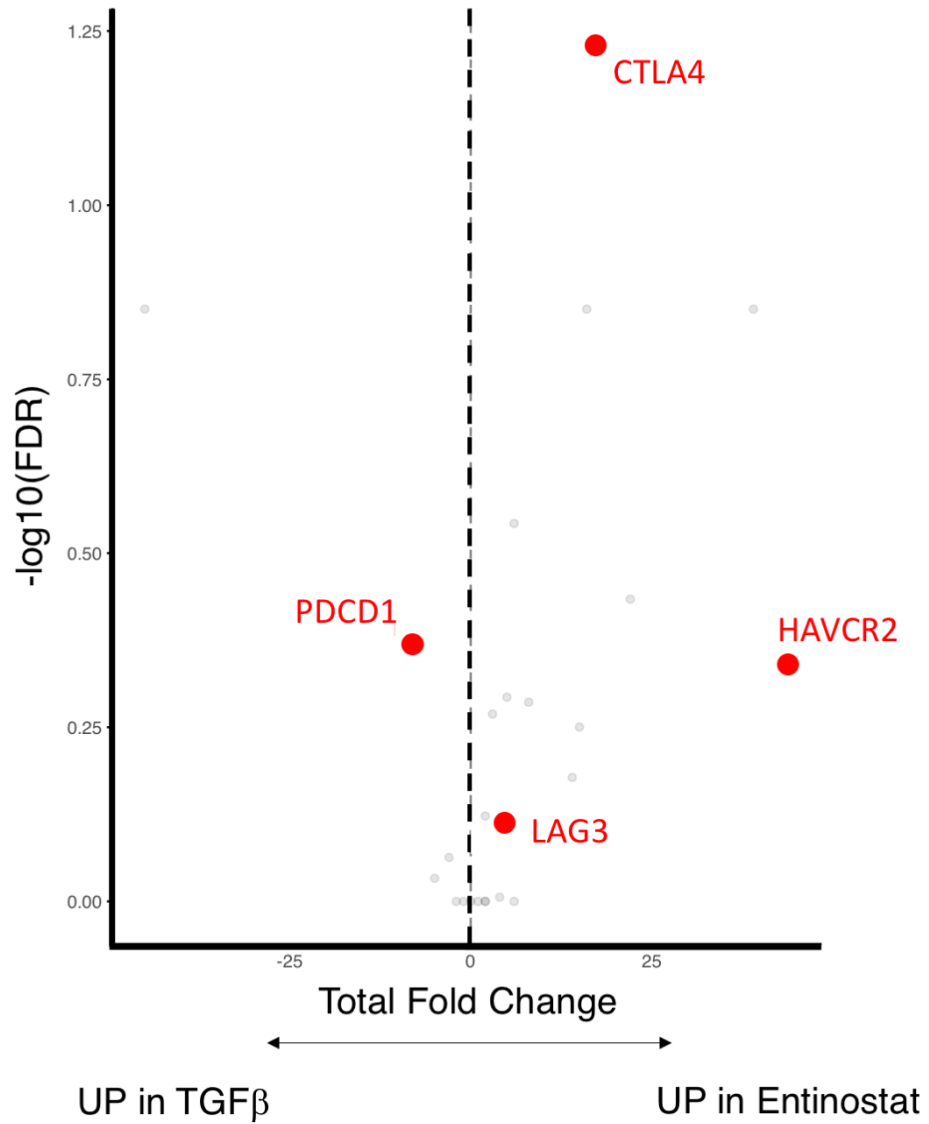
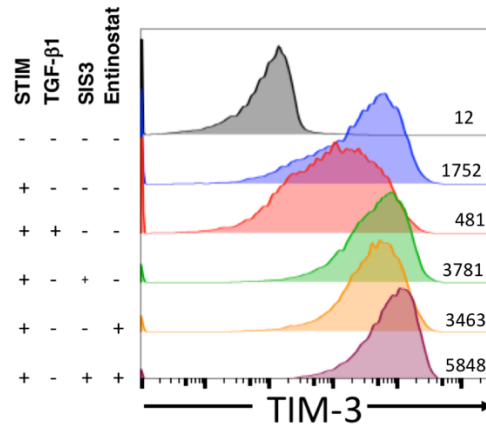


Figure 6: TGF- β 1 and Entinostat differentially affect the acetylation of immune checkpoint promoters

T cells activated *in vitro* demonstrate differential effects of TGF- β 1 and entinostat on promoter acetylation at PD-1 and CTLA-4, LAG-3, and TIM-3.

Figure 7

A



B

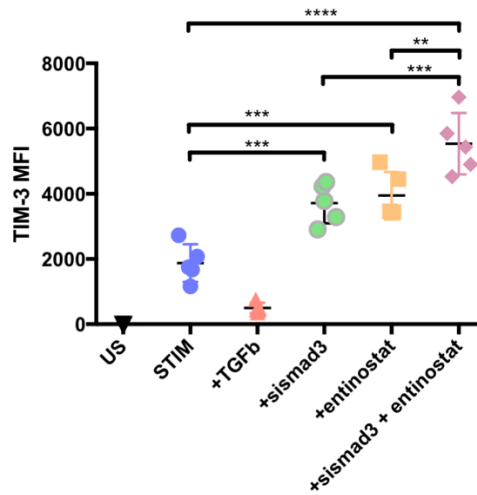


Figure 7: Combining SIS3 and entinostat additively enhances expression of TIM-3

A) Human CD8+ T cells were activated for 96 hours with anti-CD3/anti-CD28 microbeads *in vitro* and TIM-3 expression was measured by flow cytometry. T cells were activated in media, presence of TGF-β1, SIS3, entinostat, or combination of SIS3 and entinostat.

B) Summary of experimental results repeated with 5 different human donors.

Figure 8

**H3KAc ChIP-Seq
TGF- β 1 vs ENTISIS3**

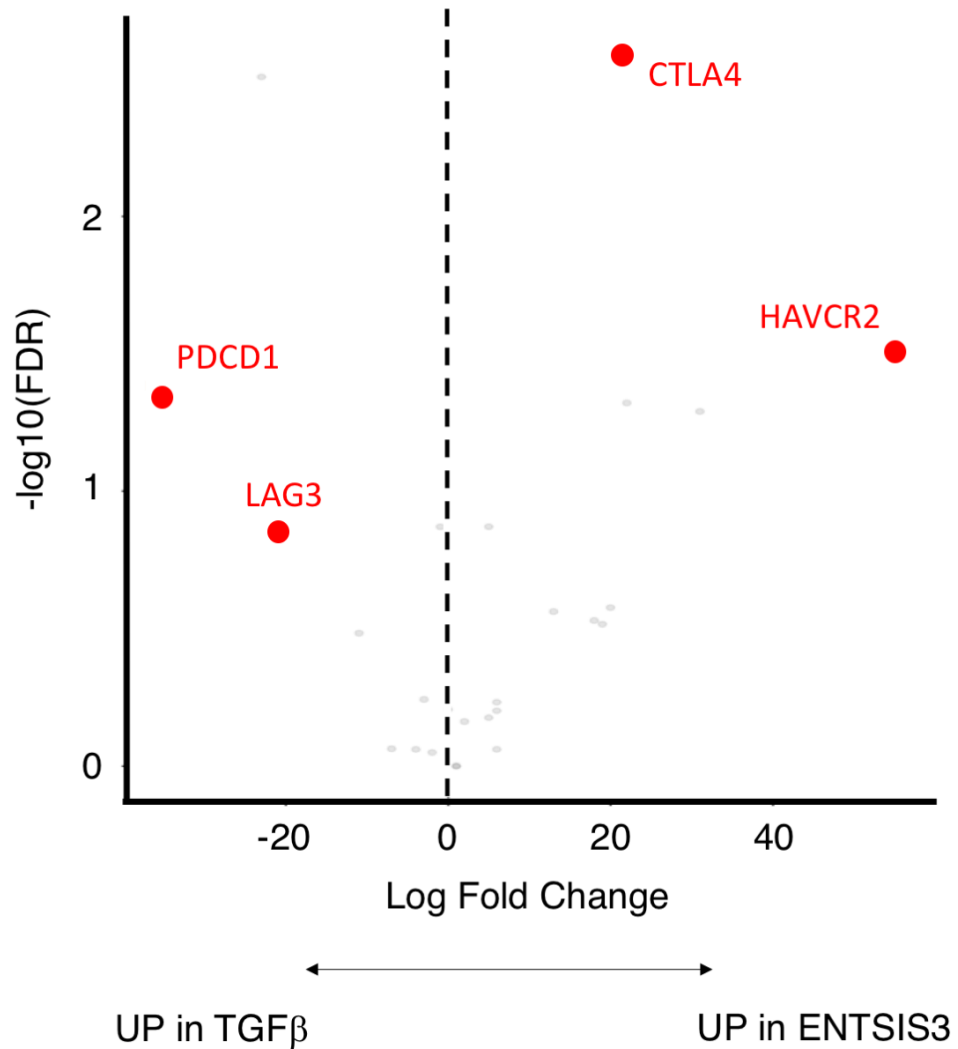


Figure 8: Combination of entinostat and SIS3 results in the largest fold change difference in promoter acetylation in CTLA-4 and TIM-3

T cells activated *in vitro* demonstrate differential effects of TGF- β 1 and entinostat on promoter acetylation at PD-1 and CTLA-4, LAG-3, and TIM-3. The combination of entinostat and SIS3 additively enhances this effect.

CHAPTER 3

Inhibition of the TGF- β 1 / Class I HDAC Axis Promotes the Differentiation of Functionally Distinct T Cell Subsets

Introduction

The persistence of antigen and an inability to completely clear it from the host leads to chronic stimulation of antigen-specific T cells. Chronically stimulated T cells undergo a hierarchical loss of function leading to the development of a state called T cell exhaustion. Exhausted T cells lose proliferative potential and production of IL-2 early. Later, production of TNF α is lost followed by late loss of IFN γ production capacity. This process is driven by chronic TCR stimulation. However, other receptors have a role in the generation of the exhausted state. PD-1 is a major inhibitory receptor from the CD28 superfamily which appears to be an important mediator of exhaustion. Evidence for this exists in both murine models, where blockade of the interaction between PD-1 and its binding partner PD-L1 by antibodies improves viral clearance and tumor protection, and human studies, where PD-1 blockade has led to long-term and durable responses in multiple tumor types.

It is important to note that blockade of PD-1/PD-L1 interactions is not sufficient to fully normalize the function of exhausted T cells^{22,98}. T cells subject to PD-1 blockade regain the ability to proliferate and produce effector cytokines; however, this ability is generally less than memory T cell counterparts. Exhausted T cells express multiple inhibitory checkpoints including CTLA-4, LAG-3, TIM-3, CD160, TIGIT, and others²⁶. Blockade of multiple checkpoints in combination leads to a better improvement of T cell function compared to PD-1 blockade alone^{99,100}. In the clinic, combinations of PD-1 and CTLA-4 blockade have led to higher response rates in patients with melanoma, lung cancer, and renal cell carcinoma^{35,101}. This is associated with a higher rate of immune-

related adverse events, further highlighting that co-blockade leads to greater T cell activation. Despite this evidence, it is unclear whether different inhibitory checkpoints are signaling and functioning through different pathways or are signaling through the same pathway, albeit at differing levels of signaling intensity. Furthermore, it is unclear whether all exhausted T cells recognizing the same antigen express the same checkpoints, or if T cells expressing different patterns of checkpoints represent different T cell subsets¹⁰². To begin to explore this question, we made use of the insight developed in the previous two chapters to generate *in vitro*, T cells with divergent checkpoint expression patterns. Using TGF- β 1 we were able to drive the generation of T cells with predominantly PD-1 expression and low expression of other checkpoints. Using entinostat in combination with SIS3 allowed us to generate T cells with the expression of TIM-3, CTLA4, LAG-3, and TIGIT. We profiled the transcriptome and functionality of these cells *in vitro* to arrive at new insight about the properties of T cells with differing checkpoint expression patterns.

Results

To address the question of the functional differences between CD8⁺ T cells expressing different cell surface checkpoints, we used the scheme developed in the previous chapters to generate CD8⁺ T cells with different checkpoint expression patterns *in vitro*. MACS isolated human CD8⁺ T cells were stimulated with anti-CD3/anti-CD28 microbeads for 4 days in the presence or absence of 5 ng/mL TGF- β 1, 5 μ M SIS3, 100 nM entinostat, or the combination of entinostat and SIS3. At 4 days the

transcriptional profile of these cells was analyzed by nanostring gene expression array. The nanostring system is a digital gene expression profiling technology that can count the number of RNA molecules of up to 800 different genes per sample. Thus, it avoids the need for amplification and the bias that can result from that, while retaining simplicity in its analysis. Figure 9A displays a heatmap of genes that were significantly different between the conditions tested. Two clusters of genes emerged from this analysis. A first cluster of genes was upregulated by TGF- β 1. The second cluster was downregulated by TGF- β 1. The expression of genes downregulated by TGF- β 1, could be increased by entinostat and SIS3. The combination of entinostat and SIS3 led to additive effects in enhancing the expression of those genes. PDCD1 (the gene encoding PD-1) was in a separate cluster from HAVCR2 (the gene encoding TIM-3) and TIGIT. Interestingly, PD-1 cluster of genes also included CXCR3, CCR4, and ITGAE (gene encoding CD103 – an integrin protein known to be important in tissue resident T cells). The ENT/SIS3 cluster included ITGAX (CD11c) and IL2RG. These results suggest that differing cell surface immune checkpoint expression patterns may correlate with differing functional profiles.

We next examined which sets of co-inhibitory and co-stimulator molecules were co-expressed together under these conditions. Two clusters of co-regulated molecules were found. A first cluster includes PD-1, ICOS, PD-L1, CD276, GITR, and CD70. These genes were upregulated by TGF- β 1. A second cluster included TIM-3, CTLA-4, TIGIT, A2A receptor, CD73, and CD39. These genes were downregulated by TGF- β 1 and upregulated by entinostat and SIS3 (Fig 9B). Thus, two clusters of differentially regulated

checkpoints emerge at the transcriptional level. These genes correlate nicely with those seen to be differentially regulated on a chromatin level by ChIP-seq analysis in chapter 2.

We next correlated the change in expression of immune checkpoint genes with the change in histone acetylation in their promoter regions. The fold change in expression between unstimulated and anti-CD3/anti-CD28 stimulated T cells was plotted against the fold change histone acetylation in the promoter for these genes (Fig 10). The level of correlation was quite good, indicating that the acetylation status of the promoter has a direct relationship with the expression level of the gene. TNFRSF18 (GITR), TNFRSF4 (OX40), TNFRSF9 (4-1BB), LAG3, and HAVCR2 (TIM-3) had the largest fold change in RNA expression and this correlated with them having the largest fold change in histone acetylation. The expression of CD28, CD274, and TIGIT went down upon stimulation and this also correlated with a loss of acetylation marks in the promoter.

We next sought to understand the protein level differences between T cells that have been stimulated to have pre-dominant PD-1 expression compared to those with high levels of CTLA-4 and TIM-3. To do this, T cells were stimulated in the presence of TGF- β 1 or entinostat in combination with SIS3. T cells were analyzed with several multi-color flow cytometry panels and supernatants were analyzed by multi-cytokine MSD array. These data were then all correlated against each other to find modules that co-varied under the different activation conditions. Two clusters were discovered, segregating the expression of PD-1 from TIM-3 (Fig 11). CD27, CD39, CTLA-4, and

granzyme B expression segregated with TIM-3 expression and were inversely correlated to the expression of the PD-1 cluster. PD-1 expression correlated with TNF α , IL-12, IL-2, and IL-6 expression. These data indicate that T cells activated in the presence of TGF- β 1 have a different cytokine and marker expression profile compared to those activated in the presence of entinostat in combination with SIS3.

Finally, we examined the checkpoint expression pattern at the population level when CD8⁺ T cells were activated in the presence of TGF- β 1 or combination entinostat and SIS3 (Fig 12). We found that at a population level, TGF- β 1 induces a shift in T cell distribution from a balanced expression of PD-1 alone, TIM-3 alone, and PD-1 and TIM-3, to mostly cells that co-express PD-1 and TIM-3 or those that express PD-1 alone (Fig 12A/B). Conversely, entinostat in combination with SIS3 led to the shifting of the population from T cells that had balanced expression of PD-1 and TIM-3 to those co-expressing PD-1 and TIM-3 or expressing TIM-3 alone.

Discussion

In this chapter, we examined CD8⁺ T cells *in vitro* for evidence of differential functionality when induced to express PD-1 pre-dominant checkpoint pattern compared to TIM-3 and CTLA-4 expression pattern. To push T cells towards a PD-1 predominant checkpoint expression pattern, we activated the T cells in the presence TGF- β 1. This lead to the generation of CD8⁺ T cells that expressed PD-1 at high levels, but low levels of TIM-3 and CTLA-4. To generate CD8⁺ T cells that expressed high levels of CTLA-4 and

TIM-3 with relatively lower levels of PD-1, CD8+ T cells were activated in the presence of entinostat and SIS3.

We found that 2 distinct modules of gene expression emerged that were differentially regulated at the histone acetylation level, leading to differences in expression at the RNA and protein level. PD-1 high T cells co-expressed markers of tissue residency and polyfunctionality such as TNF α , IL-2, and IL-12 production. TIM-3 and CTLA-4 positive T cells expressed granzyme B as well as other inhibitory checkpoints.

These data suggest that heterogeneity in immune checkpoint expression might suggest differences in functional capacity of CD8+ T cells. Indeed, data exists to support this idea. Several groups have demonstrated that blockade of PD-1 is insufficient to fully reinvigorate exhausted T cells and that T cells expressing more checkpoint types are more deeply exhausted. However, the idea that checkpoint molecules can be expressed independently of PD-1 has been less developed. PD-1 knockout, antigen-specific CD8+ T cells have a more robust initial response to the target antigen, proliferating well and producing effector cytokines¹⁰³. They subsequently undergo massive contraction. Importantly, the absence of PD-1 did not inhibit the development of exhaustion.

These data fit well with published observations showing distinct control mechanisms in checkpoint molecule expression. A recent study examining targets of the transcription factor EGR2 found that it could control the expression of LAG3 and 4-1BB but not PD-1¹⁰⁴. Notably, the expression of PD-1, even at high levels, in the absence of expression of other immune checkpoints correlated with highly activated and

polyfunctional CD8⁺ T cells. Expression of other immune checkpoints in association with PD-1; however, did denote T cells with reduced effector capacity.

We conclude that PD-1 expression can be controlled distinctly from the expression of other immune checkpoints by TGF- β 1 and this leads to the generation of T cells with different effector capacity compared to those expressing lower levels of PD-1 but higher levels of CTLA-4 and TIM-3.

Materials and Methods

Human T cells

The Johns Hopkins HATS clinic provided leukapheresis product and human PBMC were isolated by Ficoll gradient. PBMC were stored in liquid nitrogen and thawed prior to use. Human T cells were isolated from bulk PBMC using CD8⁺ T cell isolation kit (Miltenyi Biotech).

In vitro Activation of T cells

Human CD8⁺ T cells were activated *in vitro* with anti-human CD3/CD28 microbeads at a ratio of 1:1 per manufacturer instructions (Invitrogen). Human TGF- β 1 was purchased (Peprotech) as a lyophilized product and suspended in complete T cell media. T cells were activated in the presence or absence of 5 ng/mL of TGF- β 1. For the experiments examining the inhibition of Smad3 signaling the inhibitor SIS3 was used at a concentration of 5 μ M (Sigma). SIS3 was dissolved in DMSO at a 10 mM stock concentration and dissolved in T cell culture media to working concentration. T cell media was made as follows: RPMI 1640 (90%), Fetal Bovine Serum (10%), Penicillin-

Streptomycin (100 U/mL), L-glutamine (4 mM), HEPES (1M), Minimum essential amino acids, 50 μ M beta-mercaptoethanol.

Flow Cytometry

Samples were stained in FACS buffer (PBS containing 1% BSA) at room temperature for 30 minutes. The following antibodies were used and purchased from BD Biosciences: PD-1(EH12.1), CD4(OKT4), CD8(RPA-T8), CD3(UCHT1). Human anti-TIM-3 was purchased from R&D (344823). Anti-CTLA-4 was purchased from Biolegend (L3D10). CTLA-4 staining was carried out on the cell surface for 30 mins followed by sample fixation and permeabilization with the EBioscience FoxP3 transcription factor kit and subsequently stained intracellularly. Samples were acquired on a BD LSR II.

Nanostring

CD8+ T cells were activated alone or in the presence of TGF- β 1, SIS3, Entinostat, or Entinostat and SIS3 for four days and mRNA was harvested and isolated. Flow cytometry was performed on all samples to confirm surface phenotypes matched previous findings for the conditions. mRNA samples were analyzed for quality by the Johns Hopkins Deep Sequencing and Microarray Core Facility and all RIN numbers were 10. Samples were normalized to load the same amount of RNA into the nCounter PanCancer Immune Panel (NanoString Technologies, Inc., Seattle, WA) according to the manufacturer's protocol. All results were then normalized using the nSolver package provided by Nanostring and the normalized counts or z-scores were exported for further analysis in R.

ELISA (Granzyme B)

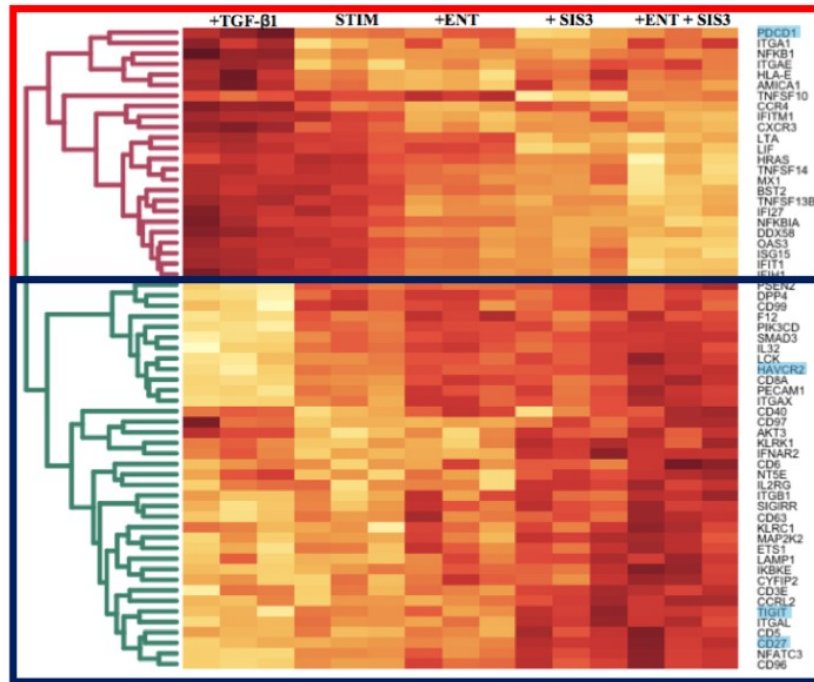
Supernatants were collected from in vitro experiments and stored at -80°C. Samples were diluted 1:1000 and granzyme B was quantitated using a commercially available ELISA (Human Granzyme B Platinum ELISA, eBiosciences) according to the manufacturer protocol.

MSD

Supernatants were evaluated for the presence of multiple cytokines using the Meso Scale Discovery multiplexed platform. IL-2, IL-6, IL-7, IL-8, IL-10, IL-12p40, IL-15, IL-16, IL-18, IP10, MIP1b, MCP1, IFN γ , and TNF α were analyzed from the supernatant samples. Samples were diluted 1:4 or 1:500 depending on the assay. The assay was performed according to the manufacturer's protocol and quantitated using QuickPlex SQ 120 (MSD). IL-7 and IL-15 were detected at levels below the limit of detection and not further analyzed.

Figure 9

A



B

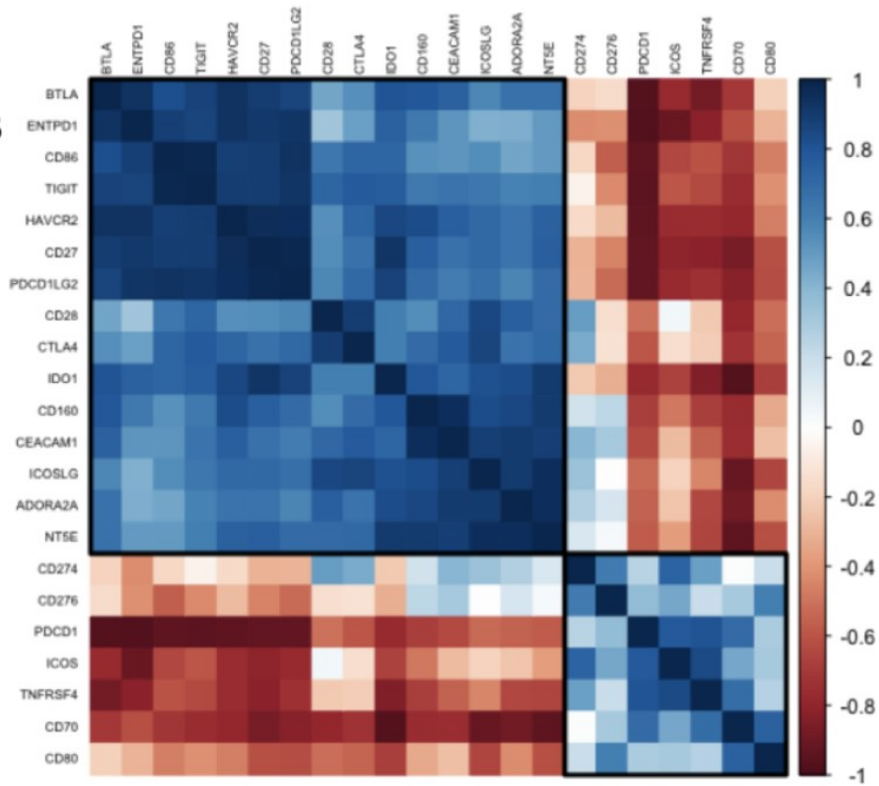


Figure 9: PD-1 and TIM-3 mark two clusters of discordantly regulated immune checkpoints

A) Heat map of z score for genes with an FDR < 0.1 for all 5 conditions identifies differential pattern of gene expression. B) Correlation matrix of checkpoint molecules. Blue represents a positive correlation with darker colors approaching $r = 1$ and red represents a negative correlation with darker colors approaching $r = -1$. Clustering analysis was performed using H clust for 2 clusters with black boxes assigned accordingly.

Figure 10

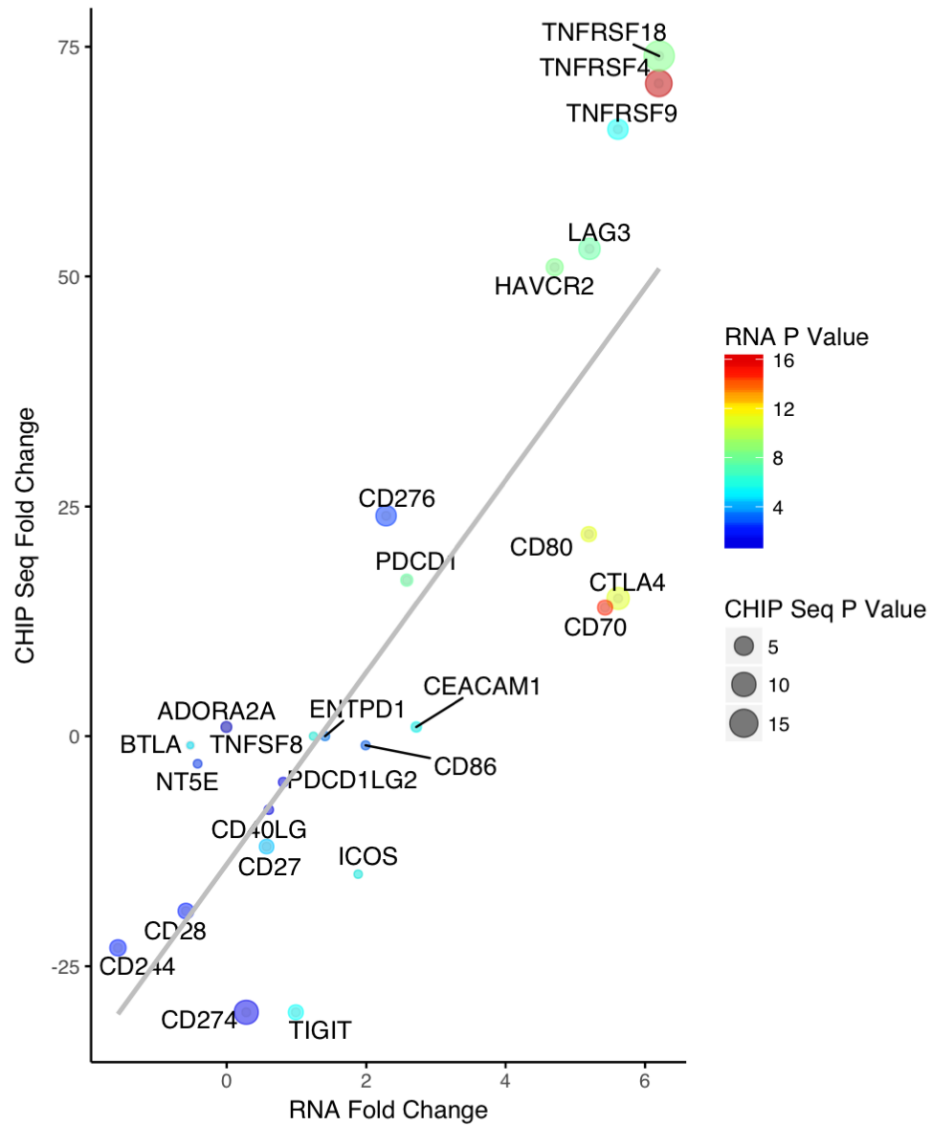


Figure 10: Promoter acetylation status is directly related to RNA expression of immune checkpoint genes.

Human CD8+ T cells were activated *in vitro*. DNA and RNA were analyzed for expression status using nanostring and promoter acetylation using ChIP-seq. Fold change was calculated comparing cells stimulated for 96 hours with unstimulated cells from the same donor. Three biological replicates for nanostring and two biological replicates for ChIP-seq.

Figure 11

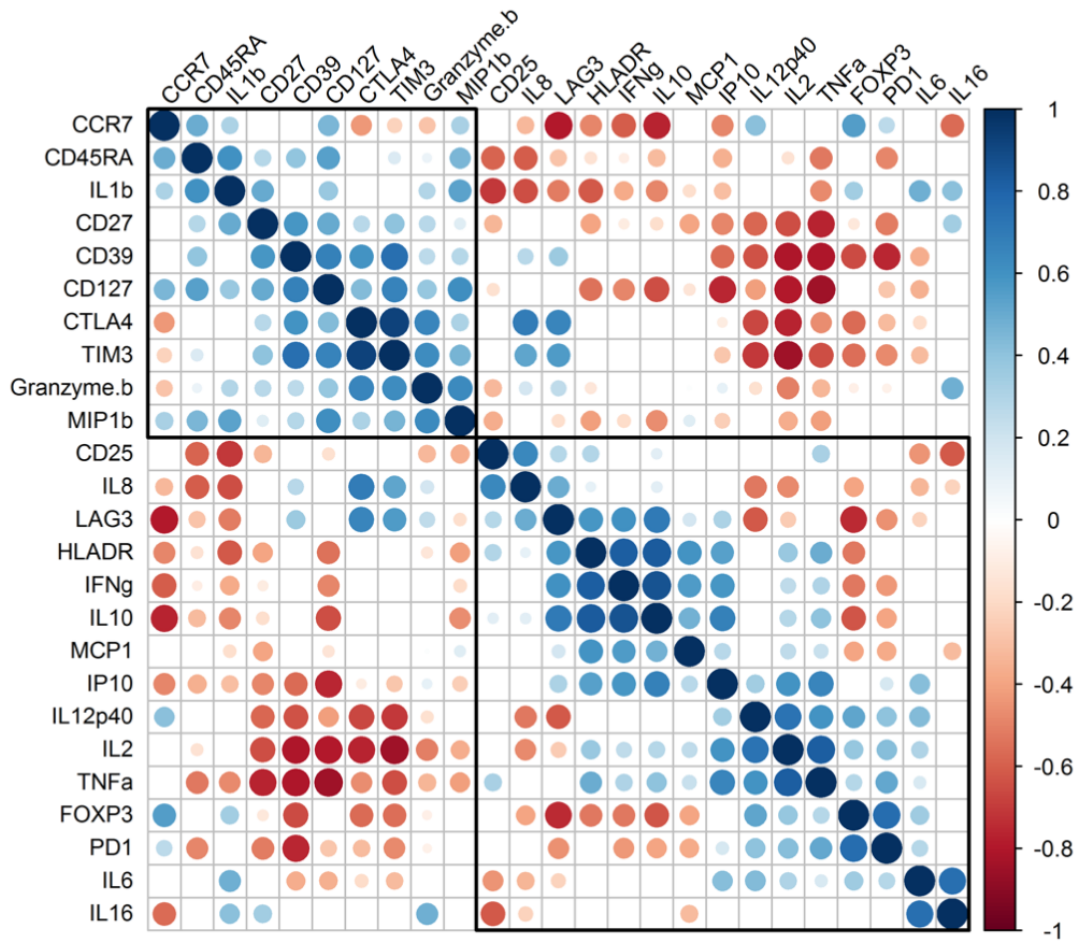


Figure 11: PD-1 and TIM-3 are discordantly regulated and associated with different functional states

Correlation matrix of multiple surface protein makers on human CD8+ T cells measured by flow cytometry and supernatant cytokines measured by MSD multiplexed platform. Blue represents a positive correlation with darker colors approaching $r = 1$ and red represents a negative correlation with darker colors approaching $r = -1$. Circle size represents the p value and p values are not significant for squares lacking circles. Clustering analysis was performed using H clust for 3 clusters. Black boxes represent independent clusters highlighting TIM-3 and PD-1 separation.

Figure 12

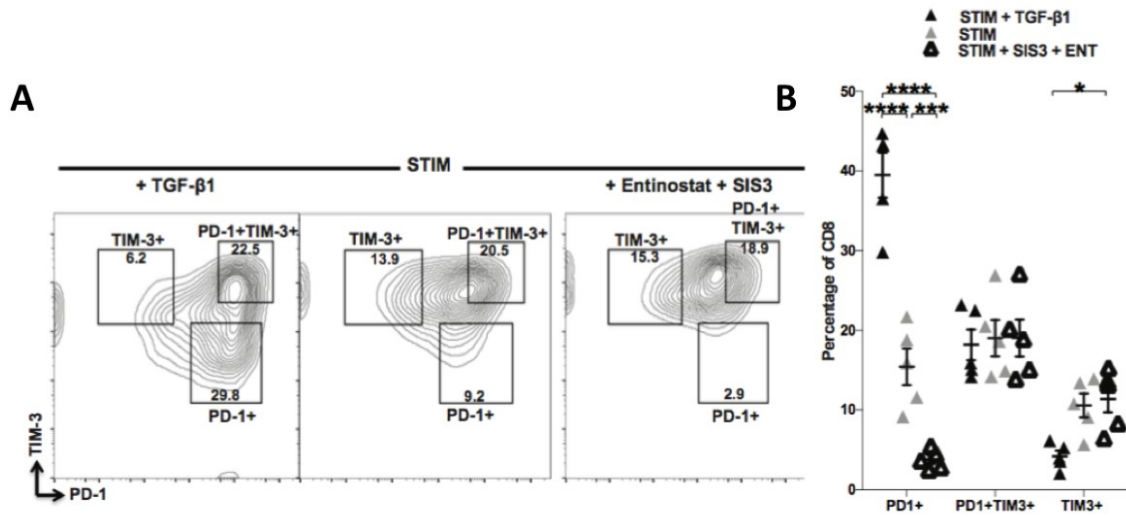


Figure 12: TGF-β1 and HDAC inhibition change the distribution of T cell population level checkpoint expression

PD-1+ vs PD-1+ TIM-3+ vs TIM-3+ expression in human CD8+ T cells activated in the presence of TGF-β1 or SIS3 with Entinostat. Representative plots from 1 of 5 donors. Percentages of CD8+ T cells in each subset of PD-1+, PD-1 TIM-3+, or TIM-3+ in T cells activated in presence of TGF-β1 or Entinostat and SIS3.

CHAPTER 4

Modulation of checkpoint expression profiles on T cells *in vivo*

Introduction

During a viral infection host CD8⁺ T cells are presented with viral peptides in the context of MHC class I on an antigen-presenting cell. If a T cell with an appropriate TCR specificity recognizes this peptide on the antigen-presenting cell, a T cell response can be mounted. T cells go on to proliferate and acquire effector properties such as cytotoxicity and cytokine production. Over the course of a typical viral infection, T cells will efficiently eliminate the pathogen over the course of an approximately 2-week period^{105–107}. Once the pathogen has been eliminated, a majority of the T cells die, and a small pool remain as memory T cells, ready to rapidly proliferate and respond to the virus if it is encountered again. During this process, T cells express immune checkpoint molecules as a consequence of activation. The expression of these checkpoints is downregulated as the virus is cleared and immunological memory is formed. In contrast to this scenario, chronic infections continue to stimulate the immune response and prevent the formation of memory. Checkpoints remain upregulated on the responding T cells, contributing to their acquired dysfunction or exhaustion. Experiments done primarily in the acute and chronic lymphocytic choriomeningitis virus (LCMV) models have provided insight into the role of immune checkpoints in mediating the exhausted state.

LCMV was first discovered by Charles Armstrong while investigating an encephalitis epidemic in St. Louis in 1933^{108–111}. It is a member of the arenaviridae family of single-stranded RNA viruses. Many important discoveries in immunology have been made using this model system, including the discovery of MHC restriction by Doherty

and Zinkernagel^{112,113}. The LCMV Armstrong strain of the virus generates a large-magnitude CD8+ T cell driven immune response which leads to viral clearance in a two-week period. The LCMV Clone 13 strain leads to a long-term persistent infection that can be cleared in a 2-3 month period or can become lifelong if CD4+ T cells are depleted during the priming phase, commonly with the GK1.5 clone anti-CD4 antibody.

Interestingly, this striking difference in viral biology and immune response is driven by a small difference in the viral nucleotide sequence. Modern sequencing technologies revealed LCMV Armstrong and Clone 13 differ in 5 of 10,600 nucleotides. This leads to a 2 amino acid difference between the virus strains. It is surprising to see the difference in immune response duration, magnitude, and tissue distribution driven by such an amino acid substitution. Nonetheless, this model has provided valuable insights into T cell exhaustion that have led to understanding of T cell function in HIV and Hepatitis C infection, and cancer.

In this chapter we address two important and previously unanswered questions in the field. First, can the checkpoint expression profile of antigen-specific CD8+ T cells be altered *in vivo* in response to manipulation of the class I HDAC/TGF- β 1 axis? Second, what consequence does this have for viral clearance and persistence in acute and chronic infections? We utilized the LCMV Armstrong and Clone 13 models to study these two questions due to their tractability and the availability of excellent reagents to track antigen-specific T cell responses to LCMV virus *in vivo*.

Results

To address the question of altering checkpoint expression profiles on antigen-specific CD8⁺ T cells, an experimental scheme was developed to mirror our *in vitro* experiments with human CD8⁺ T cells (Fig 13A). Mice were infected with LCMV Armstrong or Clone 13 on day 0. From day 0 to day 6 mice were treated once each day orally with entinostat, twice each day orally with galunisertib (a TGF- β R inhibitor), or both. In the case of clone 13 infection, mice were given 200 μ g GK1.5 CD4 depleting antibody on day -1 and day +1. Spleens and blood were collected on day 7, 14, 28, and 56 and antigen-specific T cell populations were analyzed by flow cytometry. We found that among gp33 specific CD8⁺ T cells a significantly greater proportion expressed multiple immune checkpoints in both Armstrong and Clone 13 infection at day 7 post-infection (Fig 13B). Entinostat and galunisertib treated mice both expressed more checkpoint types than mice treated with the vehicle control. Mice treated with both had the highest proportion of cells expressing multiple immune checkpoints in both the acute and chronic infection models.

In the LCMV Armstrong model, we found that entinostat, galunisertib and combination treatment all led to increases in the proportion of antigen-specific T cells expressing up to 4 inhibitory checkpoints at day 7 post-infection (Fig 14). Combinations of three checkpoints being expressed together were also significantly increased with treatment of entinostat, galunisertib, and combination of the two. Three checkpoint combinations that included CTLA-4 were generally increased while those without CTLA-4 were not. The proportion of CD8⁺ T cells expressing combinations of 2 checkpoints went

down with HDAC inhibitor, TGF- β R inhibitor, and combination treatment, seemingly indicating a shifting of gp33 specific T cells to expressing more checkpoint molecules.

In LCMV clone 13 a similar pattern to Armstrong was seen at day 7 post-infection (Fig 15). The proportion of gp33 specific CD8+ T cells expressing 4 different checkpoints was significantly increased with entinostat, galunisertib, and combination treatment. The combination led to the highest proportion of cells expressing 4 different checkpoints. While there were differences in the proportion of gp33 specific T cells expressing 3 and 2 different checkpoints, these differences were not statistically significant. There was a trend towards combination treated mice having less cells expressing 1 or 2 checkpoints, suggesting that mice treated with the combination had more cells expressing more checkpoint types.

The T cell response to LCMV is primarily driven by the expansion of CD8+ T cells, with less of a role ascribed to CD4+ T cells. To examine the proliferation kinetics of T cells during LCMV infection in the presence of TGF- β 1/Class I HDAC axis inhibition, we profiled the proportion of each T cell subsets as a fraction of live cells within the spleen (Fig 16). CD4+ T cells did not greatly change their numbers over the course of infection (Fig 16A). CD8+ T cells however greatly proliferated with a peak at day 7 post-infection, and contraction of the population after (Fig 16B/E). This also correlated with the change in gp33 antigen-specific CD8+ T cells, tracked by tetramer staining (Fig 16C/E). Chronic LCMV infection is established with depletion of CD4+ T cells at the start of infection. This is reflected in very low numbers of detected CD4+ T cells at 7 and day 14 post-infection in the LCMV clone 13 experiments. Treatment with entinostat, galunisertib or the

combination did not affect the recovery of T cell populations over time. In both acute and chronic LCMV infection, mice treated with entinostat alone or in combination with galunisertib demonstrated greater expansion during the priming phase of infection at the bulk CD8+ T cells level (Fig 16B/E). However, these changes were not statistically significant in acute infection (Fig 16C). In chronic LCMV, antigen-specific CD8+ T cells persisted at higher levels compared to galunisertib and vehicle treated mice till day 28, however, at day 56 (2 months post-infection) levels were similar among all groups.

We next asked whether the cytokine production capacity of antigen-specific CD8+ T cells was altered by drug treatment. At day 7 post-infection, LCMV Armstrong infected mice treated with entinostat had more IFN γ producing cells than vehicle controls (Fig 17). This effect was not present in galunisertib treated animals and addition of galunisertib to entinostat in the combination group abrogated the entinostat effect. Granzyme B expression was also present in higher proportion of CD8+ T cells in the entinostat treated group and this effect persisted in the combination group. There was no significant difference in the proportion of CD8+ T cells producing TNF α . There was no significant difference in IFN γ or TNF α production among the difference groups in LCMV Clone 13 infection, though there was a trend to significance with galunisertib treatment in IFN γ + cells (P=0.07). However, granzyme B production was seen in a larger proportion of CD8+ T cells in combination treated animals.

We next examined the cytokine production capacity of gp33 specific T cells at day 28 post-infection. By this time, Armstrong infected mice have cleared the infection and formed immunological memory, while clone 13 infected mice have T cells that have

developed exhaustion and produce low levels of cytokines and have reduced proliferative potential. Mice in the LCMV Armstrong group treated with entinostat had significantly lower proportion of their CD8⁺ T cells producing IFN γ and TNF α at day 28 post-infection (Fig 17). Granzyme B was unaffected. The pattern was surprisingly different in clone 13 infection. Both entinostat and galunisertib treated mice had a greater proportion of cells expressing IFN γ and the combination had a significantly greater proportion of cells expressing IFN γ compared to the vehicle control group (Fig 17). TNF α production was also significantly higher in the combination group. Granzyme B production was significantly elevated in the entinostat treated group but not the galunisertib treated group. The combination group also had elevated granzyme B production which was not statistically significant (P=0.066).

TCF1, a transcription factor encoded by the gene TCF7, is important in self-renewal and generation of memory T cells. It is asymmetrically distributed in T cells undergoing division, with TCF1^{high} cells retaining memory and self-renewal and TCF1^{low} cells becoming terminally differentiated effector cells. It has been reported that TCF1^{high} and low populations occur during chronic viral infections, and TCF1^{high} cells are responsible for the proliferative burst that follows anti-PD-1 therapy. We hypothesized that inhibition of the TGF- β 1/HDAC axis might alter the balance of TCF1^{high} and low cells during LCMV infection. Human CD8⁺ T cells activated *in vitro* and stained with a cell division tracking dye, showed approximately half of the T cells developing into TCF1^{high} and TCF1^{low} after several rounds of division (Fig 18A). Activation in the presence of entinostat increased the proportion of TCF1^{high} cells by

about 10% *in vitro*. To investigate this *in vivo* gp33 specific CD8+ T cells were stained for TCF1 expression. In both Armstrong and Clone 13 infection at day 7 post-infection, a timepoint at which a majority of the gp33 specific T cells in the vehicle control group express little to no TCF1, entinostat treated groups had approximately 40% TCF1 high cells (Fig 18B/C). While galunisertib had no effect on TCF1 level of gp33 T cells, the combination of entinostat and galunisertib had significantly more TCF1 high cells.

The T-box transcription factors Tbet and Eomes have been described to delineate two groups of exhausted anti-viral CD8+ T cells. Tbet high cells have the ability to proliferate in response to antigen, express lower levels of PD-1 and can have some functionality restored by blockade of PD-1. In contrast, Eomes high subsets are thought to represent a terminally exhausted CD8+ T cell group that no longer has the ability to proliferate but retains cytotoxicity. We examined the effect of TGF- β 1/Class I HDAC axis inhibition on the generation of these two cell subsets (Fig 19). In both acute and chronic LCMV, expression of Tbet was reduced at early time points with treatment (Fig 19A). Expression of Eomes was generally unchanged in both acute and chronic infection, with the exception of an increase seen with galunisertib treatment at 2 months post-infection in Clone 13. In Clone 13, despite the initially lower expression of Tbet seen at day 7, by day 56 expression was higher than vehicle in entinostat and combination groups. It has been further reported that the PD-1+ Eomes+ subset of exhausted antigen-specific CD8+ T cells represent a terminally exhausted subset that cannot be rescued by PD-1 blockade. We did not see any difference in the proportion of PD-1+ Eomes+ CD8+ T cells with any treatment group.

Finally, we measured the LCMV viral load in the serum of the mice by qPCR to assess whether there was a functional consequence to TGF- β 1/Class I HDAC inhibition. In acute LCMV infection there was no difference in viral load at any timepoint and with any treatment (Fig 20A). In chronic LCMV, entinostat and combination group had a higher viral at day 7, 14, and 28. But in the combination group this level reduced to the same as vehicle control and galunisertib by 2 months. Interestingly, entinostat treated mice remained with higher viral loads at 2 months, representing potentially a lack of ability to control virus levels (Fig 20B).

Discussion

In this chapter we attempted to answer two questions. First, is it possible to alter checkpoint expression profiles on antigen-specific CD8+ T cells *in vivo* using TGF- β 1/Class I HDAC inhibitors. Second, does alteration of checkpoint profile have a consequence for T cell functionality. These questions have not been previously addressed in the field and have important implications for how we think about treating viral infections and cancer.

Our results in both the LCMV acute and chronic infection models indicate that checkpoint expression patterns on antigen-specific CD8+ T cells can be altered using TGF- β 1/Class I HDAC inhibitors. We found that mice treated with entinostat or galunisertib or the combination expressed a greater number of checkpoint types on CD8+ T cells. In both acute and chronic infection, the number of cells expressing multiple immune checkpoints increases with treatment. However, the pattern followed

was not similar between the two. With acute infection, there was not only an increase in the proportion of cells expressing 4 checkpoints, there was also an increase in certain 3 checkpoint combinations with a concomitant decrease in two and single checkpoint expressing combinations. With chronic infection there was a large increase in T cells expressing all 4 checkpoints with relatively small changes in other combinations that were not statistically significant. This suggests that the infectious context determines the effect of the inhibitors.

HDAC inhibition appeared to provide both CD4+ and CD8+ T cells with a proliferative advantage. In entinostat or combination treated mice, CD4+ T cells were almost double vehicle and galunisertib at day 7 (Fig 16A). By day 14, the vehicle and galunisertib groups reach comparable levels to entinostat and combination treated mice. The same pattern is seen with CD8+ T cells in both acute and chronic infection (Fig 16B/E). This is not seen at the level of gp33 specific T cells as measured by tetramer staining. A possible explanation is that the precursor frequency for LCMV specific CD8+ T cells is relatively constant across C57BL/6 mice. Thus, while there is greater expansion of CD8+ T cells in entinostat treated mice, this number is similar between all groups when judged as a proportion of the total number of CD8+ T cells. Thus, while percentages of tetramer positive CD8+ T cells is similar between groups at the peak of infection (day 7) in both acute and chronic models, the number of cells is different. In the chronic infection model, entinostat and combination groups kept a higher percentage of gp33-specific T cells till day 28, though by 2 months these had contacted to the same levels as other mice. Thus, it is not conclusively clear whether HDAC inhibition has an effect on

memory generation, but the data suggest that it may aid in the development of T cell memory, leading to higher numbers of remaining memory T cells.

The early increase in the number of antigen-specific T cells in response to LCMV correlated with slightly increased levels of IFN γ production and granzyme B production in response to *ex vivo* challenge with gp33 peptide. In both acute and chronic LCMV, cytokine production levels were roughly equivalent at day 7. However, by day 28 in acute infection the production of both IFN γ and TNF α was significantly lower in mice treated with entinostat. In the chronic infection model, it was the opposite, with greater production of IFN γ , TNF α , and granzyme B seen in entinostat treated and combination groups. The effects of HDAC inhibition appear to be context dependent. In an acute infection which is cleared by 2 weeks, the generation of a memory response seems dampened by treatment with HDACi during the priming phase. In contrast in a chronic infection, with continuous stimulation of the T cells by persistent virus, no memory develops. At day 28, the T cells primed in the presence of HDACi continue to demonstrate greater *ex vivo* effector capacity. It would be interesting to examine this phenomenon in the context of a prolonged infection that is eventually cleared. Would effector function be greater in mice treated with HDACi up to the point that virus is cleared and decline afterwards? Based on this data, we would hypothesize that would be the case.

Interestingly, entinostat treated groups had a higher proportion of TCF1 high cells during the acute phase of the infection. Resting, naïve, and memory T cells are TCF1^{high} and this transcription factor is important for the maintenance of the naïve and

memory state^{59,114}. Upon antigen encounter and proliferation, TCF1 expression is maintained for the first three to four divisions, subsequently a large number of T cells lose expression with a minority retaining TCF1 expression. Vehicle and galunisertib treated mice displayed this pattern. In line with published reports, at day 7 approximately 20% of vehicle and galunisertib treated mice had TCF1 high cells (Fig 18). Groups treated with entinostat or combination had nearly double this amount in both acute and chronic infection. At day 7, this is particularly surprising since most gp33 specific cells at this time point are TCF1 low. Several groups have now linked the TCF1 high population to the cells providing the proliferative burst and enhanced effector function seen with PD-1 axis blockade¹¹⁵⁻¹¹⁷. It would be interesting in future experiments to test whether entinostat in combination with anti-PD-1 would lead to an enhanced anti-virus or anti-tumor immune response.

We attempted to answer the question of whether T cell functionality is impacted by TGF- β 1/Class I HDAC inhibition in several complementary ways. First, cytokine production appears to be decreased in the context of an acute immune response after memory formation and enhanced in the context of an ongoing chronic infection. Second, we examined kinetics of the T cell response and saw that HDACi augment the expansion of antigen-specific T cells in both acute and chronic infection. Third, the number of TCF1 high cells is doubled in HDACi treated mice, demonstrating a population with potentially greater capacity to generate memory and greater capacity for reinvigoration in response to checkpoint blockade. The fourth method used was to assess the proportion of Tbet and Eomes expressing antigen-specific T cells and the

levels of PD-1 and Eomes co-expressing cells (Fig 19). Tbet high Eomes low CD8+ T cells have been reported to be less exhausted than those expressing high levels of Eomes and low levels of Tbet. Eomes high PD-1 high T cells are thought to represent a terminally exhausted CD8+ T cell population²⁷. Therefore, differences in the numbers and proportions of these populations might give a clue as to the function of the T cells. We did not see any large differences in the levels of these transcription factors being expressed in T cells during the course of infection, regardless of treatment group or infection type.

Lastly, we measured the viral load in the serum of mice at different time points by qPCR to see if infection control was altered by TGF- β 1/Class I axis inhibition. There was no difference seen in LCMV Armstrong. All mice went on to clear the virus and levels of virus in the serum were not different at various time points. In the LCMV clone 13 infection no difference was seen in the viral load between vehicle and galunisertib treated mice. However, entinostat treatment significantly increased the viral load at all time points. This was also the case in the combination treatment group; however, by 2 months post-infection the viral load was equivalent to vehicle and galunisertib. This indicates that the galunisertib, while not improving viral control compared to the vehicle group, did contribute in improving the function of entinostat treated mice. This last piece of evidence, when combined with the previous data, indicates that HDAC inhibition overall likely worsens T cell exhaustion and dysfunction; however, these T cells may have greater effector potential due to their high expression of TCF1 and

increased cytokine production *ex vivo* if complemented with the correct checkpoint blockade partner.

Materials and Methods

Mice

Six- to eight-week-old female C57BL/6 mice were used for all experiments. All mice were maintained in an American Association for the Accreditation of Laboratory Animal Care International accredited facility (AAALAC) according to the National Institute of Health Animal Care guidelines, Institutional Biosafety Committee guidelines, and procedures were carried out under protocols approved by the Johns Hopkins and Columbia University Animal Care and Use Committee. Mice were housed in a specific-pathogen free colony. C57BL/6 were purchased from Jackson Laboratory.

LCMV Infections

Mice were injected with 2×10^5 LCMV Armstrong intraperitoneally (i.p.) or 4×10^6 PFU of LCMV clone 13 intravenously (i.v.). For Clone 13 experiments only, mice were injected with 200 μ g anti-CD4 GK1.5 antibody on day -1 and +1. At indicated time points, spleens were isolated from mice and dissociated through a 100- μ M filter, RBC lysis was carried out in ACK lysing solution, quenched with PBS, and splenocytes were stained for flow cytometry. LCMV was a kind gift of Jonathan Powell and was propagated in the lab as previously published.

In Vivo Drug Treatment

Entinostat (Selleckchem) was dosed at 5 mg/kg by intraoral gavage. Drug was formulated in 2% DMSO, 30% PEG200, 68% water and was given once daily for 6 consecutive days starting at the time of vaccination. Galunisertib (Selleckchem) was dosed at 100 mg/kg by intraoral gavage. Drug was formulated in 1% sodium carboxymethylcellulose, 0.4% sodium lauryl sulfate, 0.05% anti-foam A and 0.085% polyvinylpyrrolidone and given twice daily for 6 consecutive days starting at the time of vaccination.

Flow Cytometry

Single cell suspensions of splenocyte were stained in FACS buffer with OVA tetramer at room temperature for 45 minutes. Next, cells were washed and stained for cell surface markers and viability. Fixation and permeabilization were carried out using the eBioscience Foxp3 fixation and permeabilization kit. Intracellular targets were stained in permeabilization buffer and cells were acquired on a BD FACSCelesta instrument. For cytokine staining, cells were stimulated *in vitro* for 6 hours in the presence of 1 μ M gp33 peptide and eBioscience protein transport inhibitor cocktail.

qPCR For Viral Titer Determination

Whole blood was collected from mice at the indicated time points and allowed to coagulate at room temperature for 30 minutes. Blood was centrifuged at 12,000g for 10 minutes and serum was separated. 100 μ L of serum was mixed with 300 μ L Trizol LS. RNA was extracted per the manufacturer's instructions. RNA was converted to cDNA using the Clontech RNA to cDNA EcoDry Premix kit. qPCR was carried out using 10 ng

cDNA per reaction. LCMV GP primers are as follows: Forward
(TGCCTGACCAAATGGATGATT), Reverse (CTGCTGTGTTCCCGAAACT)

Data Analysis

Flow cytometry data was analyzed on FlowJo software (Treestar). Statistical analysis was carried in GraphPad Prism v7.

Figure 13

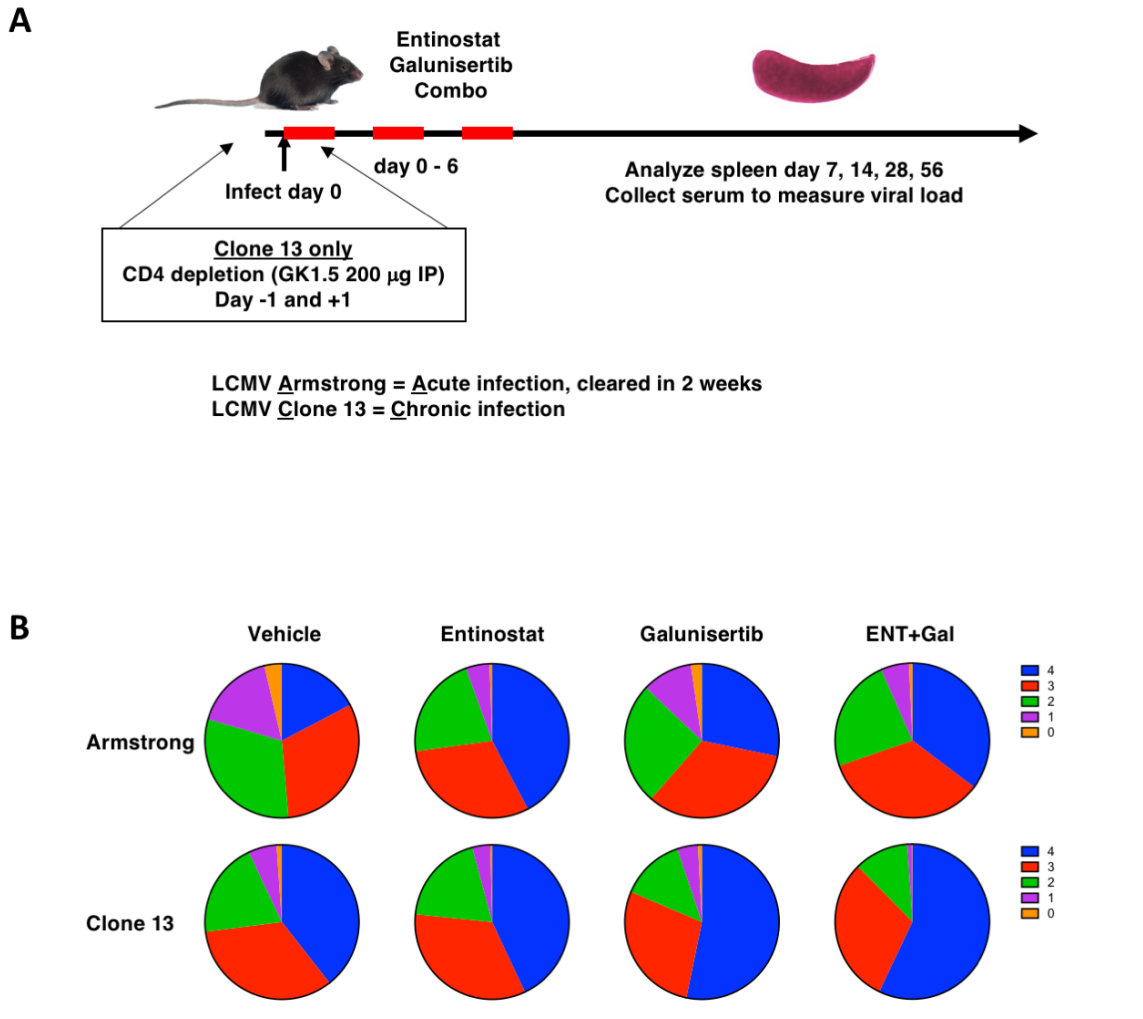


Figure 13: TGF- β 1/Class I HDAC inhibition increases the number of checkpoints expressed on CD8+ T cells

A) Experimental schematic.

B) Proportion of gp33 specific CD8+ T cells expressing 1, 2, 3, or 4 checkpoint molecules simultaneously at day 7 post-infection.

Figure 14

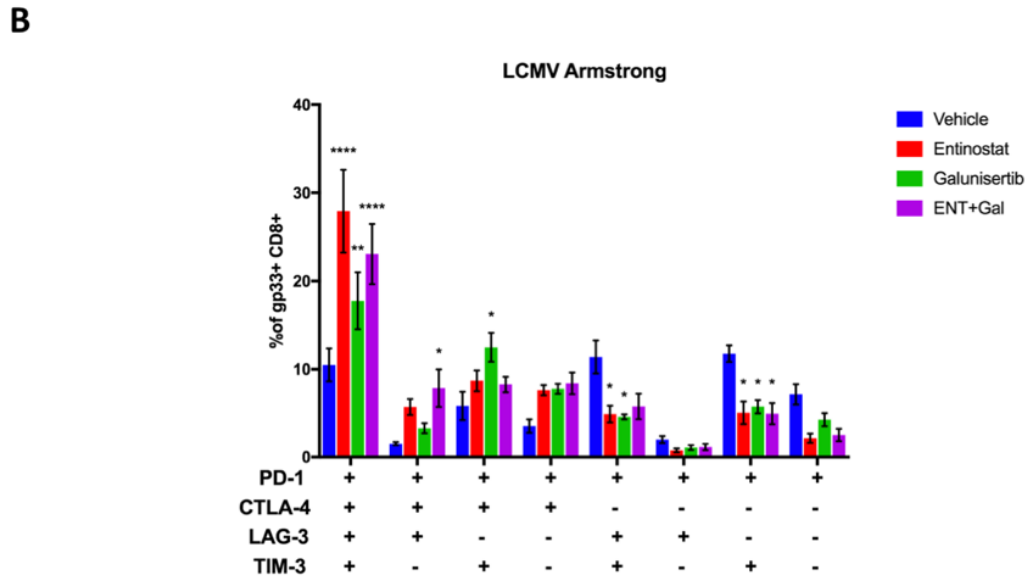
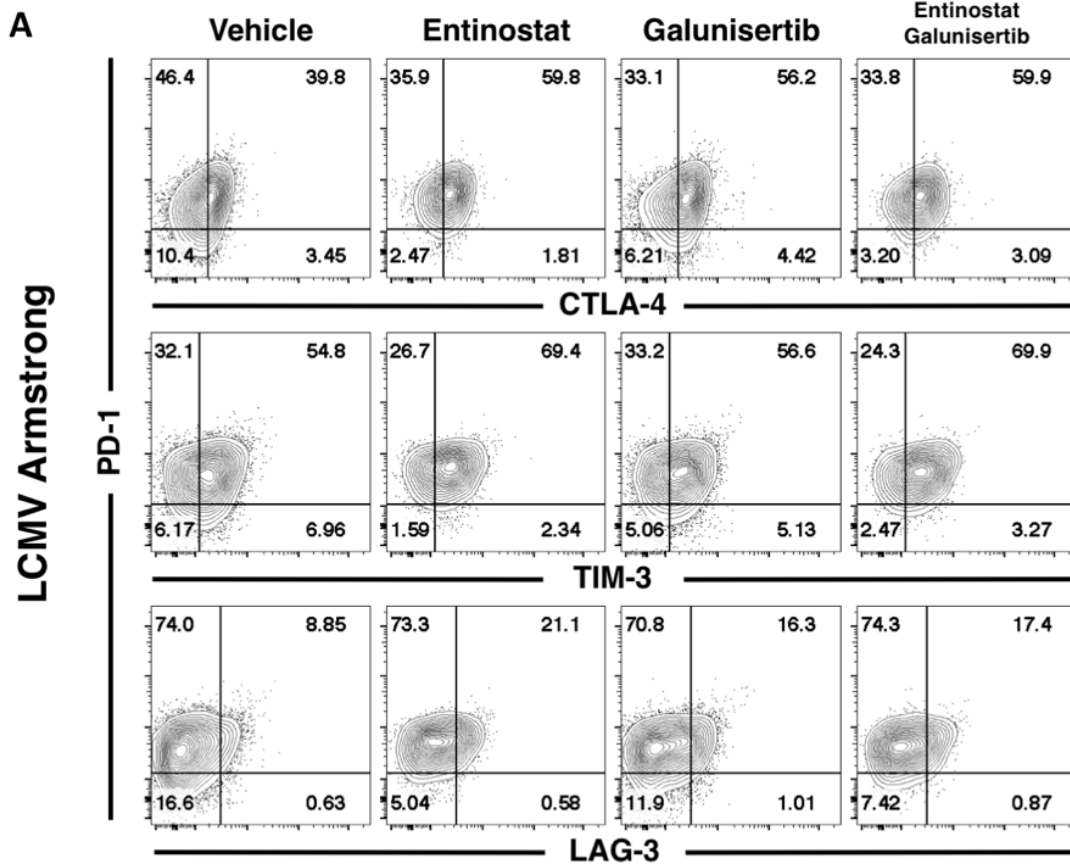


Figure 14: TGF- β 1/Class I HDAC inhibition induces the expression of multiple checkpoints in acute infection

A) Representative flow plots at day 7 post-infection showing co-expression of CTLA-4, TIM-3, and LAG-3 with PD-1

B) Summary statistics for combinations of co-expressed immune checkpoints at day 7 post-infection. Stars indicate results of t-test in comparison to vehicle control. * $p < 0.05$, ** $p < 0.005$, *** $p < 0.0005$

Figure 15

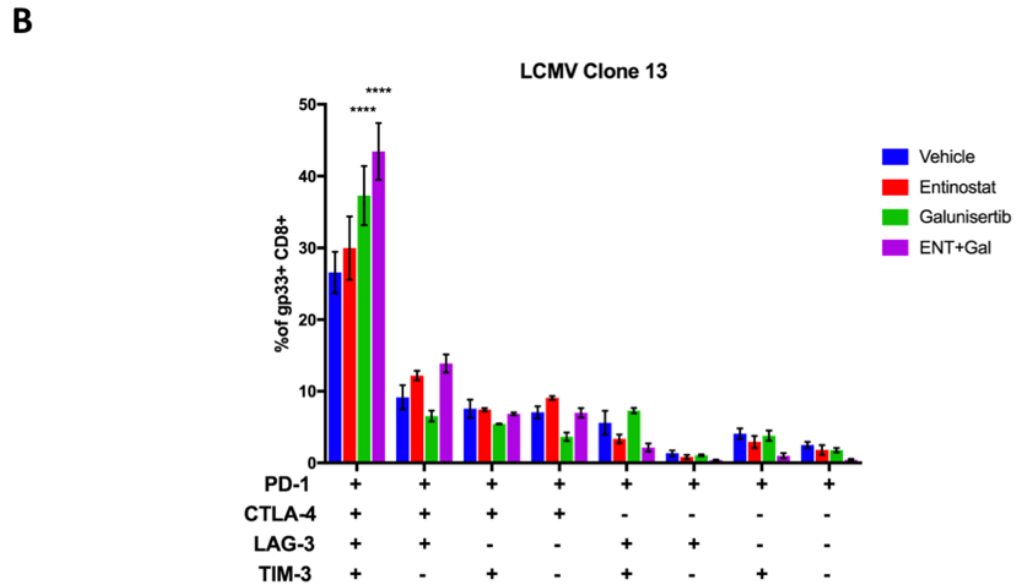
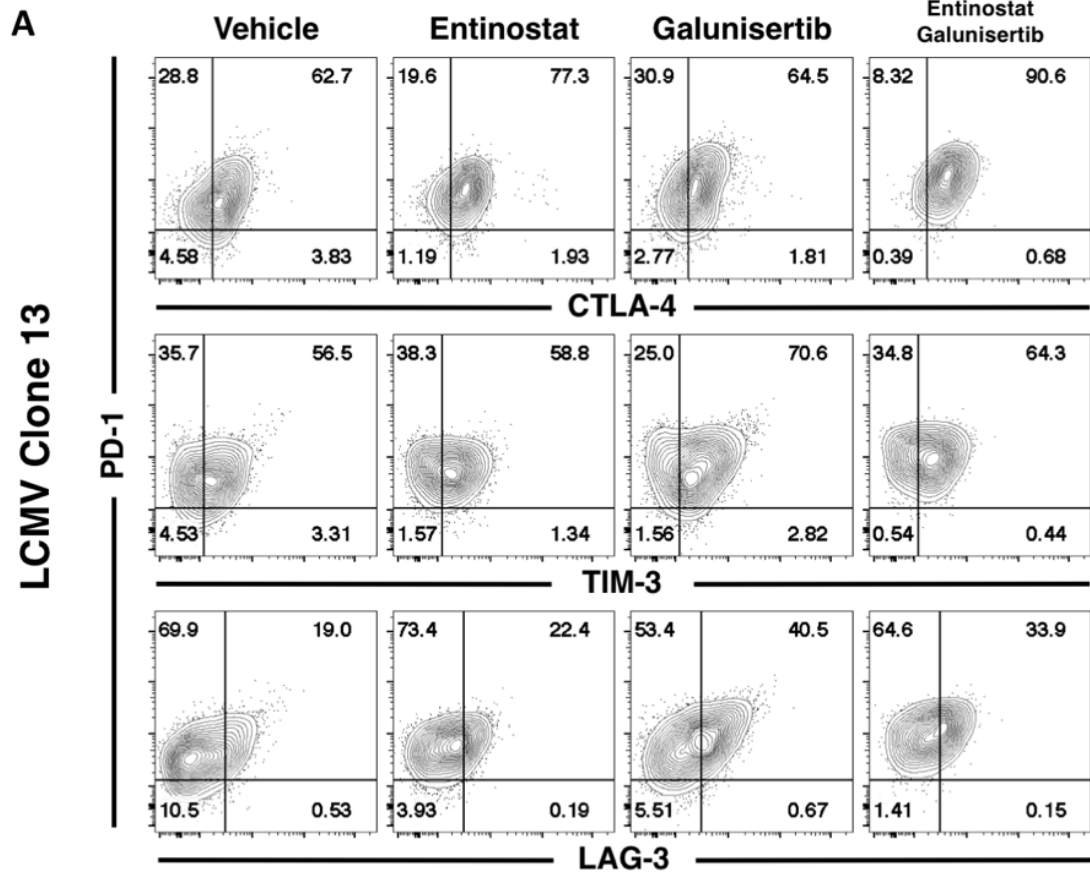


Figure 15: TGF- β 1/Class I HDAC inhibition induces the expression of multiple checkpoints in chronic infection

A) Representative flow plots at day 7 post-infection showing co-expression of CTLA-4, TIM-3, and LAG-3 with PD-1

B) Summary statistics for combinations of co-expressed immune checkpoints at day 7 post-infection. Stars indicate results of t-test in comparison to vehicle control. * $p < 0.05$, ** $p < 0.005$, *** $p < 0.0005$

Figure 16

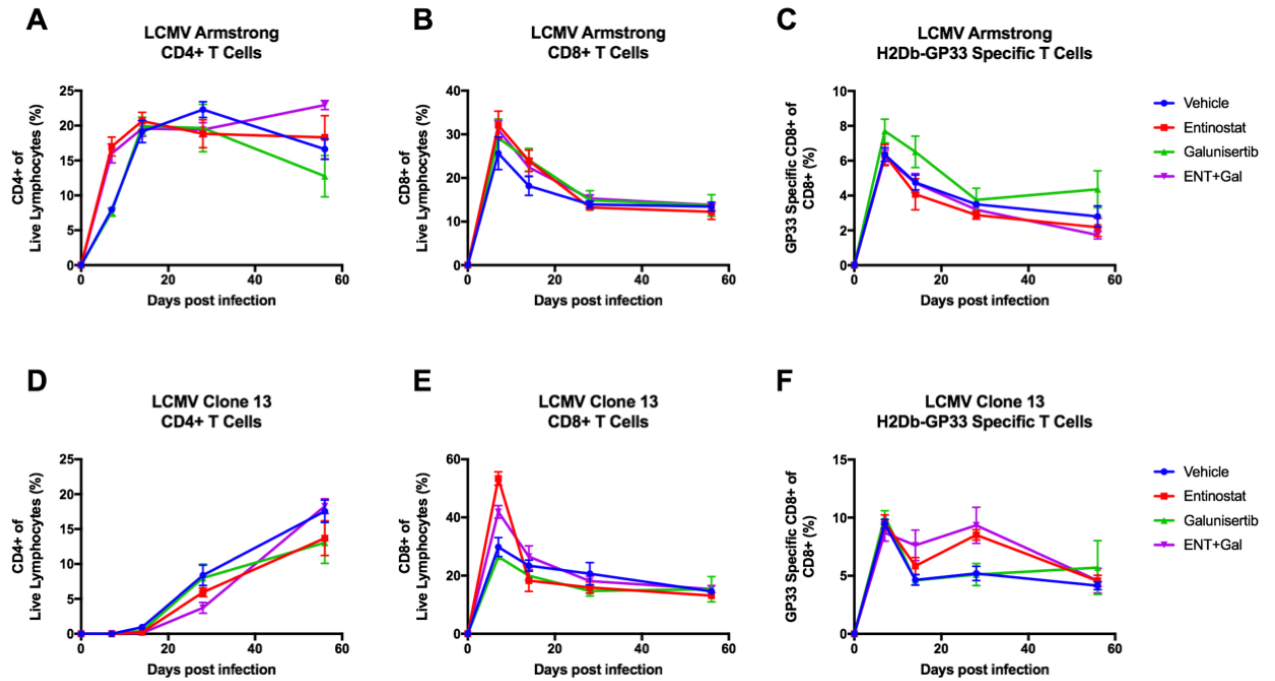


Figure 16: HDAC inhibition promotes T cell expansion during the priming phase of infection

A,B,C) T cell subsets in LCMV Armstrong (Acute infection)

D,E,F) T cell subsets in LCMV Clone 13 (Chronic infection)

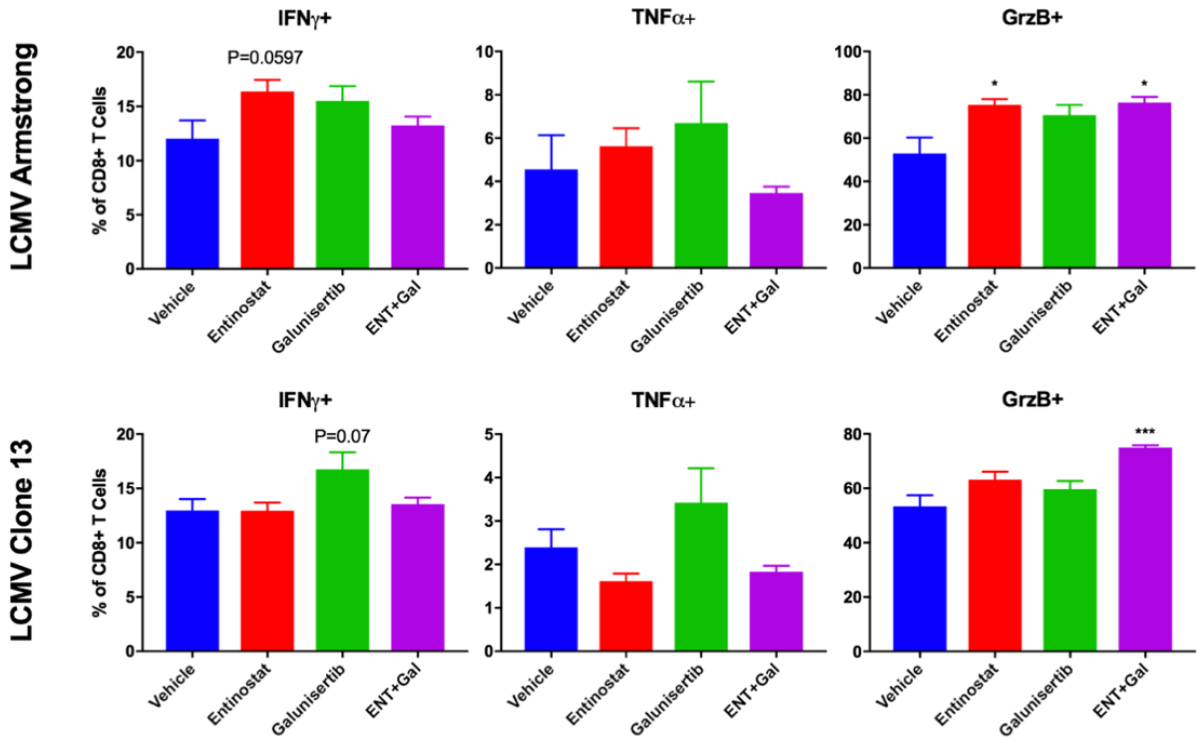
A/D) CD4+ T cells as proportion of live lymphocytes over time

B/E) CD8+ T cells as a proportion of live lymphocytes over time

C/F) H2Db-GP33 tetramer positive T cells as a percentage of CD8+ T cells over time

Figure 17

Day 7 Post Infection



Day 28 Post Infection

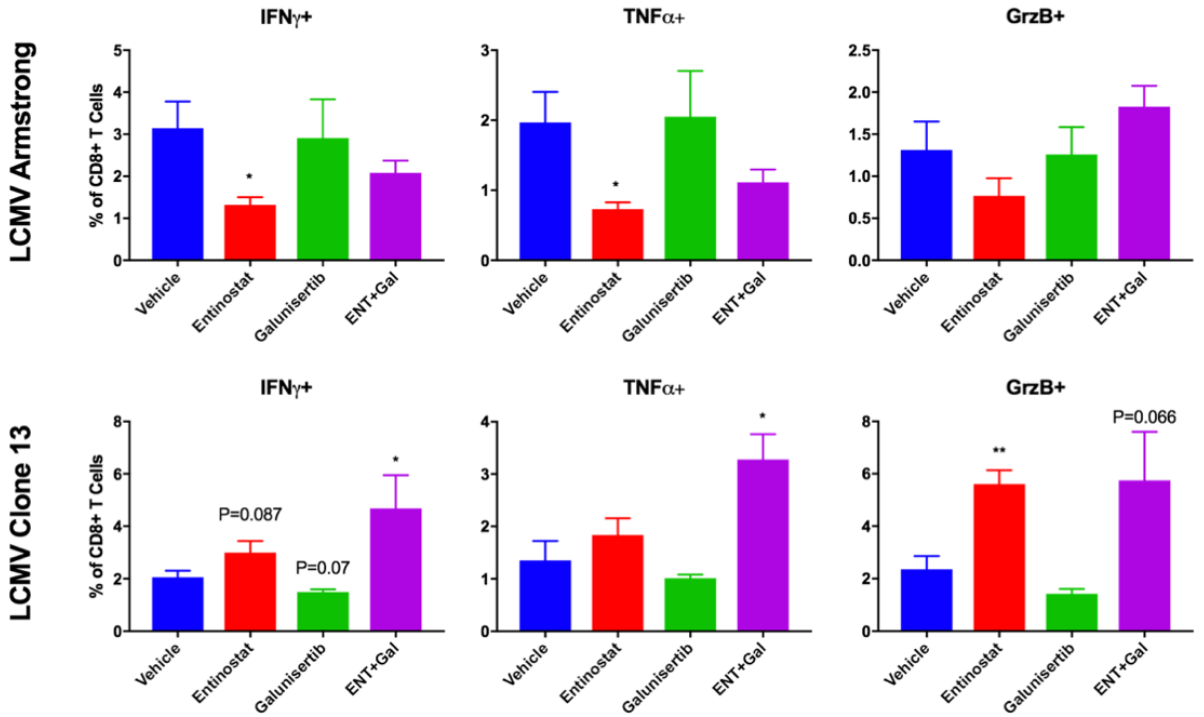


Figure 17: Cytokine production is altered by TGF- β 1/Class I HDAC inhibition during acute and chronic infection

Top Panel: Proportions of IFN γ , TNF α , and granzyme B producing CD8 $^+$ T cells after 6 hours *ex vivo* stimulation with GP33 peptide at day 7 post-infection

Bottom Panel: Proportions of IFN γ , TNF α , and granzyme B producing CD8 $^+$ T cells after 6 hours *ex vivo* stimulation with GP33 peptide at day 28 post-infection

Figure 18

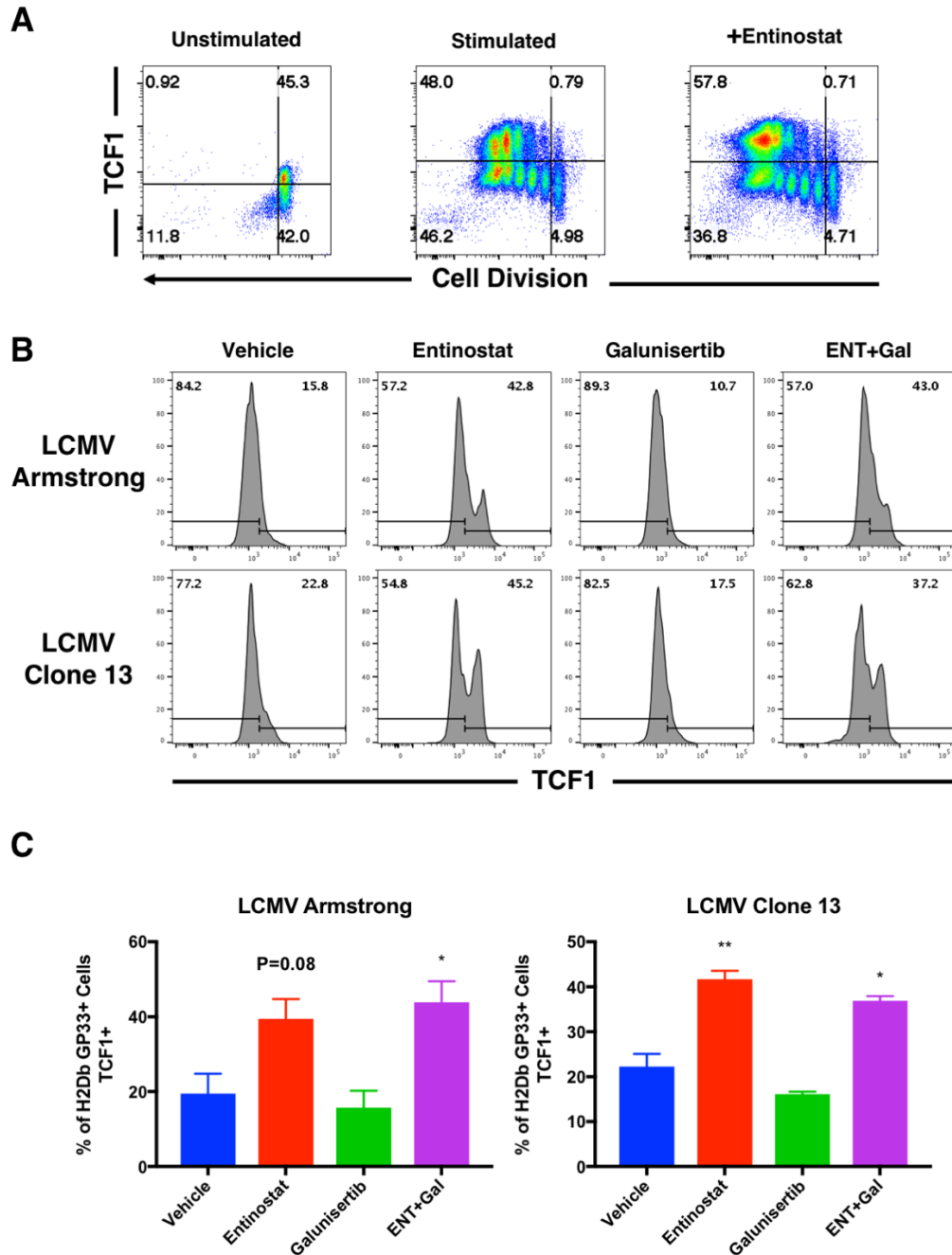


Figure 18: TCF1 expression is retained in a higher proportion of antigen-specific CD8+ T cells in mice treated with class I HDAC inhibition

A) Human CD8+ T cells were stimulated *in vitro* for 4 days in the presence of 100 nM entinostat and TCF1 expression was examined in relationship to cell division

B) TCF1 expression in gp33 tetramer positive CD8+ T cells at day 7 post-infection

C) Summary of TCF1+ gp33 tetramer positive CD8+ T cells at day 7 post-infection

Figure 19

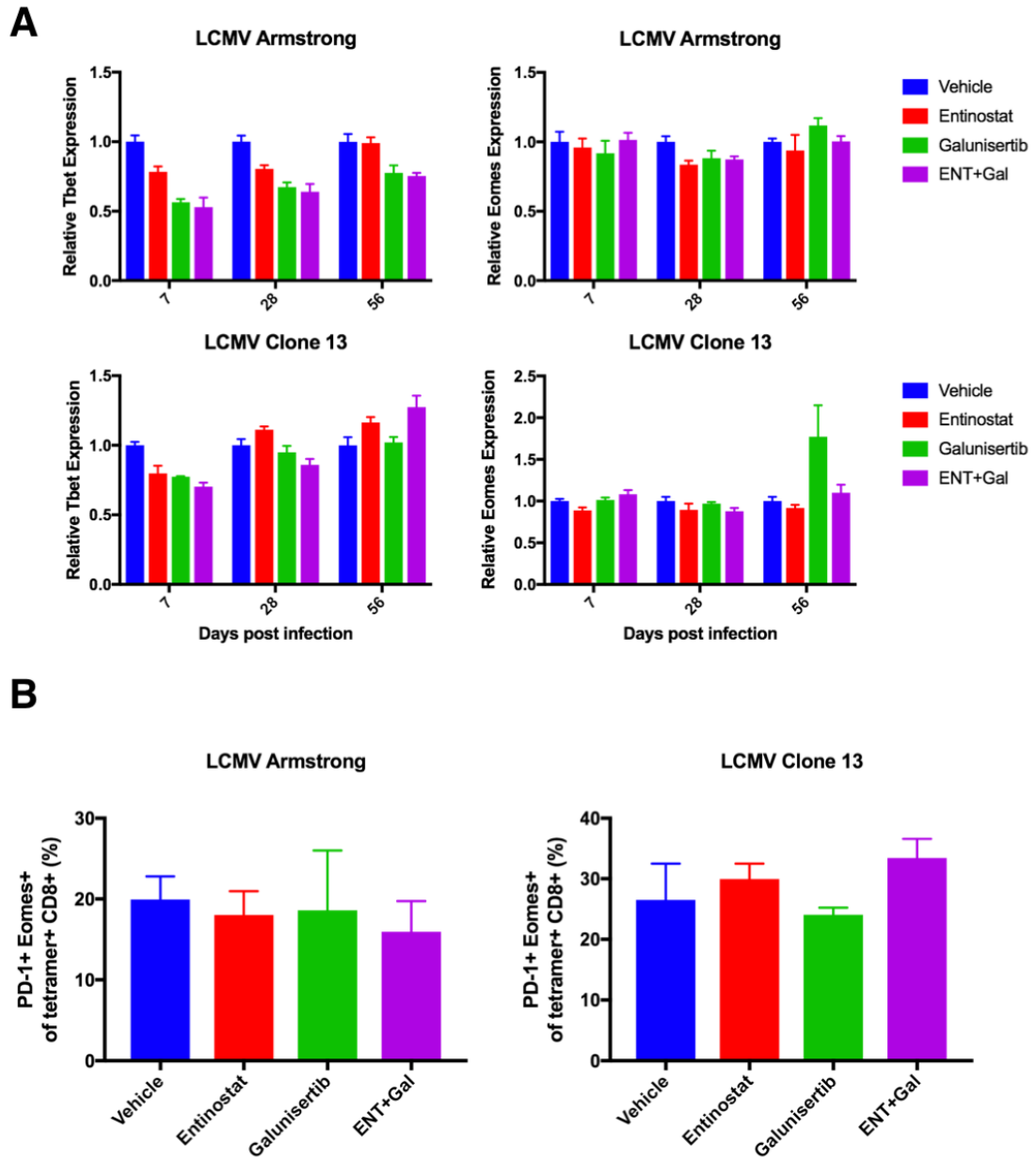


Figure 19: Tbet and Eomes expression are similar between TGF- β 1/class I HDAC inhibited CD8+ T cells

A) Tbet and Eomes expression at days 7, 28, and 56 in gp33 tetramer positive CD8+ T cells, normalized at each time point to the vehicle control group by MFI

B) PD-1+ Eomes+ gp33 tetramer positive CD8+ T cells at day 7 post-infection

Figure 20

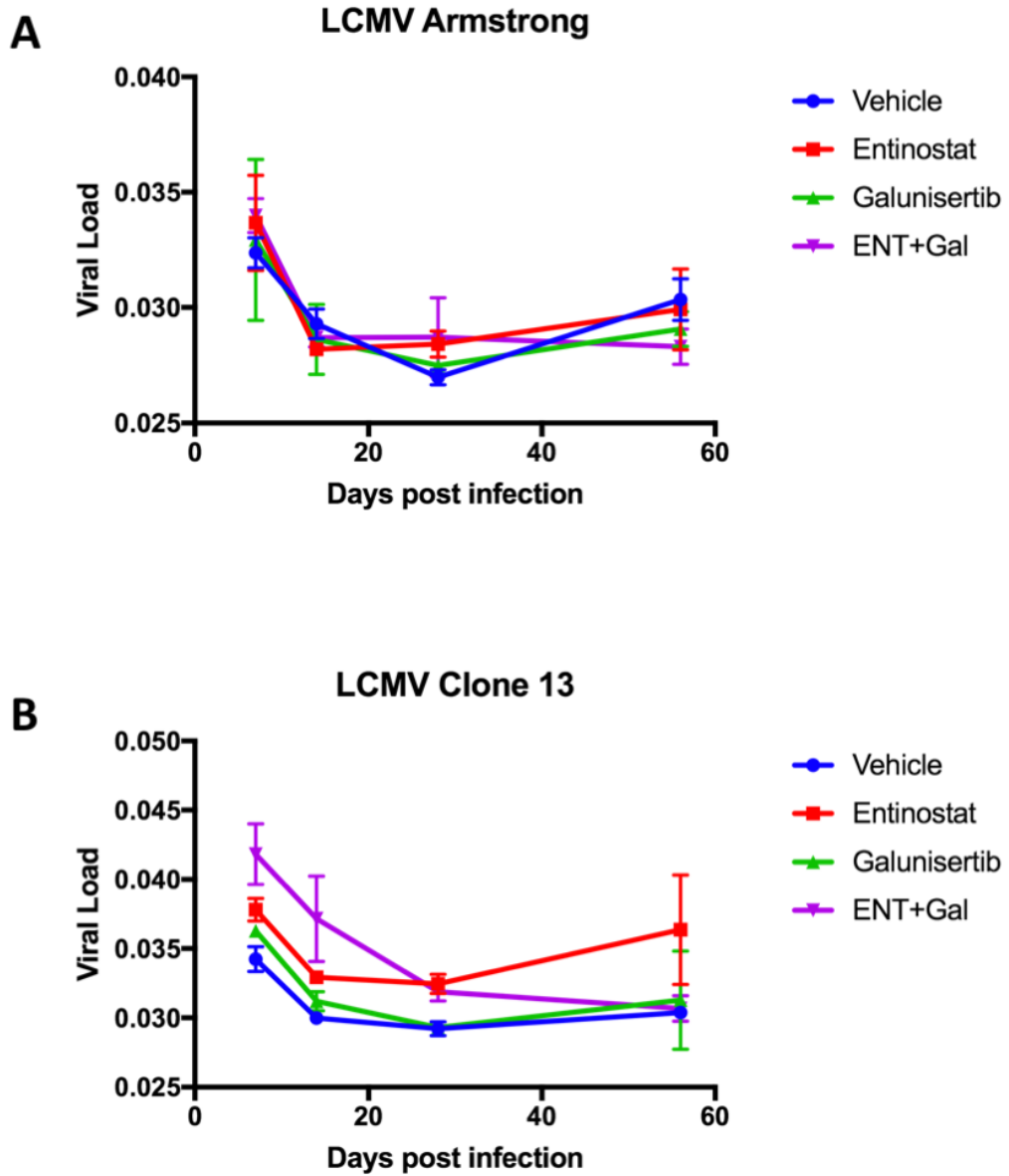


Figure 20: LCMV virus levels are higher in the serum of class I HDAC inhibited mice

A) LCMV Armstrong virus levels in the serum of mice quantified by qPCR over time

B) LCMV clone 13 virus levels in the serum of mice quantified by qPCR over time

CHAPTER 5

Entinostat synergizes with checkpoint blockade to generate anti-tumor immunity

Introduction

Cancers can express a number of different types of antigens that can be recognized by the immune system and target the cancer for destruction. These include overexpressed tissue antigens, endogenous retroviruses that become expressed as a result of genetic dysregulation, developmental antigens that are expressed during normal development, but expression is silenced in the mature tissue, and mutation-associated neoantigens (MANA)¹¹⁸. Indeed, cancers with a higher mutational burden have been shown to have a better response rate to immunotherapies¹¹⁹. However, cancers that present clinically have developed resistance mechanisms to immune attack. These suppressive mechanisms include T cell reprogramming and exclusion by immunosuppressive cytokines, the recruitment of suppressive cell populations to the tumor microenvironment (TME), and the engagement of inhibitory checkpoints on tumor-specific T cells.

Immune checkpoints can be engaged in the TME by their ligands, thereby blunting an anti-tumor response. Blockade of these checkpoints has been shown to have clinical efficacy and lead to durable remissions in subset of cancers and patients. However, a majority of patients do not respond to these therapies. Understanding the mechanisms of resistance to checkpoint blockade and the development of new strategies to render the immune systems of these patients responsive is an area of unmet need and active research.

Based on our data in the LCMV model of acute and chronic infection, we hypothesized that epigenetic therapy may alter the phenotypic and functional

characteristics of tumor-specific CD8+ T cells. Entinostat induces the expression of multiple immune checkpoints on antigen-specific CD8+ T cells, likely correlating with a heightened activation and effector status. However, these cells are also the most susceptible to inhibition by the TME, since they express more targets for negative regulatory engagement. We hypothesized that combining class I HDACi with the appropriate checkpoint blockade would lead to an improved anti-tumor immune response compared to checkpoint blockade alone. In this chapter, we test this hypothesis in the challenging Myc-CaP model of murine prostate cancer¹²⁰. This syngeneic tumor model was derived as an androgen-dependent cell from a c-myc transgenic mouse with prostate cancer. This cell line faithfully reproduces the behavior of prostate cancer in humans, with castration leading to an initial rapid and deep tumor regression, followed by the emergence of castration resistance. We have previously shown that castration is an immune priming event in prostate cancer, leading to the presentation of prostate cancer antigens in the draining lymph nodes and that this tumor model is generally unresponsive to checkpoint immunotherapy^{121–123}. We tested the hypothesis that HDACi in combination with checkpoint blockade can lead to an anti-tumor immune response in this model.

Results

To test the hypothesis that HDACi would enhance the efficacy of immune checkpoint we utilized the Myc-CaP model of androgen-dependent prostate cancer. Two million Myc-CaP cells were implanted subcutaneously, and tumors were treated

upon reaching an approximate volume of 500 mm³. Upon reaching that volume, mice were given degarelix, a GnRH antagonist, which leads to pharmacological castration. Simultaneously, mice were given entinostat in combination with checkpoint blockade agents as detailed in the experimental schematic (Fig 21A). Reflecting previous results, we saw that castration in combination with the isotype control antibody led to an initial regression of tumors followed by castration-resistance and tumor growth. As has been demonstrated previously by the lab, PD-L1/PD-1 axis blockade had no therapeutic effect. Likewise, TIM-3 blocking antibody was unable to induce an effective anti-tumor immune response with tumors growing similarly to the isotype control group (Fig 21B). Depleting IgG2a CTLA-4 antibody was able to achieve some efficacy both alone and in combination with entinostat (Fig 21B). While there was an effect on tumor outgrowth, CTLA-4 alone did not lead to a survival advantage compared to isotype control, leading to a 6 day increase in median survival but not achieving the threshold of statistical significance (Fig 21C). Entinostat in combination with CTLA-4 blockade led to a median survival of 39 days, reaching the threshold of statistical significance and leading to a survival benefit compared to vehicle control. In comparison to entinostat only (not shown) the survival was greater (median survival 33 days vs 39); however, did not achieve statistical significance.

Since the combination of entinostat and anti-CTLA-4 had led to a statistically significant survival benefit, we investigated the changes in T cell composition within the TME. T cell infiltration was greatly increased in groups containing anti-CTLA-4 (Fig 22A). As a percentage of total T cells, there was no difference in CD4+ and CD8+ T cell

infiltration between groups. However, the number of CD4+ and CD8+ T cells per milligram of tumor was greatly increased in mice treated with anti-CTLA-4. The addition of entinostat to anti-CTLA-4 did not significantly change the level of T cell infiltration, therefore, it is unlikely that the mechanism by which the combination treatment leads to a survival advantage is due to increased T cell recruitment alone.

We next investigated the changes in checkpoint expression after entinostat treatment and checkpoint blockade. For this we focused on entinostat in combination with CTLA-4, since this was the only combination to have any survival advantage. Tumors were harvested at day 7 post-castration and single cell suspensions were examined by flow cytometry. The expression of LAG-3 and TIM-3 were similar and unchanged between all groups (data not shown). CTLA-4 was the only checkpoint molecule with changes in expression on CD8+ T cells. Interestingly, entinostat alone was able to induce expression of CTLA-4 on CD8+ tumor-infiltrating lymphocytes (TIL). CTLA-4 treatment further increased the expression of CTLA-4 on TIL and the combination of entinostat and CTLA-4 led to the highest level of PD-1 and CTLA-4 co-expression on CD8+ TIL (Fig 22B/C). The expression of checkpoints on CD8+ TIL can either be a marker of activation or a marker of exhaustion. Expression alone is insufficient to establish the functional status of these T cells.

In light of the longer survival of mice treated with the combination of entinostat and CTLA-4 checkpoint blockade, we hypothesized that the heightened expression of CTLA-4 on these cells might be an indicator of greater effector capacity. To test this, single cell suspensions of tumor were stimulated *ex vivo* and stained intracellularly for

cytokine production. While entinostat alone and CTLA-4 checkpoint blockade alone had modest effects on the production of cytokines, the combination led to a large increase in the number of cells producing IFN γ , TNF α , and GrzB (Fig 23 A/B), indicating that CD8+ TIL from combination treated mice expressed the highest levels of PD-1 and CTLA-4 and also produced the most effector cytokines. Thus, the heightened expression of immune checkpoints in this context correlated with greater effector function.

CTLA-4 is highly expressed regulatory T cells in comparison to non-Treg CD4+ and CD8+ T cells (Fig 24A). Indeed, the average level of CTLA-4 expression on Treg was 14-fold higher than CD8+ T cells. Thus, we hypothesized that a second mechanism by which the anti-CTLA-4 treatment leads to a survival advantage was through targeting of Treg populations. Anti-CTLA-4 treatment led to a relative depletion of Treg as a percentage of all CD4+ T cells (Fig 24B). However, closer examination revealed that Treg infiltration was actually increased in tumors treated with anti-CTLA-4 alone or in combination with entinostat. Thus, the depletion effect seen is primarily driven by massive non-Treg CD4+ and CD8+ T cell infiltration of the tumor, diluting the Treg population within the T cell compartment as a whole (Fig 24C). Within the Treg compartment there was comparatively less PD-1, CTLA-4 and PD-1, 4-1BB co-expressing Treg in mice treated with anti-CTLA-4 or combination. These Treg have been reported to have a more activated phenotype which correlates with greater suppressive capacity. Therefore, anti-CTLA-4 treatment leads to the infiltration of large numbers of T cells into the tumor. This T cell mixture contains CD4, CD8, and Treg cells. However, the relative number of Treg compared to other T cell types is diluted. Furthermore, in mice treated with

entinostat in combination with anti-CTLA-4, the CD8+ T cells have greater effector function.

Discussion

Here, we have examined the effect of combining HDACi with checkpoint blockade in a challenging murine tumor model that is generally unresponsive to immunotherapy. We found, consistent with previous results, that most checkpoint blockades were ineffective in eliciting anti-tumor immunity in this model¹²³. Anti-CTLA-4 treatment in combination with HDACi led to a survival benefit. This was accompanied by greater T cell infiltration to the TME, greater activation status of CD8+ T cells, and greater effector function. Regulatory T cells were reduced in the TME as a percentage of all T cells and Tregs corresponding to a highly suppressive phenotype were depleted.

As was shown in previous chapters, HDACi alter the checkpoint expression profile of CD8+ T cells. This correlated with greater effector potential. In the LCMV model, in the absence of checkpoint blockade, this led to greater exhaustion and T cell dysfunction leading to higher viral load. This is likely due to the engagement of the expressed checkpoints by their ligands. The TME is rich in immunosuppressive mechanisms, therefore, HDACi alone are unlikely to yield a better immune response. However, pairing HDACi with an appropriate checkpoint blockade such as anti-CTLA-4 in this example, led to a better anti-tumor immune response. CD8+ T cells with greater effector capacity infiltrated the tumor and provided a survival benefit.

These data highlight the complexity of combining epigenetic modulating agents, such as HDACi, with traditional immunotherapies like checkpoint blockade. These drugs are not cell-type specific and can have effects on multiple cells. Tumor, stromal, myeloid, and lymphoid cells can all be affected by HDACi. While we have attempted to understand some of the effects that HDACi have on CD8+ T cells, their effects on regulatory T cells, conventional CD4+ effector T cells, and myeloid cells has not been well studied^{124–130}. Predicting the sum total of HDACi effects on these cell populations and its effect on anti-tumor immunity is challenging and can only be understood after understanding the effects of these inhibitors on each subset. The effects of entinostat on regulatory T cells and myeloid-derived suppressor cells (MDSC) have been published. However, these studies are incomplete, with outstanding questions remaining in the field. Entinostat has been reported to render both Tregs and MDSC less suppressive by several groups. However, the finding that entinostat, even at low *in vivo* doses such as used in these studies (5 mg/kg, direct anti-tumor dose greater than 20 mg/kg), can lead to T cell dysfunction is novel. These data will help inform future pre-clinical and clinical development of combination immunotherapies using HDACi.

Materials and Methods

Eight-to-10-week-old male FVB/NJ mice were used for all experiments. All mice were maintained in an American Association for the Accreditation of Laboratory Animal Care International accredited facility (AAALAC) according to the National Institute of Health Animal Care guidelines, Institutional Biosafety Committee guidelines, and procedures

were carried out under protocols approved by the Johns Hopkins and Columbia University Animal Care and Use Committee. Mice were housed in a specific-pathogen free colony. FVB/NJ mice were purchased from Jackson Laboratory.

Myc-CaP tumor experiments

Myc-CaP, derived from prostate cancer in c-Myc transgenic mice, was a generous gift from Dr. Charles Sawyers and was maintained in complete DMEM media. Cells were tested to be mycoplasma free. Eight-to-10 week old mice were implanted with 1.5×10^6 tumor cells in the right flank in 100 μ L PBS. Tumor diameters were measured every 3 days. Tumor volume was calculated using the formula: length x (width)² x 0.5. When tumor volumes reached 500 mm³ mice were randomly assigned to treatment groups. Castration was carried out with 0.625 mg degarelix in 100 μ L water per mouse via subcutaneous injection. Overall survival was defined as the time between castration and death or tumor volume exceeding 2000 mm³, whichever event occurred first.

Immune checkpoint blockade

Anti-PD-L1 (clone 10F.9G2), and anti-TIM-3 (clone RMT3-23) were purchased from BioXCell. Anti-CTLA-4 (murine IgG2a) was a gift from Bristol Myers Squibb. Murine IgG2a (clone C1.18.4) was used as an isotype control (BioXCell). Antibody treatment was given as indicated in the experimental schematic at a dose of 200 μ g per mouse by intraperitoneal injection.

In Vivo Drug Treatment

Entinostat (Selleckchem) was dosed at 5 mg/kg by intraoral gavage. Drug was formulated in 2% DMSO, 30% PEG200, 68% water and was given once daily for 7 consecutive days starting at the time of castration.

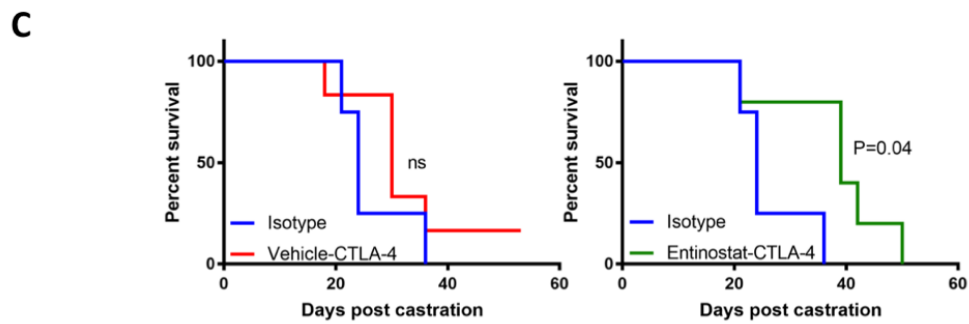
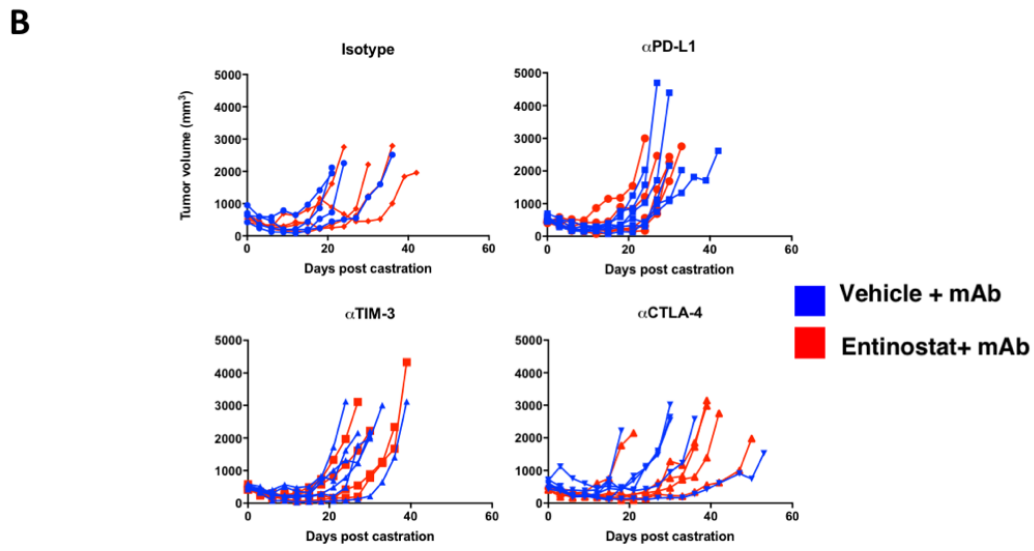
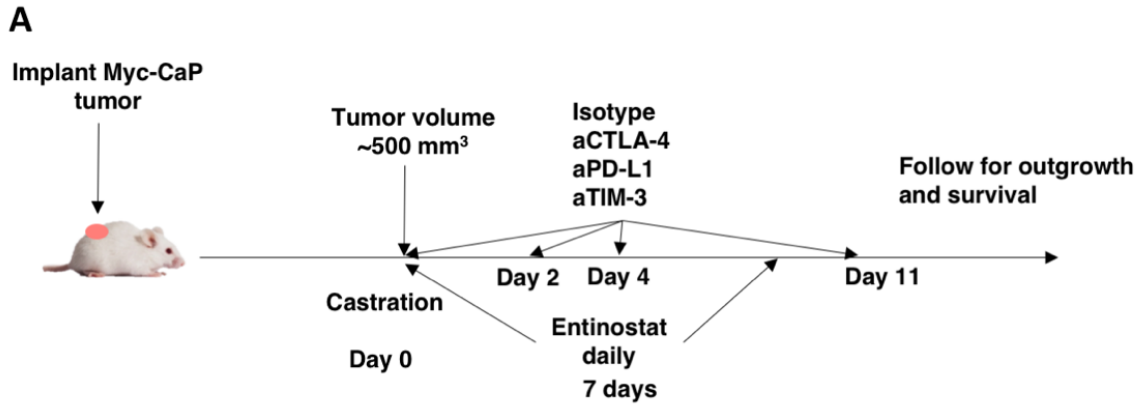
Flow Cytometry

Single-cell suspensions were prepared from tumors as follows: tumors were finely minced with scissors to 1-2 mm sized fragments. Tumor fragments were digested in a Miltenyi GentleMACS instrument using the Miltenyi mouse tumor dissociation kit. Cell suspensions were stained at room temperature for 30 minutes with fluorochrome conjugated antibodies and LIVE/DEAD viability dye. For intracellular staining, samples were permeabilized with the eBioscience FoxP3 fix/perm kit. *Ex vivo* stimulation was carried out using PMA (50 ng/mL) and ionomycin (500 ng/mL) for 4 hours in the presence of protein transport inhibitor cocktail (eBioscience).

Data Analysis

Flow cytometry data was analyzed on FlowJo software (Treestar). Statistical analysis was carried in GraphPad Prism v7.

Figure 21



Group	Median Survival (Days)
Vehicle	24
aCTLA-4	30
Entinostat+ aCTLA-4	39

Figure 21: Entinostat in combination with anti-CTLA-4 leads to survival advantage

A) Experimental schematic B) Spaghetti plots for tumor growth. Each line represents an individual mouse. Day 0 is the day of castration. C) Survival curves for indicated groups. Significance was calculated using the Log-rank test

Figure 22

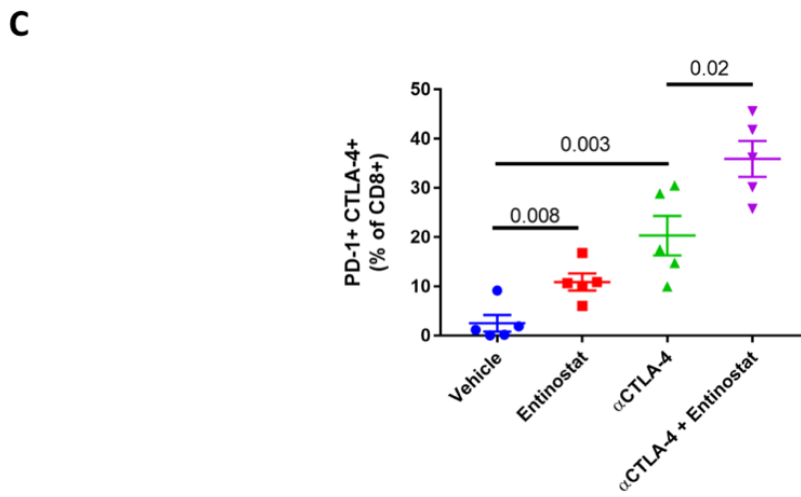
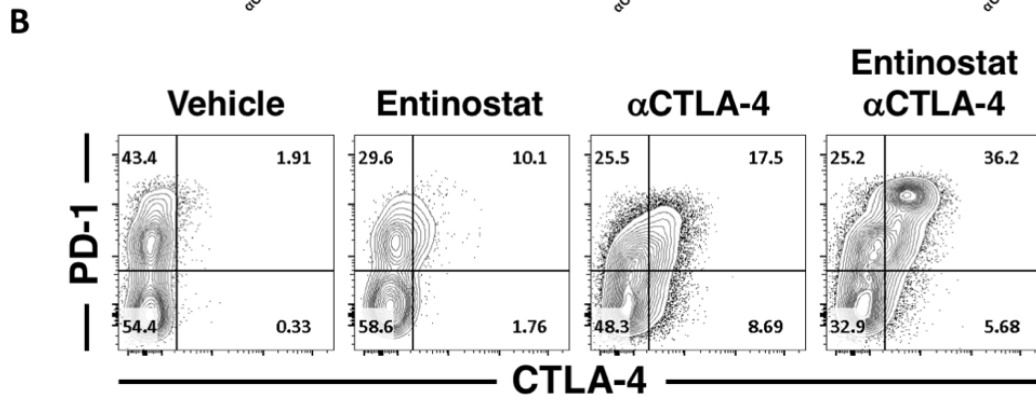
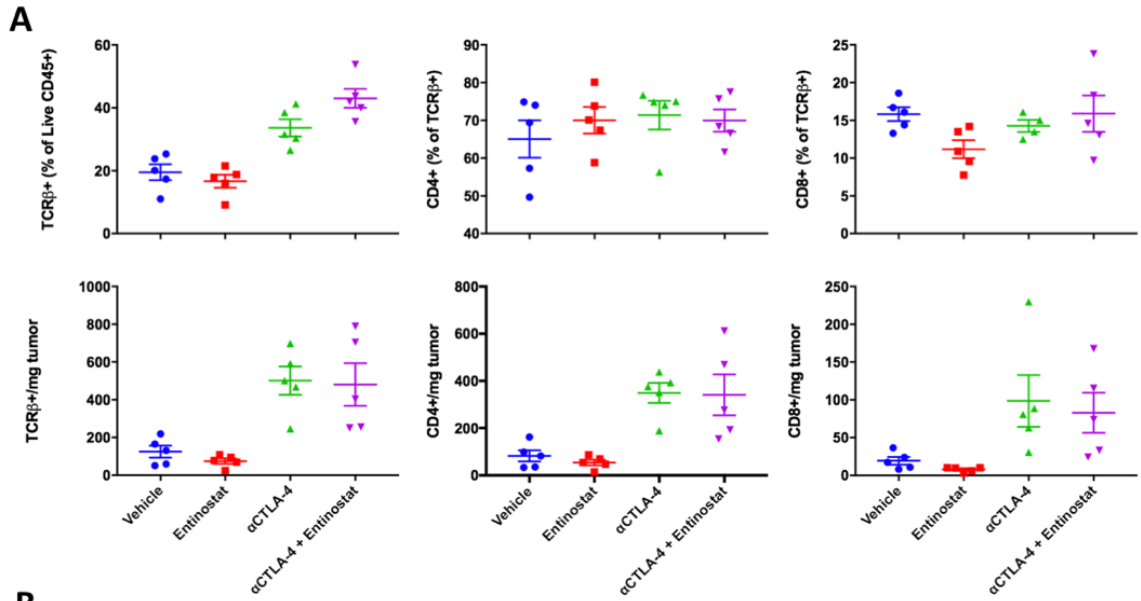


Figure 22: Combination anti-CTLA-4 and HDACi treatment lead to T cell infiltration to tumor and effector function

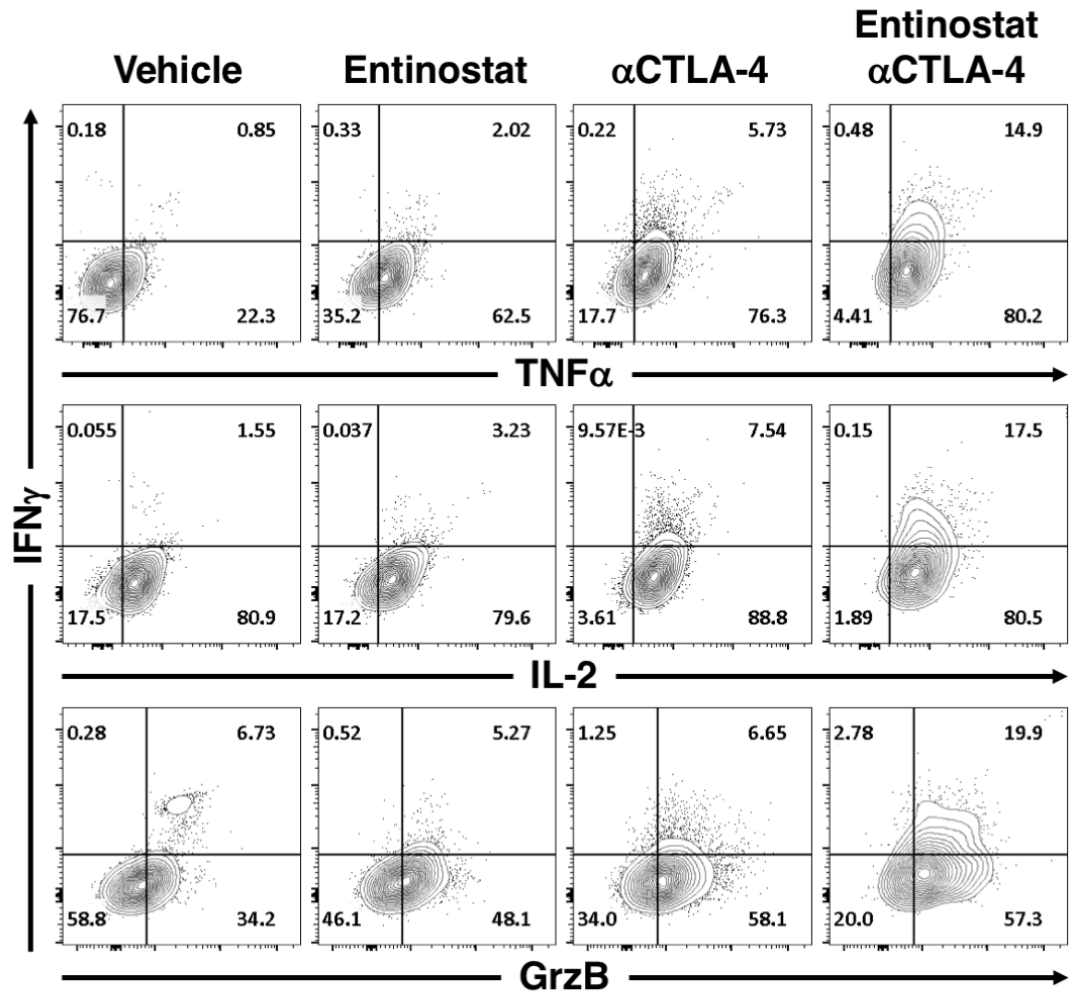
A) *Top row:* Total T cells (TCR β +), CD4+, and CD8+ T cell percentages are shown. *Bottom row:* Total T cells (TCR β +), CD4+, and CD8+ T cell numbers per milligram of tumor weight are shown

B) Representative flow cytometry plots showing PD-1 and CTLA-4 expressing CD8+ T cells in the TME.

C) Summary results for PD-1 and CTLA-4 co-expressing CD8+ T cells in the TME.

Figure 23

A



B

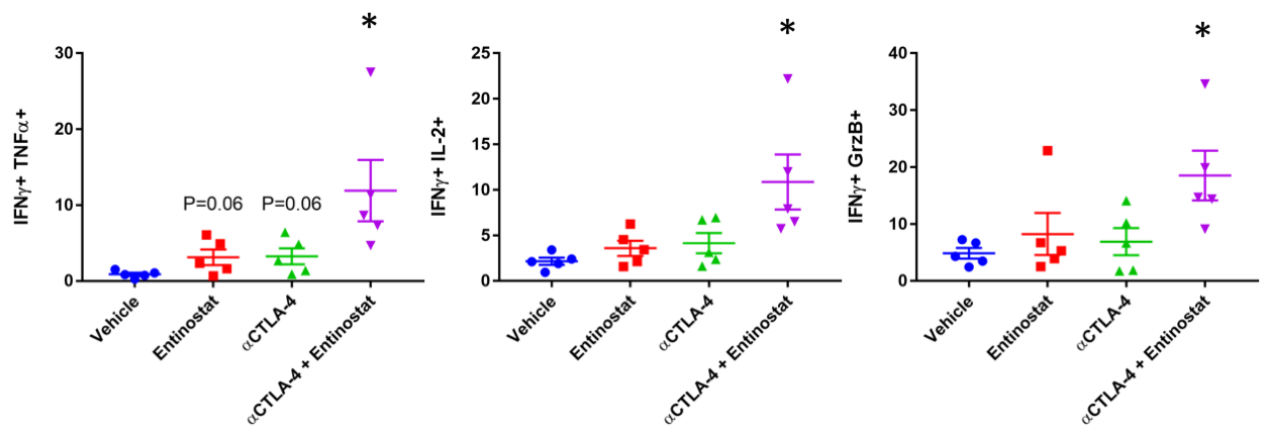


Figure 23: Combination entinostat and anti-CTLA-4 treatment lead to cytokine production in CD8+ TIL

A) Representative flow cytometry plots demonstrating co-production of IFN γ with TNF α , IL-2, and granzyme B.

B) Summary graphs for cytokine production in CD8+ TIL.

Figure 24

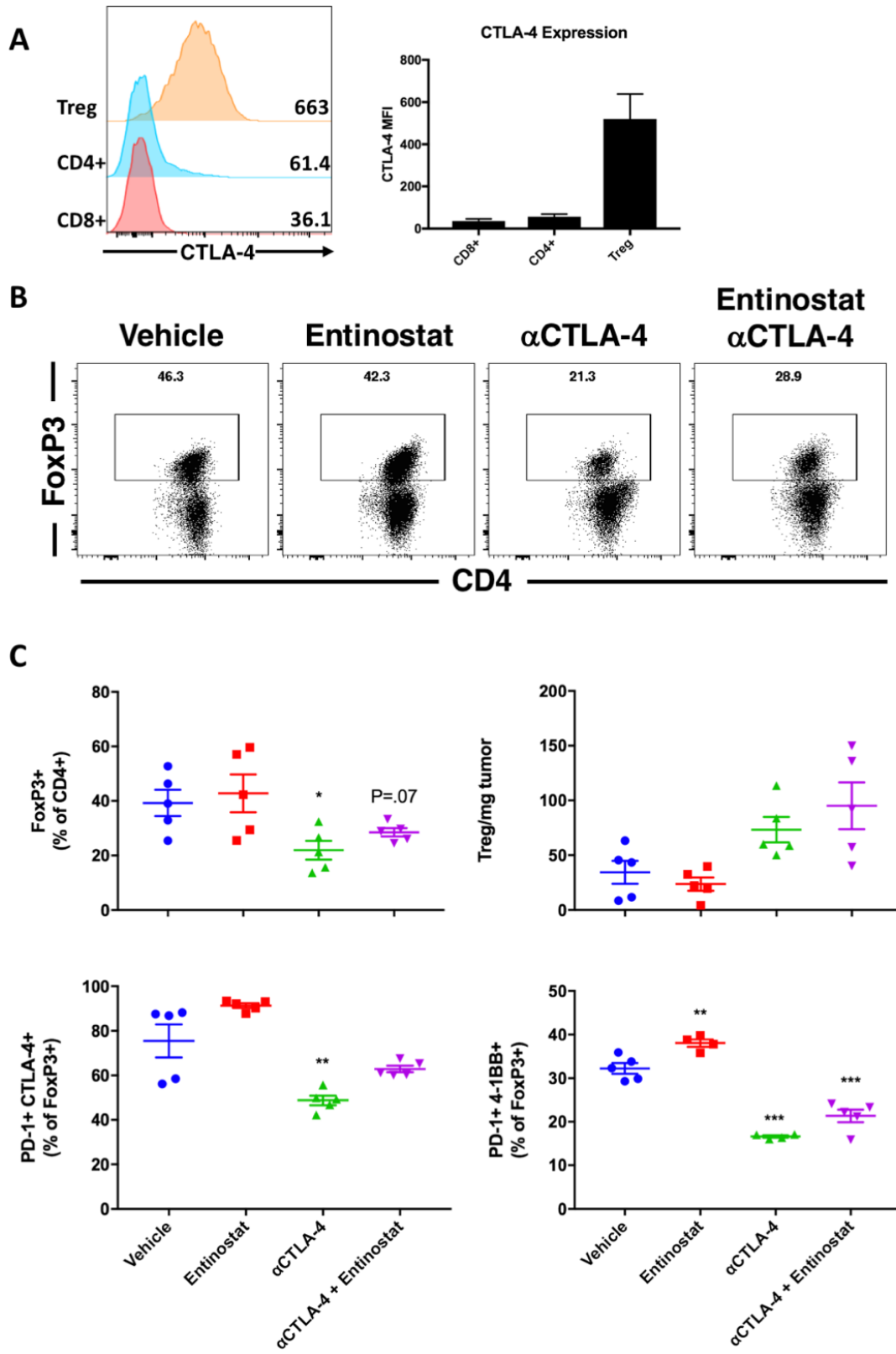


Figure 24: Anti-CTLA-4 reduces the percentage of regulatory T cells in the TME

A) Histogram and bar graph comparing the MFI of CTLA-4 in T cell populations within the TME

B) Representative flow cytometry plots of Treg abundance in the TME.

C) Summary graphs showing Treg abundance, Treg per milligram of tumor tissue, PD-1 and CTLA-4 co-expression on Treg, and PD-1 and 4-1BB co-expression on Treg

CONCLUSIONS AND FUTURE DIRECTIONS

The immune system has evolutionarily developed mechanisms to restrain overexuberant activation to prevent damage to the host. The importance of these mechanisms can be appreciated in patients with autoimmune disorders and those with chronic viral infections and cancer. These tolerance mechanisms include immunological ignorance, central and peripheral tolerance, anergy, exhaustion and senescence¹³¹. Exhaustion occurs in the setting of chronic T cell stimulation through the T cell receptor¹³². Persistent antigen encounter and chronic inflammation lead to the development of the exhausted state which is characterized by functional hyporesponsiveness in T cells. The “default” T cell program in response to a pathogen involves an initial rapid proliferation and acquisition of effector cytokine production and cytolytic capacity followed by a contraction of the T cell population to a small number of long-lived memory T cells with rapid recall ability to guard the host against subsequent encounters with the pathogen⁷⁵. In exhaustion, this program is altered. Chronic stimulation imprints a genetic and epigenetic program on T cells characterized by progressive and hierarchical loss of effector functions, upregulation and co-expression of multiple immune checkpoints, metabolic derangements and a failure to progress to the memory state in which T cells can persist in the absence of antigen. Checkpoints have been shown to have a role in the development and maintenance of the exhaustion program. However, the mechanisms which govern checkpoint expression of T cells are not well-studied. This work was undertaken with the goal of furthering our understanding of immune checkpoint regulation on CD8+ T cells, and to develop a

better understanding of how these mechanisms impact patients with cancer and chronic viral infections.

In chapter 1, we demonstrate that the immunoregulatory cytokine TGF- β 1 upregulates the expression of the immune checkpoint PD-1. This was dependent on signaling downstream of Smad3, a transcription factor involved in TGF- β 1 signaling. The upregulation of PD-1 occurred at both the RNA and protein level, suggesting that the action of TGF- β 1 was not at the post-transcriptional level. We followed up on this observation by examining the effect of TGF- β 1 on the expression of other immune checkpoints. For this analysis we selected CTLA-4 and TIM-3, two well-known and studied checkpoints expressed on CD8+ T cells. To our surprise we found that the expression of both checkpoints was strongly downregulated by TGF- β 1. We thought that this might be dependent on TGF- β 1 signaling through a Smad3 mediated signaling pathway. We found that a specific inhibitor of Smad3 was able to reverse this effect. Therefore, we conclude that TGF- β 1 differentially regulates some immune checkpoints. It upregulates the expression of PD-1, while down regulating the expression of CTLA-4, and TIM-3.

In chapter 2, we tested the hypothesis that coordinated, chromatin level programs involving histone acetylation might be involved in the regulation of immune checkpoints. We found that in response to activation *in vitro* CD8+ T cells increased the acetylation level of histone H3 in the promoter and proximal regulatory areas of immune checkpoint genes. This correlated well with increased expression of these genes. Because of the involvement of histone acetylation, we screened a limited

number of histone acetylation modifying drugs for their effect on immune checkpoint expression and found that the class I HDAC inhibitors upregulated the expression of TIM-3 and not PD-1. Since TGF- β 1 upregulated PD-1 expression and downregulated TIM-3, while class I HDAC inhibitors upregulated TIM-3 but not PD-1, we examined the histone acetylation landscape in proximity to immune checkpoints during T cell activation in the presence of TGF- β 1 or entinostat. We found that CTLA-4 and TIM-3 had increased promoter acetylation during activation with entinostat but PD-1 had increased promoter acetylation during activation with TGF- β 1. Since Smad3 inhibition also increased the expression of TIM-3 and CTLA-4, we tested whether the combination of the two would have additive effects on the expression of these two immune checkpoints. We found that the combination of SIS3 and entinostat led to the highest expression of TIM-3. This combination also correlated to the largest difference in histone acetylation at the promoters of these genes relative to TGF- β 1. Thus, we concluded that TGF- β 1 differentially regulates immune checkpoints on a chromatin level, in a process dependent on class I HDACs cooperating with Smad3.

In chapter 3, we asked do T cells expressing different patterns of immune checkpoints have different functional capabilities? To probe this, we used TGF- β 1 and combination entinostat and SIS3 treatment to drive T cells to phenotypes either expressing high levels of PD-1 and intermediate to low levels of other checkpoints, or to express high levels of other immune checkpoints in co-expression with intermediate levels of PD-1. We discovered two clusters of TGF- β 1 regulated genes. A cluster which was upregulated by TGF- β 1 and this included PD-1. A second cluster was identified

which was downregulated by TGF- β 1 and included CTLA-4, TIM-3, TIGIT, CD39, A2AR, CEACAM1, and BTLA. The expression of the second cluster could be increased by combination treatment with entinostat and SIS3. The correlation and patterns of expression of these two clusters were found on both the RNA and protein level. The PD-1 high T cells expressed higher levels of IL-2 and TNF α while the TIM-3, CTLA-4 high cells expressed high levels of IL-1 β and granzyme B. We conclude, TGF- β 1 drives a particular T cell fate characterized by high levels of PD-1, lower levels of other checkpoints, and the production of IL-2. Inhibition of this pathway combined with class I HDAC inhibition led to the development of T cells that expressed high levels of granzyme B and IL-1 β . Importantly, the question arises if the cells treated with HDACi and Smad3 inhibitor are more susceptible to exhaustion due to the expression of multiple immune checkpoints.

In chapter 4, we took our *in vitro* observations to a well-established *in vivo* model of T cell activation and exhaustion, utilizing the LCMV model of acute and chronic infection. We found results that were similar to those obtained in the *in vitro* system. Treatment of mice with entinostat, galunisertib (a Smad3 inhibitor), or the combination of the two led to increased number of antigen-specific T cells that expressed multiple immune checkpoints in both acute and chronic infection. The expression of more immune checkpoints correlated with enhanced proliferation and expansion of antigen-specific populations during the course of both acute and chronic infection; however, at late time points population levels were equivalent. Despite this, the difference in cytokine production was not great between the different treatment groups. Nor were there large differences in the expression of transcription factors known to be important

in the programming of exhaustion. Ultimately, we found that the viral load was higher in chronic infection in mice treated with HDACi or the combination, leading us to conclude that these cells were not as capable as their control counterparts at controlling infection and are likely more exhausted.

In chapter 5, we pursued two goals. First, to test the hypothesis that HDAC inhibition will induce checkpoint expression in a cancer model. Second, to test the hypothesis that HDAC inhibition when combined with an appropriate checkpoint blockade agent, may lead to survival benefit and anti-tumor immunity. For these studies, we chose the challenging Myc-CaP model of prostate cancer that is poorly responsive to immunotherapy^{120,123}. We found that entinostat in combination with anti-CTLA-4 led to both a reduction in tumor outgrowth and a survival advantage. This correlated with high levels of PD-1 and CTLA-4 co-expression. CD8+ TIL from combination treated mice also produced high levels of effector cytokines. We concluded that entinostat in combination with appropriate checkpoint blockade can have anti-tumor effect.

Our findings in this thesis, represent a novel finding regarding HDAC regulation of T cell exhaustion. The role of HDAC enzymes in this regulation suggests that chromatin structure can inhibit expression of transcriptional programs that lead to the production of multiple checkpoint molecules. However, it remains unclear and a subject for future work how the balance of chromatin changes by HDACs and transcriptional activation by specific factors cooperate to regulate the expression of inhibitory molecules.

PD-1 has been previously shown to be regulated by epigenetic modifications, in particular the role of DNA methylation has been well-studied in this context. The PD-1 promoter is demethylated during chronic LCMV expression, leading to PD-1 expression^{61,63,133}. This demethylation is durable, even when the cells are transferred to a new environment lacking the antigen with even higher PD-1 expression levels upon rechallenge. ATAC-seq profiling studies have shown that exhausted T cells have a chromatin landscape distinct from that of effector and memory T cells⁷²⁻⁷⁴. Blockade of PD-L1, the ligand for PD-1, does not substantially alter the epigenetic profile of these T cells. This suggests that rewiring of the exhaustion epigenetic program is unlikely to occur with single checkpoint blockade, despite the temporary reversal of exhaustion characteristics and T cell reinvigoration. It also implies that discontinuation of checkpoint blockade in both mice and people that have responded to checkpoint blockade will lead to reacquisition of the exhaustion phenotype in T cells. Our data suggests that signaling through molecular mechanism other than the checkpoint molecules themselves may regulate the exhaustion program and that reversal of this program will require chromatin level program changes that might be induced by epigenetic agents.

We have demonstrated, for the first time, that checkpoint molecules are regulated by different chromatin level programs. We saw TGF- β 1 upregulated PD-1, but decreased the expression of TIM-3, CTLA-4, LAG-3, and ENTPD1 (CD39). Giving credence to this finding a recent study examining the role of EGR2 in the development of T cell exhaustion in murine tumors found that a subset of checkpoints was controlled by EGR2

including LAG-3 and 4-1BB (TNFRSF9), but not PD-1¹⁰⁴. Our findings similarly showed that 4-1BB and LAG-3 were coregulated with TIM-3 and CTLA-4, but not with PD-1. Of course, to simply say that all checkpoints besides PD-1 are regulated coordinately is likely inaccurate. Under the conditions that we have examined in this body of work we have found them to co-regulated. However, as is the case of the EGR2 study above, the interaction of specific transcription factors with chromatin dynamics likely controls the expression of individual checkpoints. In some physiological contexts, this regulation will be coordinate, and in others distinct. In the context of TGF- β 1, PD-1 is distinctly controlled from other checkpoints. However, it is important to note that in both murine and human tumors, PD-1 is often co-expressed with multiple checkpoints including CTLA-4, LAG-3, and TIM-3. Thus, in the context of a complex TME, it is the sum total of all molecular influences that will dictate the total checkpoint expression profile of a T cell, and in turn, its susceptibility to dysfunction and responsiveness to checkpoint blockade.

PD-1 expression does not necessarily mean T cells are exhausted. Previous work has shown that exhaustion may develop independently of PD-1. Genetic deficiency of PD-1 in CD8+ T cells in chronic LCMV infection did not inhibit the development of exhaustion and, in fact, led to higher levels of other inhibitory molecules on the dysfunctional CD8+ T cells¹⁰³. Our findings support these observations. In our *in vitro* model, high expression of PD-1 and low expression of other immune checkpoints driven by TGF- β 1 led to the development of T cells with effector cytokine production capacity and polyfunctionality. In contrast, abrogation of TGF- β 1 signaling or inhibition of class I

HDAC led to T cells that had a loss of polyfunctionality and expressed higher levels of granzyme B, consistent with a less functional phenotype.

Our findings suggest a previously unappreciated role for TGF- β 1 in regulating CD8+ T cell exhaustion. Contrary to what might have been expected, given its known immunoregulatory functions^{134,135}, inhibition of TGF- β 1 signaling *in vitro* and *in vivo* led to the development of T cells with more profound dysfunction. While further work is needed to carefully dissect this phenotype and understand the molecular mediators involved, it appears that TGF- β 1 may promote a state of tempered exhaustion associated with greater functionality. This suggests the intriguing hypothesis that TGF- β 1 may act as a molecular thermostat, regulating the depth of exhaustion that a T cell may achieve during chronic antigen encounter. This is particularly important in the setting of chronic infections. Exhausted T cells, while hypofunctional, are not inert and play an important role in maintaining the stalemate between pathogen and host. Loss of these T cell population quickly leads to the host succumbing to infection. Thus, understanding the role of TGF- β 1 in chronic infection and by extension cancer, its major sources of production, and the locations in which it may influence T cell behavior and the development of exhaustion is important. Several groups have begun to probe this question and have demonstrated that TGF- β 1 excludes T cells from the TME in several different mouse models^{136,137}. Combining TGF- β 1 inhibitors with checkpoint blockade demonstrates synergistic effect and these combinations are being examined in the clinic.

A major strength of this body of work is that findings have been consistent in both mouse and human T cells, *in vitro* and *in vivo*. Further work is needed, particularly in murine tumor models to fully understand the mechanisms at play in the epigenetic and environmental control of T cell exhaustion.

In summary, we have identified a novel mechanism by which the environment can influence epigenetic programming of T cell dysfunction. These data suggest that different molecular and epigenetic programs control checkpoint expression and development of exhaustion. The functional and therapeutic consequences of this regulation remain to be more fully examined; however, initial evidence points to a therapeutic opportunity if epigenetic agents are rationally combined with immune checkpoint blockade. These data also serve as a cautionary tale that combining these powerful agents empirically may lead to worsening of the exhaustion phenotype that we are trying to reverse, potentially leading to worse outcomes for patients. Done correctly, this may lead to advances in how we think about rationally combining epigenetic reprogramming with checkpoint blockade in the clinic.

References:

1. Hanahan, D. & Weinberg, R. A. Hallmarks of Cancer: The Next Generation. *Cell* **144**, 646–674 (2011).
2. Pardoll, D. M. The blockade of immune checkpoints in cancer immunotherapy. *Nature reviews. Cancer* **12**, 252–64 (2012).
3. Topalian, S. L., Drake, C. G. & Pardoll, D. M. Targeting the PD-1/B7-H1(PD-L1) pathway to activate anti-tumor immunity. *Current opinion in immunology* **24**, 207–12 (2012).
4. Shankaran, V. *et al.* IFN γ and lymphocytes prevent primary tumour development and shape tumour immunogenicity. *Nature* **410**, 1107–1111 (2001).
5. Mittal, D., Gubin, M. M., Schreiber, R. D. & Smyth, M. J. New insights into cancer immunoediting and its three component phases—elimination, equilibrium and escape. *Curr Opin Immunol* **27**, 16–25 (2014).
6. BUET, M. Cancer; a biological approach. I. The processes of control. *British medical journal* **1**, 779–86 (1957).
7. Schreiber, R. D., Old, L. J. & Smyth, M. J. Cancer Immunoediting: Integrating Immunity's Roles in Cancer Suppression and Promotion. *Science* **331**, 1565–1570 (2011).
8. Koebel, C. M. *et al.* Adaptive immunity maintains occult cancer in an equilibrium state. *Nature* **450**, 903 (2007).
9. Zaretsky, J. M. *et al.* Mutations Associated with Acquired Resistance to PD-1 Blockade in Melanoma. *The New England Journal of Medicine* **375**, 819–829 (2016).
10. Topalian, S. L., Drake, C. G. & Pardoll, D. M. Immune checkpoint blockade: a common denominator approach to cancer therapy. *Cancer cell* **27**, 450–61 (2015).
11. Calcinotto, A. *et al.* IL-23 secreted by myeloid cells drives castration-resistant prostate cancer. *Nature* **559**, 1 (2018).
12. Kumar, V., Patel, S., Tcyganov, E. & Gabrilovich, D. I. The Nature of Myeloid-Derived Suppressor Cells in the Tumor Microenvironment. *Trends in Immunology* **37**, 208–220 (2016).
13. Parker, K. H., Beury, D. W. & Ostrand-Rosenberg, S. Myeloid-Derived Suppressor Cells: Critical Cells Driving Immune Suppression in the Tumor Microenvironment. *Advances in cancer research* **128**, 95–139 (2015).

14. Plitas, G. *et al.* Regulatory T Cells Exhibit Distinct Features in Human Breast Cancer. *Immunity* **45**, 1122–1134 (2016).
15. Josefowicz, S. Z., Lu, L.-F. F. & Rudensky, A. Y. Regulatory T cells: mechanisms of differentiation and function. *Annual review of immunology* **30**, 531–64 (2012).
16. Ghasemzadeh, A., Bivalacqua, T. J., Hahn, N. M. & Drake, C. G. New Strategies in Bladder Cancer: A Second Coming for Immunotherapy. *Clinical Cancer Research* **22**, 793–801 (2016).
17. Tivol, E. *et al.* Loss of CTLA-4 leads to massive lymphoproliferation and fatal multiorgan tissue destruction, revealing a critical negative regulatory role of CTLA-4. *Immunity* **3**, 541–7 (1995).
18. Waterhouse, P. *et al.* Lymphoproliferative disorders with early lethality in mice deficient in Ctl4. *Science (New York, N.Y.)* **270**, 985–8 (1995).
19. Nishimura, H., Minato, N., Nakano, T. & Honjo, T. Immunological studies on PD-1 deficient mice: implication of PD-1 as a negative regulator for B cell responses. *International immunology* **10**, 1563–1572 (1998).
20. Nishimura, H., Nose, M., Hiai, H., Minato, N. & Honjo, T. Development of lupus-like autoimmune diseases by disruption of the PD-1 gene encoding an ITIM motif-carrying immunoreceptor. *Immunity* **11**, 141–151 (1999).
21. Nishimura, H. *et al.* Autoimmune dilated cardiomyopathy in PD-1 receptor-deficient mice. *Science (New York, N.Y.)* (2001).
22. Wherry, E. & Kurachi, M. Molecular and cellular insights into T cell exhaustion. *Nature reviews. Immunology* **15**, 486–99 (2015).
23. Wherry, E., Blattman, J. N., Murali-Krishna, K., van der Most, R. & Ahmed, R. Viral persistence alters CD8 T-cell immunodominance and tissue distribution and results in distinct stages of functional impairment. *Journal of virology* **77**, 4911–27 (2003).
24. Barber, D. L. *et al.* Restoring function in exhausted CD8 T cells during chronic viral infection. *Nature* **439**, 682 (2006).
25. Wherry, E., Ha, S., Kaech, Haining, W. & Sarkar, S. Molecular signature of CD8+ T cell exhaustion during chronic viral infection. (2007).
26. Blackburn, S. D. *et al.* Coregulation of CD8+ T cell exhaustion by multiple inhibitory receptors during chronic viral infection. *Nat Immunol* **10**, 29–37 (2009).

27. Paley, M. A. *et al.* Progenitor and terminal subsets of CD8+ T cells cooperate to contain chronic viral infection. *Science (New York, N.Y.)* **338**, 1220–5 (2012).
28. Leach, D., Krummel, M. & Allison, J. Enhancement of antitumor immunity by CTLA-4 blockade. *Science (New York, N.Y.)* **271**, 1734–6 (1996).
29. Linsley, P., Greene, J., Brady, W. & Bajorath, J. Human B7-1 (CD80) and B7-2 (CD86) bind with similar avidities but distinct kinetics to CD28 and CTLA-4 receptors. (1994).
30. Weber, J. S., Yang, J. C., Atkins, M. B. & Disis, M. L. Toxicities of Immunotherapy for the Practitioner. *J Clin Oncol* **33**, 2092–2099 (2015).
31. Simpson, T. R. *et al.* Fc-dependent depletion of tumor-infiltrating regulatory T cells co-defines the efficacy of anti-CTLA-4 therapy against melanoma. *The Journal of experimental medicine* **210**, 1695–710 (2013).
32. JAGO, C., YATES, J., CÂMARA, O. N., LECHLER, R. & LOARDI, G. Differential expression of CTLA-4 among T cell subsets. *Clin Exp Immunol* **136**, 463–471 (2004).
33. Topalian, S. L. *et al.* Safety, activity, and immune correlates of anti-PD-1 antibody in cancer. *The New England journal of medicine* **366**, 2443–54 (2012).
34. rrott, D. F. *et al.* Survival, Durable Response, and Long-Term Safety in Patients With Previously Treated Advanced Renal Cell Carcinoma Receiving Nivolumab. *Journal of clinical oncology : official journal of the American Society of Clinical Oncology* **33**, 2013–20 (2015).
35. Postow, M. A. *et al.* Nivolumab and Ipilimumab versus Ipilimumab in Untreated Melanoma. *The New England journal of medicine* (2015). doi:10.1056/nejmoa1414428
36. Le, D. T. *et al.* PD-1 Blockade in Tumors with Mismatch-Repair Deficiency. *The New England journal of medicine* **372**, 2509–20 (2015).
37. Robert, C. *et al.* Pembrolizumab versus Ipilimumab in Advanced Melanoma. *The New England journal of medicine* (2015). doi:10.1056/nejmoa1503093
38. Powles, T. *et al.* MPDL3280A (anti-PD-L1) treatment leads to clinical activity in metastatic bladder cancer. *Nature* **515**, 558–62 (2014).
39. Kamphorst, A. O. *et al.* Rescue of exhausted CD8 T cells by PD-1–targeted therapies is CD28-dependent. *Science* eaaf0683 (2017). doi:10.1126/science.aaf0683
40. Hui, E. *et al.* T cell costimulatory receptor CD28 is a primary target for PD-1–

mediated inhibition. *Science* **355**, 1428–1433 (2017).

41. Yao, S., Zhu, Y. & Chen, L. Advances in targeting cell surface signalling molecules for immune modulation. *Nat Rev Drug Discov* **12**, 130 (2013).

42. Casey, S. C. *et al.* MYC regulates the antitumor immune response through CD47 and PD-L1. *Science* **352**, aac9935 (2016).

43. Hogg, S. J. *et al.* BET-Bromodomain Inhibitors Engage the Host Immune System and Regulate Expression of the Immune Checkpoint Ligand PD-L1. *Cell Reports* **18**, 2162–2174 (2017).

44. Zhu, H. *et al.* BET Bromodomain Inhibition Promotes Anti-tumor Immunity by Suppressing PD-L1 Expression. *Cell Reports* **16**, 2829–2837 (2016).

45. Spranger, S. *et al.* Up-regulation of PD-L1, IDO, and T(regs) in the melanoma tumor microenvironment is driven by CD8(+) T cells. *Science translational medicine* **5**, 200ra116 (2013).

46. Ribas, A. Adaptive Immune Resistance: How Cancer Protects from Immune Attack. *Cancer Discov* **5**, 915–919 (2015).

47. Oestreich, K. *et al.* NFATc1 Regulates PD-1 Expression upon T Cell Activation. *The Journal of Immunology* doi:10.4049/jimmunol.181.7.4832

48. Kao, C. *et al.* Transcription factor T-bet represses expression of the inhibitory receptor PD-1 and sustains virus-specific CD8+ T cell responses during chronic infection. *Nat Immunol* **12**, 663 (2011).

49. Lu, P. *et al.* Blimp-1 represses CD8 T cell expression of PD-1 using a feed-forward transcriptional circuit during acute viral infection. *The Journal of Experimental Medicine* **211**, 515–527 (2014).

50. aron, M. *et al.* The Transcription Factor FoxO1 Sustains Expression of the Inhibitory Receptor PD-1 and Survival of Antiviral CD8+ T Cells during Chronic Infection. *Immunity* **41**, 802–814 (2014).

51. Park, B. *et al.* TGF 1-Mediated SMAD3 Enhances PD-1 Expression on Antigen-Specific T Cells in Cancer. *Cancer Discov* **6**, 1366–1381 (2016).

52. Stephen, T. L. *et al.* SATB1 Expression Governs Epigenetic Repression of PD-1 in Tumor-Reactive T Cells. *Immunity* **46**, 51–64 (2017).

53. Gray, S. M., Kaech, S. M. & Staron, M. M. The interface between transcriptional and

- epigenetic control of effector and memory CD8⁺ T-cell differentiation. *Immunological Reviews* **261**, 157–68 (2014).
54. Jones, P. A. Functions of DNA methylation: islands, start sites, gene bodies and beyond. *Nature Reviews Genetics* **13**, 484 (2012).
55. Okano, M., Bell, D., Haber, D. & Li, E. DNA methyltransferases Dnmt3a and Dnmt3b are essential for de novo methylation and mammalian development. *Cell* **99**, 247–57 (1999).
56. Lee, P. *et al.* A critical role for Dnmt1 and DNA methylation in T cell development, function, and survival. *Immunity* **15**, 763–74 (2001).
57. Thomas, R. M., Gamper, C. J., Ladle, B. H., Powell, J. D. & Wells, A. D. De novo DNA methylation is required to restrict T helper lineage plasticity. *The Journal of biological chemistry* **287**, 22900–9 (2012).
58. Ladle, B. H. *et al.* De novo DNA methylation by DNA methyltransferase 3a controls early effector CD8⁺ T-cell fate decisions following activation. *Proceedings of the National Academy of Sciences* 201524490 (2016). doi:10.1073/pnas.1524490113
59. Lin, W.-H. W. *et al.* CD8⁺ T Lymphocyte Self-Renewal during Effector Cell Determination. *Cell Reports* **17**, 1773–1782 (2016).
60. Scharer, C. D., Barwick, B. G., Youngblood, B. A., Ahmed, R. & Boss, J. M. Global DNA methylation remodeling accompanies CD8 T cell effector function. *Journal of immunology (Baltimore, Md. : 1950)* **191**, 3419–29 (2013).
61. Youngblood, B. *et al.* Chronic virus infection enforces demethylation of the locus that encodes PD-1 in antigen-specific CD8(+) T cells. *Immunity* **35**, 400–12 (2011).
62. Youngblood, B., Hale, S. J. & Ahmed, R. T-cell memory differentiation: insights from transcriptional signatures and epigenetics. *Immunology* **139**, 277–84 (2013).
63. Ahn, E. *et al.* Demethylation of the PD-1 promoter is imprinted during the effector phase of CD8 T cell exhaustion. *Journal of virology* (2016). doi:10.1128/JVI.00798-16
64. Ernst, J. *et al.* Mapping and analysis of chromatin state dynamics in nine human cell types. *Nature* **473**, 43 (2011).
65. Ernst, J. & Kellis, M. Discovery and characterization of chromatin states for systematic annotation of the human genome. *Nature Biotechnology* **28**, 817 (2010).
66. Phillips, J. E. & Corces, V. G. CTCF: master weaver of the genome. *Cell* **137**, 1194–211

(2009).

67. Araki, Y., Fann, M., Wersto, R. & Weng, N. Histone Acetylation Facilitates Rapid and Robust Memory CD8 T Cell Response through Differential Expression of Effector Molecules (Eomesodermin and Its Targets: Perforin and Granzyme B). *The Journal of Immunology* **180**, 8102–8108 (2008).

68. DiSpirito, J. R. & Shen, H. Histone Acetylation at the Single-Cell Level: A Marker of Memory CD8+ T Cell Differentiation and Functionality. *The Journal of Immunology* **184**, 4631–4636 (2010).

69. Buenrostro, J. D., Giresi, P. G., Zaba, L. C., Chang, H. Y. & Greenleaf, W. J. Transposition of native chromatin for fast and sensitive epigenomic profiling of open chromatin, DNA-binding proteins and nucleosome position. *Nature methods* **10**, 1213–8 (2013).

70. Buenrostro, J. D. *et al.* Single-cell chromatin accessibility reveals principles of regulatory variation. *Nature* **523**, 486–490 (2015).

71. Buenrostro, J. D., Wu, B., Chang, H. Y. & Greenleaf, W. J. ATAC-seq: A Method for Assaying Chromatin Accessibility Genome-Wide. *Current Protocols in Molecular Biology* **109**, 21.29.1-21.29.9 (2015).

72. Pauken, K. E. *et al.* Epigenetic stability of exhausted T cells limits durability of reinvigoration by PD-1 blockade. *Science* **354**, 1160–1165 (2016).

73. Sen, D. R. *et al.* The epigenetic landscape of T cell exhaustion. *Science (New York, N.Y.)* **354**, 1165–1169 (2016).

74. Mognol, G. P. *et al.* Exhaustion-associated regulatory regions in CD8+ tumor-infiltrating T cells. *Proceedings of the National Academy of Sciences* 201620498 (2017). doi:10.1073/pnas.1620498114

75. Kaech, S. M. & Cui, W. Transcriptional control of effector and memory CD8+ T cell differentiation. *Nature Reviews Immunology* **12**, 749–61 (2012).

76. Gallimore, A. *et al.* Induction and exhaustion of lymphocytic choriomeningitis virus-specific cytotoxic T lymphocytes visualized using soluble tetrameric major histocompatibility complex class I-peptide complexes. *The Journal of experimental medicine* **187**, 1383–93 (1998).

77. Zajac, A. *et al.* Viral immune evasion due to persistence of activated T cells without effector function. *The Journal of experimental medicine* **188**, 2205–13 (1998).

78. Chihara, N. *et al.* Induction and transcriptional regulation of the co-inhibitory gene module in T cells. *Nature* 1–6 (2018). doi:10.1038/s41586-018-0206-z
79. Wang, C., Singer, M. & Anderson, A. C. Molecular Dissection of CD8+ T-Cell Dysfunction. *Trends in Immunology* **38**, 567–576 (2017).
80. Singer, M. *et al.* A Distinct Gene Module for Dysfunction Uncoupled from Activation in Tumor-Infiltrating T Cells. **166**, 1500-1511.e9 (2016).
81. Pasero, C. *et al.* Inherent and Tumor-Driven Immune Tolerance in the Prostate Microenvironment Impairs Natural Killer Cell Antitumor Activity. *Cancer Research* **76**, 2153–2165 (2016).
82. Wojtowicz-Praga, S. Reversal of tumor-induced immunosuppression by TGF-beta inhibitors. *Investigational new drugs* **21**, 21–32 (2003).
83. Rodeck, U. *et al.* Transforming growth factor beta production and responsiveness in normal human melanocytes and melanoma cells. *Cancer research* **54**, 575–81 (1994).
84. Gorelik, L. & Flavell, R. A. Abrogation of TGFβ Signaling in T Cells Leads to Spontaneous T Cell Differentiation and Autoimmune Disease. *Immunity* **12**, 171–181 (2000).
85. Best, J. *et al.* Transcriptional insights into the CD8(+) T cell response to infection and memory T cell formation. *Nature immunology* **14**, 404–12 (2013).
86. Shin, H. *et al.* Epigenetic Modifications Induced by Blimp-1 Regulate CD8+ T Cell Memory Progression during Acute Virus Infection. *Immunity* **39**, 661–675 (2013).
87. Gray, S. M., Amezcua, R. A., Guan, T., Kleinstein, S. H. & Kaech, S. M. Polycomb Repressive Complex 2-Mediated Chromatin Repression Guides Effector CD8+ T Cell Terminal Differentiation and Loss of Multipotency. *Immunity* (2017). doi:10.1016/j.immuni.2017.03.012
88. Kakaradov, B. *et al.* Early transcriptional and epigenetic regulation of CD8+ T cell differentiation revealed by single-cell RNA sequencing. *Nat Immunol* (2017). doi:10.1038/ni.3688
89. Yu, B. *et al.* Epigenetic landscapes reveal transcription factors that regulate CD8+ T cell differentiation. *Nature Immunology* **18**, 573–582 (2017).
90. Phan, A. T., Goldrath, A. W. & Glass, C. K. Metabolic and Epigenetic Coordination of T Cell and Macrophage Immunity. *Immunity* **46**, 714–729 (2017).

91. Philip, M. *et al.* Chromatin states define tumour-specific T cell dysfunction and reprogramming. *Nature* **545**, 452–456 (2017).
92. Schietinger, A. *et al.* Tumor-Specific T Cell Dysfunction Is a Dynamic Antigen-Driven Differentiation Program Initiated Early during Tumorigenesis. *Immunity* (2016). doi:10.1016/j.immuni.2016.07.011
93. Schietinger, A., Delrow, J. J., Basom, R. S., Blattman, J. N. & Greenberg, P. D. Rescued tolerant CD8 T cells are preprogrammed to reestablish the tolerant state. *Science (New York, N.Y.)* **335**, 723–7 (2012).
94. Anderson, A. C. *et al.* T-bet, a Th1 transcription factor regulates the expression of Tim-3. *Eur J Immunol* **40**, 859–866 (2010).
95. Huang, Y.-H. *et al.* CEACAM1 regulates TIM-3-mediated tolerance and exhaustion. *Nature* **517**, 386–390 (2014).
96. Gibson, H. M. *et al.* Induction of the CTLA-4 gene in human lymphocytes is dependent on NFAT binding the proximal promoter. *Journal of immunology (Baltimore, Md. : 1950)* **179**, 3831–40 (2007).
97. Nixon, B. G. & Li, M. O. Satb1: Restraining PD1 and T Cell Exhaustion. *Immunity* **46**, 3–5 (2017).
98. Pauken, K. E. & Wherry, E. J. Overcoming T cell exhaustion in infection and cancer. *Trends Immunol* **36**, 265–276 (2015).
99. Jin, H.-T. *et al.* Cooperation of Tim-3 and PD-1 in CD8 T-cell exhaustion during chronic viral infection. *Proceedings of the National Academy of Sciences* **107**, 14733–14738 (2010).
100. Sakuishi, K. *et al.* Targeting Tim-3 and PD-1 pathways to reverse T cell exhaustion and restore anti-tumor immunity. *J Exp Medicine* **207**, 2187–2194 (2010).
101. Larkin, J. *et al.* Combined Nivolumab and Ipilimumab or Monotherapy in Untreated Melanoma. *The New England Journal of Medicine* (2015). doi:10.1056/nejmoa1504030
102. Huang, A. C. *et al.* T-cell invigoration to tumour burden ratio associated with anti-PD-1 response. *Nature* (2017). doi:10.1038/nature22079
103. Odorizzi, P. M., Pauken, K. E., Paley, M. A., Sharpe, A. & Wherry, J. E. Genetic absence of PD-1 promotes accumulation of terminally differentiated exhausted CD8+ T cells. *The Journal of Experimental Medicine* **212**, 1125–1137 (2015).

104. Williams, J. B. *et al.* The EGR2 targets LAG-3 and 4-1BB describe and regulate dysfunctional antigen-specific CD8+ T cells in the tumor microenvironment. *The Journal of experimental medicine* (2017). doi:10.1084/jem.20160485
105. Sowell, R. T. & Kaech, S. M. Probing the Diversity of T Cell Dysfunction in Cancer. *Cell* **166**, 1362–1364 (2016).
106. Farber, D. L., Netea, M. G., Radbruch, A., Rajewsky, K. & Zinkernagel, R. M. Immunological memory: lessons from the past and a look to the future. *Nature Reviews Immunology* **16**, 124–8 (2016).
107. Farber, D. L., Yudanin, N. A. & Restifo, N. P. Human memory T cells: generation, compartmentalization and homeostasis. *Nat Rev Immunol* **14**, nri3567 (2013).
108. Zehn, D. & Wherry, E. J. *Advances in Experimental Medicine and Biology*. 137–152 (2015). doi:10.1007/978-3-319-15774-0_10
109. Bocharov, G., Argilaguuet, J. & Meyerhans, A. Understanding Experimental LCMV Infection of Mice: The Role of Mathematical Models. *J Immunol Res* **2015**, 1–10 (2015).
110. Zhou, X., vidya Ramachandran, Mann, M. & Popkin, D. L. Role of Lymphocytic Choriomeningitis Virus (LCMV) in Understanding Viral Immunology: Past, Present and Future. *Viruses* **4**, 2650–2669 (2012).
111. Welsh, R. M. & Seedhom, M. O. *Current Protocols in Microbiology*. 15A.1.1-15A.1.11 (2008). doi:10.1002/9780471729259.mc15a01s8
112. Zinkernagel, R. M. & Doherty, P. C. The discovery of MHC restriction. *Immunol Today* **18**, 14–17 (1997).
113. ZINKEAGEL, R. & DOHERTY, P. Restriction of in vitro T cell-mediated cytotoxicity in lymphocytic choriomeningitis within a syngeneic or semiallogeneic system. *Nature* **248**, 248701a0 (1974).
114. Nish, S. A. *et al.* CD4 + T cell effector commitment coupled to self-renewal by asymmetric cell divisions. *The Journal of Experimental Medicine* jem.20161046 (2016). doi:10.1084/jem.20161046
115. Im, S. *et al.* Defining CD8+ T cells that provide the proliferative burst after PD-1 therapy. *Nature* **537**, 417–421 (2016).
116. He, R. *et al.* Follicular CXCR5-expressing CD8+ T cells curtail chronic viral infection. *Nature* **537**, 412–416 (2016).

117. Wu, T. *et al.* The TCF1-Bcl6 axis counteracts type I interferon to repress exhaustion and maintain T cell stemness. *Science immunology* **1**, (2016).
118. Coulie, P. G., den Eynde, B. J., van der Bruggen, P. & Boon, T. Tumour antigens recognized by T lymphocytes: at the core of cancer immunotherapy. *Nat Rev Cancer* **14**, nrc3670 (2014).
119. Rizvi, N. A. *et al.* Cancer immunology. Mutational landscape determines sensitivity to PD-1 blockade in non-small cell lung cancer. *Science (New York, N.Y.)* **348**, 124–8 (2015).
120. Watson, P. A. *et al.* Context-dependent hormone-refractory progression revealed through characterization of a novel murine prostate cancer cell line. *Cancer research* **65**, 11565–71 (2005).
121. Drake, C. G. *et al.* Androgen ablation mitigates tolerance to a prostate/prostate cancer-restricted antigen. *Cancer cell* **7**, 239–49 (2005).
122. Drake, C. G. Prostate cancer as a model for tumour immunotherapy. *Nature reviews. Immunology* **10**, 580–93 (2010).
123. Shen, Y.-C. *et al.* Combining intratumoral Treg depletion with androgen deprivation therapy (ADT): preclinical activity in the Myc-CaP model. *Prostate Cancer and Prostatic Diseases* **1** (2017). doi:10.1038/s41391-017-0013-x
124. Pili, R. *et al.* Immunomodulation by entinostat in renal cell carcinoma patients receiving high dose interleukin 2: a multicenter, single-arm, phase 1/2 trial (NCI-CTEP#7870). *Clinical Cancer Research* **23**, clincanres.1178.2017 (2017).
125. Orillion, A. *et al.* Entinostat Neutralizes Myeloid-Derived Suppressor Cells and Enhances the Antitumor Effect of PD-1 Inhibition in Murine Models of Lung and Renal Cell Carcinoma. *Clinical Cancer Research* **23**, 5187–5201 (2017).
126. Shen, L., Orillion, A. & Pili, R. Histone deacetylase inhibitors as immunomodulators in cancer therapeutics. *Epigenomics* **8**, 415–428 (2016).
127. Shen, L. *et al.* Class I histone deacetylase inhibitor entinostat suppresses regulatory T cells and enhances immunotherapies in renal and prostate cancer models. *PLoS one* **7**, e30815 (2012).
128. Falkenberg, K. J. & Johnstone, R. W. Histone deacetylases and their inhibitors in cancer, neurological diseases and immune disorders. *Nature reviews. Drug discovery* **13**, 673–91 (2014).

129. West, A. C. & Johnstone, R. W. New and emerging HDAC inhibitors for cancer treatment. *The Journal of clinical investigation* **124**, 30–9 (2014).
130. West, A. C. *et al.* An intact immune system is required for the anticancer activities of histone deacetylase inhibitors. *Cancer research* **73**, 7265–76 (2013).
131. Schietinger, A. & Greenberg, P. D. Tolerance and exhaustion: defining mechanisms of T cell dysfunction. *Trends in immunology* **35**, 51–60 (2014).
132. Attanasio, J. & Wherry, E. Costimulatory and Coinhibitory Receptor Pathways in Infectious Disease. *Immunity* **44**, 1052–68 (2016).
133. Ghoneim, H. E. *et al.* De Novo Epigenetic Programs Inhibit PD-1 Blockade-Mediated T Cell Rejuvenation. *Cell* (2017). doi:10.1016/j.cell.2017.06.007
134. Liu, M., Li, S. & Li, M. O. TGF- β Control of Adaptive Immune Tolerance: A Break From Treg Cells. *Bioessays* 1800063 (2018). doi:10.1002/bies.201800063
135. Sanjabi, S., Oh, S. A. & Li, M. O. Regulation of the Immune Response by TGF- β : From Conception to Autoimmunity and Infection. *Cold Spring Harbor perspectives in biology* **9**, a022236 (2017).
136. Tauriello, D. V. *et al.* TGF β drives immune evasion in genetically reconstituted colon cancer metastasis. *Nature* (2018). doi:10.1038/nature25492
137. Mariathasan, S. *et al.* TGF β attenuates tumour response to PD-L1 blockade by contributing to exclusion of T cells. *Nature* (2018). doi:10.1038/nature25501

Curriculum Vitae

Ali Ghasemzadeh

Email: aghasemzadeh@jhmi.edu

Johns Hopkins University
1830 E. Monument St.
Suite 2-300
Baltimore, MD 21231

Birthplace: Philadelphia, PA
Date of Preparation: July 30, 2019

EDUCATIONAL HISTORY

- | | |
|----------------|---|
| 2012 – Present | Johns Hopkins University School of Medicine, Baltimore MD
Medical Scientist Training Program
Graduate Program in Immunology
M.D., Ph.D.
Expected graduation: May 2020 |
| 2008 – 2012 | Marquette University, Milwaukee WI
B.S. Magna Cum Laude
Biomedical Sciences |
| 2005 – 2008 | Allameh Tabatabaei High School, Sari, Iran
High School Diploma |

AWARDS AND HONORS

- | | |
|------|---|
| 2018 | Rein Saral, M.D. Scholarship for Outstanding Students in the Field of Oncology, Johns Hopkins University School of Medicine |
| 2016 | Excellence in Medical Student Research: Basic Science
Johns Hopkins University Medical Student Research Symposium |
| 2013 | Dean's Summer Research Fellowship
Johns Hopkins University School of Medicine
<i>Department of Plastic and Reconstructive Surgery</i>
<i>Mentors: Dr. Amir Dorafshar, Dr. Justin Sacks</i> |

2012	Award for outstanding research by graduating Biomedical Sciences major, Marquette University
2011	Alpha Sigma Nu – National Jesuit Honor Society
2011	Honorable Mention, Barry M. Goldwater Scholarship
2010	Basic Science Research Award, 1 st place undergraduate research award, Marquette University
2009 – 2011	Marquette University Summer Research Fellowship
2008 – 2012	Dean’s List, Marquette University
2008 – 2012	Marquette University Ignatius Scholar

RESEARCH EXPERIENCE

2017 - 2018	Graduate Student and Research Assistant Columbia Center for Translational Immunology <i>Laboratory of Dr. Charles Drake</i> Columbia University Medical Center
2015 – 2016	Graduate Student and Research Assistant Department of Oncology <i>Laboratory of Dr. Charles Drake</i> Johns Hopkins University School of Medicine
2014 – 2015	Rotating Graduate Student Department of Oncology <i>Laboratory of Dr. Jonathan Powell</i> <i>Laboratory of Dr. Charles Drake</i> Johns Hopkins University School of Medicine
2012 – Present	Research Assistant Department of Plastic and Reconstructive Surgery Johns Hopkins Hospital
2009 – 2011	Research Assistant Department of Microbiology Tarbiat Modares University, Tehran, Iran
2008 – 2012	Research Assistant Department of Biomedical Sciences Marquette University, Milwaukee, WI

LEADERSHIP

2016-2017	Johns Hopkins University School of Medicine Immunology Seminar Series Organizer
2013-2016	Johns Hopkins University School of Medicine Medical Student Research Symposium Co-Chair
2013-2014	Johns Hopkins University School of Medicine Nathans College Treasurer
2012-2013	Johns Hopkins University School of Medicine Nathans College First Year Representative
2012-2013	Johns Hopkins University School of Medicine Medical Student Research Day Committee First Year Representative

PUBLICATIONS

Peer reviewed scientific articles

1. Marciscano AE, **Ghasemzadeh A**, Nirschl TR, Theodros D, Kochel CM, Francica BJ, Muroyama Y, Anders RA, Sharabi AB, Velarde E, Mao W, Chaudhary KR, Chaimowitz MG, Wong J, Selby M, Thudium KB, Korman AJ, Ulmert D, Thorek DL, DeWeese TL, Drake CG. Elective nodal irradiation attenuates the combinatorial efficacy of stereotactic radiation therapy and immunotherapy. *Clin Cancer Res.* 2018 Jun 13.
2. Francica BJ, **Ghasemzadeh A**, Desbien AL, Theodros D, Sivick KE, Reiner GL, Hix Glickman L, Marciscano AE, Sharabi AB, Leong ML, McWhirter SM, Dubensky TW, Pardoll DM, Drake CG. TNFalpha and radio-resistant stromal cells are essential for therapeutic efficacy of cyclic dinucleotide STING agonists in non-immunogenic tumors. *Cancer Immunol Res.* 2018 Feb 22.
3. Shen YC, **Ghasemzadeh A**, Kochel CM, Nirschl TR, Francica BJ, Lopez-Bujanda ZA, Carrera Haro MA, Tam A, Anders RA, Selby MJ, Korman AJ, Drake CG. Combining intratumoral Treg depletion with androgen deprivation therapy (ADT): Preclinical activity in the Myc-CaP model. *Prostate Cancer Prostatic Dis.* 2017 Dec 4.

4. Muroyama Y, Nirschl TR, Kochel CM, Lopez-Bujanda Z, Theodros D, Mao W, Carrera-Haro MA, **Ghasemzadeh A**, Marciscano AE, Velarde E, Tam AJ, Thoburn CJ, Uddin M, Meeker AK, Anders RA, Pardoll DM, Drake CG. Stereotactic radiotherapy increases functionally suppressive regulatory T cells in the tumor microenvironment. *Cancer Immunol Res*. 2017 Oct 2.
5. Park BV, Freeman ZT, **Ghasemzadeh A**, Chattergoon MA, Rutebemberwa A, Steigner J, Winter ME, Huynh TV, Sebald SM, Lee SJ, Pan F, Pardoll DM, Cox AL. TGF- β 1-Mediated Smad3 Enhances PD-1 Expression on Antigen-Specific T Cells in Cancer. *Cancer Discov*. 2016 Sep 28.
6. Patel MA, Kim JE, Theodros D, Tam A, Velarde E, Kochel CM, Francica B, Nirschl TR, **Ghasemzadeh A**, Mathios D, Harris-Bookman S, Jackson CC, Jackson C, Ye X, Tran PT, Tyler B, Coric V, Selby M, Brem H, Drake CG, Pardoll DM, Lim M. J Immunother Cancer. 2016 May 17;4:28.
7. **Ghasemzadeh A**, Bivalacqua TJ, Hahn NM, Drake CG. New Strategies in Bladder Cancer: A Second Coming for Immunotherapy. *Clin Cancer Res*. 2016 Feb 15;22(4):793-801.
8. **Ghasemzadeh A**, Mundinger GS, Swanson EA, Utira AF, Dorafshar AH. Pediatric Condylar and Subcondylar Fractures: A 20 Year Experience. *Plast Reconstr Surg*. 2015 Dec; 136(6):1279-88.
9. Swanson EW, Susarla SM, **Ghasemzadeh A**, Mundinger GS, Redett RJ, Tufaro AP, Manson, PN, Dorafshar AH. Application of the Mandible Injury Severity Score (MISS) to pediatric mandibular fractures. *J Oral Maxillofac Surg*. 2015 July; 73(7): 1341-9.
10. Utria AF, Mundinger GS, Bellamy JL, Zhou J, **Ghasemzadeh A**, Yang R, Jallo GI, Ahn ES, Dorafshar AH. The Importance of Timing in Optimizing Cranial Vault Remodeling in Syndromic Craniosynostosis. *Plast Reconstr Surg*. 2014 Dec 12.
11. Talebi Bezmin Abadi A, **Ghasemzadeh A**, Mohabati Mobarez A. Low frequency of cagA-positive *Helicobacter pylori* strains isolated from Iranian patients with MALT lymphoma. *Intern Emerg Med*. 2013 Feb;8(1):49-53.
12. Taghvaei T, Talebi Bezmin Abadi A, **Ghasemzadeh A**, Naderi BK, Mohabati Mobarez A. Prevalence of horB gene among the *Helicobacter pylori* strains isolated from dyspeptic patients: first report from Iran. *Intern Emerg Med*. 2012 Dec;7(6):505-8.
13. Talebi Bezmin Abadi A, **Ghasemzadeh A**, Taghvaei T, Mobarez AM. Primary resistance of *Helicobacter pylori* to levofloxacin and moxifloxacin in Iran. *Intern*

Emerg Med. 2012 Oct;7(5):447-52. Epub 2011 Mar 25.

14. Abadi AT, Taghvaei T, **Ghasemzadeh A**, Mobarez AM. High frequency of A2143G mutation in clarithromycin-resistant *Helicobacter pylori* isolates recovered from dyspeptic patients in Iran. *Saudi J Gastroenterol*. 2011 Nov-Dec;17(6):396-9.

Publications in Preparation/Submission

1. **Ghasemzadeh A***, Freeman ZT*, Patel CH, Sun IH, Massaccesi G, Mao W, Oh M, Marciscano AE, Theodros D, Clement JM, Tomasi AG, Vergara C, Powell JD, Pardoll DM, Chattergoon MA, Drake CG, Cox AL. Immune Checkpoints Are Discordantly Regulated by Chromatin Remodeling. In submission to *Journal of Clinical Investigation*
*denotes equal authorship
2. **Ghasemzadeh A**, Freeman ZT, Mao W, Marciscano AE, Aggen DH, Theodros D, Chaimowitz MG, Lopez Bujanda ZA, Drake CG. Entinostat increases T cell exhaustion in tumors and chronic viral infections. Manuscript in preparation.

Poster and Podium Presentations

1. Discordant regulation of immune checkpoints by TGF- β 1 and class I HDAC. Poster presentation at the Third CRI-CIMT-EATI-AACR International Cancer Immunotherapy Conference. Mainz, Germany. September 6, 2017.
2. Class I HDAC Regulate T Cell Inhibitory Checkpoint Expression and Exhaustion. Poster presentation at the Prostate Cancer Foundation Annual Scientific Retreat. San Diego, CA. October 27, 2016.
3. Prophylactic Nodal Irradiation Abrogates the Synergy of Tumor Radiotherapy and Immune Checkpoint Blockade. Poster presentation at AACR Tumor Immunology and Immunotherapy meeting. Boston, MA, October 20, 2016.
4. Addition of a Melanoma Targeting *Listeria* Vaccine Greatly Enhances the Efficacy of Immune Checkpoint Blockade. Oral presentation at Johns Hopkins School of Medicine Medical Student Research Symposium. February 10, 2016.
5. Engineered *Listeria Monocytogenes* Vaccine in Combination with Immune Checkpoint Blockade: Effects on the Tumor Microenvironment. Poster presentation at the Immunology Training Program rotation student presentation day. Baltimore, MD. January 9, 2015.

6. Management of Pediatric Condylar and Subcondylar Fractures: The Algorithmal Impact of Concomitant Mandibular Arch Fractures. Oral presentation at the Plastic Surgery Research Council Meeting 2014, New York, NY, March 8, 2014.
7. What is the Optimal Age for Cranial Vault Remodeling in Syndromic Craniosynostosis? Insights from the Johns Hopkins Experience. Oral presentation at the Plastic Surgery Research Council Meeting 2014, New York, NY, March 8, 2014.
8. The Differential Sensitivity of NMDA Receptor NR2A and NR2B Subunits to Inhibition by Long Chain Alcohols. Oral presentation at the Marquette University College of Health Sciences Undergraduate Research Day. Milwaukee, WI. July 29, 2011.
9. Differences in the Binding Sites of Alcohols to NR2A and NR2B Subunits. Poster presentation at Marquette University College of Health Sciences Undergraduate Research Day. Milwaukee, WI. July 29, 2010.